The causal role of neural oscillations in attentional and perceptual sampling mechanisms

Samson Chota

THÈSE

En vue de l'obtention du

DOCTORAT DE L'UNIVERSITÉ DE TOULOUSE

Délivré par l'Université Toulouse 3 - Paul Sabatier

Présentée et soutenue par

Samson CHOTA

Le 20 octobre 2020

Étude de la relation causale entre les oscillations cérébrales et la perception en utilisant des techniques non invasives de stimulation cérébrale

Ecole doctorale : **CLESCO - Comportement, Langage, Education, Socialisation, Cognition**

Spécialité : **Neurosciences**

Unité de recherche :
CERCO - Centre de Recherche Cerveau et Cognition

Thèse dirigée par
Rufin VANRULLEN

Jury

Mme Laura DUGUé, Rapporteure
M. Gregor THUT, Rapporteur
Mme Suliann BEN HAMED, Rapporteure
M. Rufin VANRULLEN, Directeur de thèse

The causal role of neural oscillations in attentional and perceptual sampling mechanisms.

Samson Chota

September 21, 2020

Contents

Chapter 1

General Introduction

1.1 Foreword

We stay blissfully unaware of the vast amount of information that our brain is constantly processing. And that is a good thing. Without it we would quickly be overwhelmed trying to make sense of half a billion photons that get absorbed by our retina every second. In order to successfully separate the important things from the unimportant ones in the tidal wave of incoming information, the brain had to develop a number of sophisticated tricks, some of which I will investigate in the context of this thesis.

Imagine sitting on your bike at a red traffic light. There are many cues that your brain subconsciously uses to help you know when you can safely cross the street. Is the light to your left or your right? Which of the three lights is the important one? How long has it been red already? How frequently do I have to check? Obviously some of these questions are about the right location but interestingly some of them are also about the right timing.

How does the brain manage to collect the right amount of information, from the correct location at the correct time? More and more research suggests that periodic fluctuations in our brains activity, so called brain oscillations, play an important role in this process. During my thesis I tried to investigate this theory by manipulating neural oscillations and demonstrated that this changes the way that the brain collects information over time.

1.2 Perceptual Rhythms

Perception varies from moment to moment. Some of the fluctuations in target detection, reaction times or discrimination tasks can be explained by taking a closer look at the momentary state of brain oscillations that accompanies the presentation of stimuli (Box "Dense Sampling Method). More precisely we can relate the phase of certain oscillatory frequency bands to perceptual outcomes, with some "good" phases being beneficial for perception and some "bad" phases being detrimental. This relationship implies that neural oscillations and with them perception, continuously alternates between periods of higher and lower efficiency. Over the last two decades two dominant oscillatory components, one in the 4-7 Hz theta range and one in the 10 Hz alpha range, have emerged from experiments that investigated these perceptual fluctuations (Figure 1) (VanRullen,

2016).

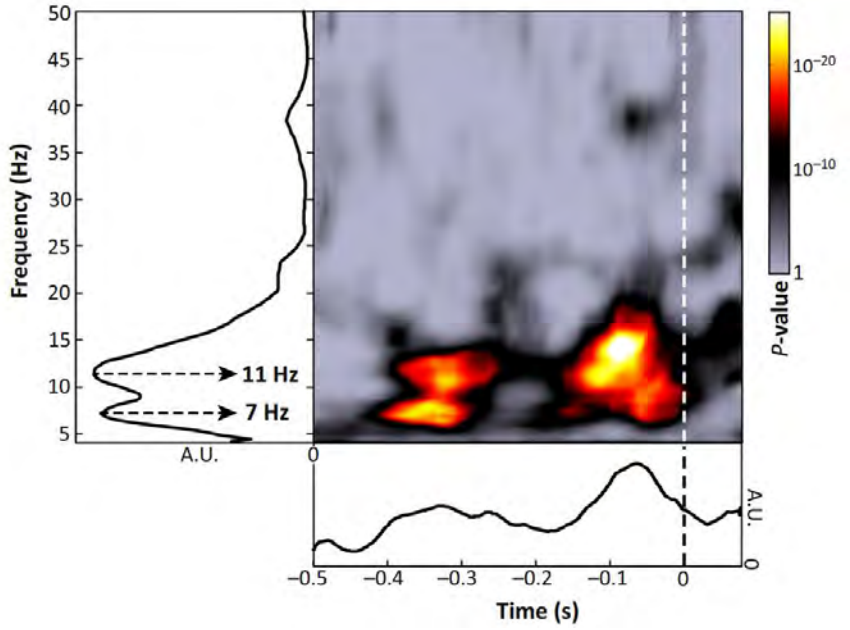

Figure 1. *Phase-Dependent Perception.* The plot depicts the time-frequency representations of 10 independent studies conducted at our laboratory. Hot colors indicate the time and frequency at which the phase of the respective oscillation influenced perceptual outcome in the corresponding task. In other words, if a specific oscillatory phase led to a certain outcome (e.g. target detected) then the opposite phase favoured the opposite outcome (target not detected). As can be seen in the figure, studies consistently reported phase effects in the 10 as well as 7 Hz frequency range with the strongest effect around 100 ms before stimulation. Figure adopted from VanRullen (2016).

Paradigms in which two stimuli compete for attentional resources, for example those in which both stimuli have to be monitored to detect a change, often show that attention alternates between the two competing stimuli at a frequency of 4 to 8 Hz. This attentional "sampling" manifests as a periodic modulation of reaction times or target detection rates over time, observed for both stimuli but in anti-phasic relationship (Busch & VanRullen, 2010; Landau & Fries, 2012; Fiebelkorn, Saalmann, & Kastner, 2013; Landau, Schreyer, van Pelt, & Fries,

2015; Dugué, Roberts, & Carrasco, 2016; Gaillard et al., 2020). We demonstrated this effect in the study found in chapter V. This observation has led to the characterization of this attentional dynamic as an "attentional spotlight" that highlights one stimulus after the other (Figure 2B) (VanRullen, Carlson, & Cavanagh, 2007). Importantly the attentional spotlight is highly flexibel, seemingly being able to sample stimuli of different set sizes at arbitrary locations in the visual field. It is task-context dependent as can be seen in cueing studies and seems to be partially object based (Fiebelkorn et al., 2013; Davidson, Alais, van Boxtel, & Tsuchiya, 2018; Gaillard et al., 2020). Primarily targets that are relevant are sampled and increasing the number of targets, hence distributing attentional resources, leads to a decrease in performance and sampling rate for individual targets (Holcombe & Chen, 2013; Fiebelkorn & Kastner, 2018). How exactly this attentional rhythm samples stimuli and which effects this has on perception is not well understood. In chapter V and VI I investigate how two different types of experimental manipulation lead to changes in attentional sampling and its perceptual consequences.

The second oscillatory component that can be observed in behavioral time courses is a 10 Hz perceptual rhythm. I refer to it as perceptual because it seems to relate more to a general low level fluctuation of excitability in the early visual pathway, not object based and associated most frequently with the occipital alpha rhythm (Figure 2A) (Busch, Dubois, & VanRullen, 2009; Lőrincz, Kékesi, Juhász, Crunelli, & Hughes, 2009; Haegens, Nácher, Luna, Romo, & Jensen, 2011). Interestingly the fluctuations at 10 Hz do not only modulate perceptual sensitivity but also seem to influence time perception in a periodic manner. We can observe experimentally that at regular intervals perceived time is distorted, leading to errors in judgments of relative timing. (Chakravarthi & Vanrullen, 2012; Samaha & Postle, 2015). This intriguing observation has given rise to several theories about the temporal structure of our conscious visual perception (Valera, Toro, Roy John, & Schwartz, 1981; VanRullen & Koch, 2003; VanRullen, 2016). Up until now the question which causal role the occipital alpha rhythm plays in our temporal perception has not been answered. In chapter II and III I investigated if we can manipulate the occipital alpha rhythm and observe how this changes the temporal dynamics of our visual temporal perception.

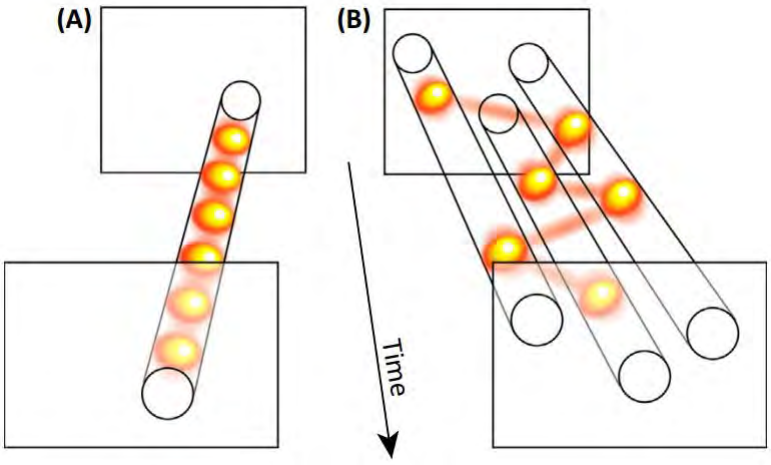

Figure 2. *Perceptual versus Attentional Sampling.* **A.** Discrete perceptual sampling of a single visual location. This sensory mechanism is hypothesized to be implemented by occipital alpha oscillations. **B.** Attentional sampling mechanism, dynamically and sequentially processing different objects in the visual field. We assume that this mechanism is related to theta oscillations in the 4 to 8 hz range. Figure adopted from VanRullen (2016)

As evident in the title I refer to these periodic fluctuations as sampling mechanisms. This implies that they have an active function, namely that of periodically collecting visual information and reducing complexity. This is contrary to the believe of some researchers who claim that the observed fluctuations, either in perception and/or on the neuronal population level are a side effect of other processes. A substantial part of this thesis is dedicated to provide evidence against this viewpoint by providing causal evidence for the involvement of brain rhythms in sampling processes. I shortly review the question of causality in the General Discussion at the end of this thesis.

1.3 Neural oscillations

1.3.1 Alpha

For both attentional and perceptual behavioral fluctuations we have began to find neurophysiological correlates in the brain. Since behavior changes periodically it is most likely that periodic neural oscillations give rise, or relate in some

way to these observations. However connecting the right oscillatory signature to the right behavioral observation is difficult since neural oscillations are ubiquitous in the brain (Box "EEG") (Buzsaki, 2006).

Among brain rhythms the alpha rhythm is the most easily observed one with a frequency of 8 to 12 Hz (Berger, 1931). Initially thought of as a cognitive idling rhythm (Pfurtscheller, Stancák, & Neuper, 1996) it has since been implicated in a vast number of cognitive functions such as attention, memory and inhibition (Klimesch, 1999; Klimesch, Sauseng, & Hanslmayr, 2007; Tuladhar et al., 2007; Jokisch & Jensen, 2007; Jensen & Mazaheri, 2010; Foxe & Snyder, 2011; Bonnefond & Jensen, 2012; Jensen, Bonnefond, & VanRullen, 2012; Klimesch, 2012). A large body of literature investigates the effects of alpha amplitude on perception, linking high alpha power to high inhibition and lower target detection rates (Thut, Nietzel, Brandt, & Pascual-Leone, 2006; Babiloni, Vecchio, Bultrini, Luca Romani, & Rossini, 2006; Hanslmayr et al., 2007). More specifically, alpha power has been shown to increase in task irrelevant areas, whereas it decreases in task relevant areas, demonstrating its role in spatial attention (Sauseng et al., 2005; Kelly, Lalor, Reilly, & Foxe, 2006; Foxe & Snyder, 2011). Alpha oscillations play an even more dynamic role in the context of temporal attention, decreasing/increasing their amplitude at the moment when a target/distractor is expected (Rohenkohl & Nobre, 2011; van Diepen, Cohen, Denys, & Mazaheri, 2015). On an even finer temporal scale we find that the phase of ongoing oscillations in the 5-15 Hz range influences perception. Busch et al. (2009) and Mathewson et al. (2009) demonstrated that the phase of alpha oscillations is predictive of stimulus detection performance, implying that excitability in the visual cortex oscillates at around 10 Hz (Busch et al., 2009; Mathewson, Gratton, Fabiani, Beck, & Ro, 2009). These findings have been replicated several times using rhythmic entrainment at 10 Hz via periodic visual stimuli or alpha-TMS. (Mathewson, Fabiani, Gratton, Beck, & Lleras, 2010; Romei, Gross, & Thut, 2010; Thut et al., 2011; Spaak, Lange, & Jensen, 2014; Dugué & VanRullen, 2017). In chapter II and III we apply such a rhythmic entrainment protocol to influence the alpha rhythm and observe how excitability fluctuations change time perception.

While alpha de-synchronization in response to visual stimulation is a relatively robust effect observed in this context, there has been an intriguing finding that shed doubt on the interpretation of its relationship to perception. By presenting

participants with white noise luminance sequences and cross-correlating them with the resulting EEG signal, one can calculate the brain's mathematical impulse response function (IRF)(VanRullen & Macdonald, 2012). Theoretically this IRF should resemble an ERP since both can be considered the brains response to an impulse, however the IRF showed an up to 1 second long reverbration of the input sequence that had a strong oscillatory 10 Hz component, and was thus coined "perceptual echo" (Figure 3). Importantly these reverbrations were only present when the EEG was cross-correlated with the exact luminance sequence of that trial and not when a random luminance sequence was used. This indicates that it is the precise visual information that is "echoed" in the brain instead of arbitrary luminance sequences leading to oscillatory entrainment . In the remainder of the manuscript I will use the term perceptual echo and IRF interchangeably. A striking observation here is that, in contrast to traditional ERP's, where we find strong de-synchronization after stimulation, the echoes show a clear increase in oscillatory power. The fact that the broadband input sequence did not favour any specific frequencies suggests that a basic property the visual system is to processes information at an intrinsic frequency of 10 Hz. The oscillatory component of the echoes initially does seem to reflect the periodic sampling of external stimuli in the fashion of chapter II and III. Theoretically the echoes can be understood as a filter that turns a continuous signal into a periodic signal, similar to what we would expect from said rhythmic sampling. However, since the IRF's are a result of the cross-correlation we must remember that their temporal unit is in lags which means that in theory every successive luminance increment is associated with a phase locked IRF. In contrast, chapter II and III hypothesize that rhythmic sampling is implemented by a single oscillation that samples all stimuli in "real-time" instead of lags. These considerations make the relationship between discrete sampling and echoes a complex one to disentangle.

A different way to understand the mechanism that generates the echoes is to assume that they are a result of an internal process that periodically reactivates specific stimuli sequences. These rhythmic reactivations could be a signature that might be expected of intra-cortical sampling, or information transfer, where one layer in the visual hierarchy samples the information in another one in a recurrent fashion. Along these lines the echoes could reflect predictive coding processes where bottom up information and top down predictions need to be aligned for comparison while taking into account neural transmission delays

(Hogendoorn & Burkitt, 2019; Alamia & VanRullen, 2019). In any case, if these findings could be extended to other sensory modalities we would have intriguing evidence that rhythmic processing is intrinsically linked to neural oscillation in the respective sensory processing areas. In chapter IV we tested if perceptual echoes can be found in the somatosensory system.

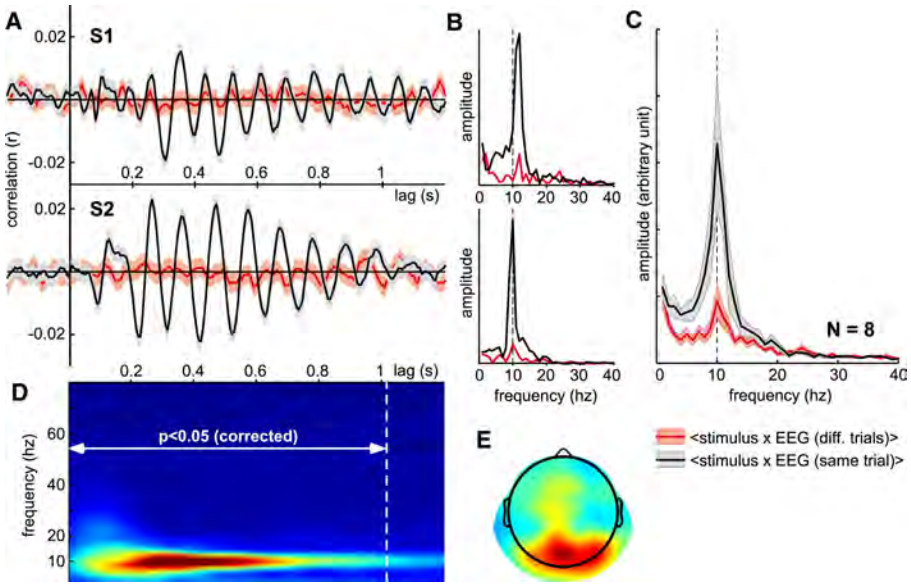

Figure 3. *Perceptual Echoes.* **A.** Visual Perceptual Echoes of two individual subjects. Cross correlation between white noise sequence and corresponding EEG leads to 1 second long periodic reverbrations. Surrogate echoes are calculated by cross-correlating white noise sequences with the EEG signal of a random trial and show no reverbrations. **B.** The power spectrum of the perceptual echoes shows strong oscillatory components at 10 Hz. **C.** Group average of the power spectrum. **D.** Average time-frequency representation of individual perceptual echoes. We can observe significantly high alpha power for up to 1 second. **E.** The Topography of the power spectrum indicates that the origin of the echo lies in parieto-occipital regions. Figure adopted from VanRullen and Macdonald (2012).

Several theories have tried to provide a broader explanation for the role of the alpha rhythm (Başar, Schürmann, Başar-Eroglu, & Karakaş, 1997; Klimesch, Sauseng, & Hanslmayr, 2007; Jensen & Mazaheri, 2010; Mathewson et al., 2011).

EEG
EEG is a an invaluable tool to measure brain activity with a high temporal resolution. It uses multiple electrodes distributed across the scalp to measure changes in the electric potential. The EEG signal is assumed to stem from large groups of pyramidal cells with parallel axional orientation, that reside in deep cortical layers.

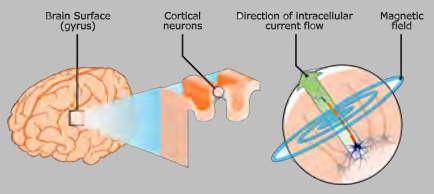

EEG measurements were used in chapter 4 to measure oscillatory responses to different input frequencies as well as broad band stimulation. Since EEG data tends to be subject to several sources of noise like line noise, eye blinks and muscle contractions, we used independent component analysis and a generalized eigenvalue decomposition approach to improve the signal to noise ratio. This allowed us to identify the channels that best represented the brains frequency response. Illustration by Nikola Vukovic (2014).

Generally these ideas agree that alpha exhibits some form of inhibitory effect on the neural population, modulated by amplitude and/or phase. It is not clear however what exactly is inhibited and at which stage(s) of the visual processing pipeline this inhibition takes place. The thalamus, more specifically the lateral geniculate nucleus (LGN), has been implicated in utilizing alpha to gate information flow towards primary visual cortex (Lőrincz et al., 2009). The LGN primarily relays information from the retina to V1 and serves as it's main afferent. It has been proposed that alpha is generated by this cortico-geniculate circuit, effectively concentrating neuronal firing to certain phases of the alpha cycle and temporally framing information transfer (Haegens et al., 2011; Vijayan & Kopell, 2012). Visual information would therefore arrive periodically in more or less discrete packages at primary visual cortex. In my thesis I was specifically interested in the consequences that this temporal framing structure has on the temporal dynamics of time perception. Of critical importance here is the theory of discrete perception which I investigated in chapter II and III. I will go into more detail on this hypothesis in the chapter "Discrete Perception".

1.3.2 Theta

Behavioral theta fluctuations in reaction times and performance measures are commonly found during attentional tasks. (Busch & VanRullen, 2010; Landau & Fries, 2012; Fiebelkorn et al., 2013; Landau et al., 2015; Dugué, McLelland, Lajous, & VanRullen, 2015). Previously the theta rhythm, as measured with EEG, has been related to attentional processes (Busch & VanRullen, 2010; Clayton, Yeung, & Cohen Kadosh, 2015; Landau et al., 2015). Using EEG and TMS, Dugue et al. have shown that performance in a visual search paradigm was dependent on the phase and amplitude of cortical theta oscillations (Dugué, Marque, & VanRullen, 2011). Furthermore they showed that information in visual cortex is vulnerable to TMS pulses every 160 ms (6 Hz). Detection rates of attended targets were demonstrated to be dependent on the phase of frontal theta oscillations (Busch & VanRullen, 2010). However electrophysiological evidence that maps behavioral attentional oscillations directly to intracortical regions displaying neural oscillations has long been missing. A recent upsurge in studies has changed this however (VanRullen, 2018). In a series of experiments it was shown that behavioral signatures of attention relate to theta oscillation in Prefrontal Cortex (PFC), highlighting its function as a top-down mechanism and finally providing convincing evidence for the the cyclic nature of attention and its oscillatory substrates (Helfrich et al., 2018; Spyropoulos, Bosman, & Fries, 2018; Fiebelkorn, Pinsk, & Kastner, 2018; Gaillard et al., 2020). These recent developments have given rise to more wholesome theories of attentional processes, incorporating several neural systems assumed to be involved in attention sampling. Fiebelkorn et. al. (2018) identified two attentional states that directly relate to two opposite phases of theta oscillations in the FEF. During one of these states, the "poor theta phase", they observed high alpha power over parietal regions (LIP), effectively inhibiting visual processing at the current locus of attention and allowing for attentional shifts to different potential targets. This state is related to the periods of low performance in periodic behavioral measures. On the other hand the "good theta phase" was associated to high beta band activity in the FEF and high gamma band activity in LIP. Burst of beta power were hypothesized to reflect surpressed attentional shifts away from the locus of attention whereas increases in gamma in the LIP is assumed

to reflect enhanced processing, leading to the observed increases in performance.

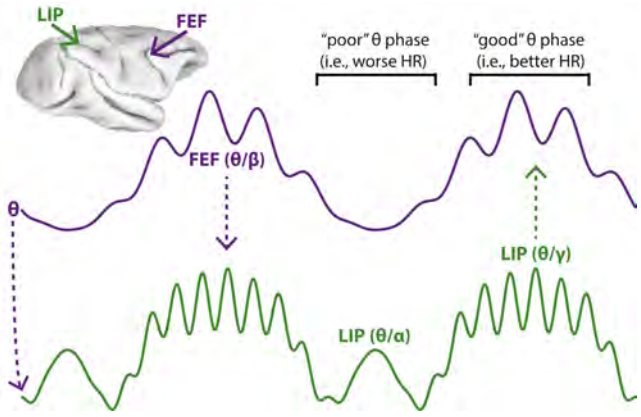

Figure 4. *The Frontoparietal attentional network. Fiebelkorn (2018).* Attentional sampling can be characterized as alternating states of processing (good phase) and shifting (bad phase). Both states map onto certain phases of FEF theta oscillations. During good phases alpha power in parietal regions (LIP) is low, a signature associated with high excitability and thus allowing for effective processing. During bad phases one can observe high alpha power, associated with increased inhibition, which allows the attentional network to shift the focus away from the now-inhibited locus of attention. Figure adopted from Fiebelkorn (2018).

Through sophisticated decoding of intracranial recordings it was demonstrated for the first time that neural signals recorded from the PFC could be used to track the locus of attention in real-time in macaque monkeys (Astrand, Wardak, Baraduc, & Ben Hamed, 2016). Recently the investigators further build upon their initial study by showing that the decoded spotlight rhythmically explores the visual field in line with previously proposed rhythmic theories of attention (Gaillard et al., 2020). The rhythmically sampled locations were highly dependent on prior expectation on the target location as well as general expectation about sensory events. Interestingly however attentional sampling was shown to not be solely restricted to the cued relevant locations in the visual field (exploitation) but also occasionally sampled uncued locations (exploration), a trade-off that potentially aids the attentional system in case of unexpected events.

In a recent study in macaques it was demonstrated that theta oscillations in V4 play an important role in attention related stimulus competition, resulting in behavioral oscillations at 6 Hz, a finding that we have since reproduced in humans (Kienitz et al., 2018; Chota et al., 2018). These studies represent important steps towards finding the neural implementation of the system that gives rise to attentional fluctuations. In chapter V I closely reproduce the behavioral findings of the macaque experiment by Kienitz in order to fill in the missing link between neural theta and behavioral theta oscillations. For a more detailed discussion of their findings I refer the reader to the introduction in chapter V.

Most of the studies I described in the previous paragraph were concerned with covered attention, that is, attention without explicitly fixating the object of interest. However one of the most useful tools of our attentional system is the ability to make saccades towards relevant stimuli in our environment (Zhao, Gersch, Schnitzer, Dosher, & Kowler, 2012). Previous research in combination with our findings in chapter V support the idea that specific theta phases are better for processing than others (Busch & VanRullen, 2010; Dugué et al., 2011; Kienitz et al., 2018; Chota et al., 2018; Gaillard et al., 2020). It thus seems important that the phase of theta is aligned with saccade execution to optimally process the stimulus that falls on the fovea when the saccade lands. Indeed saccades have been found to phase align theta oscillations in humans and non-human primates (Hoffman et al., 2013). Further evidence links theta oscillations to preparatory processes right before saccade onset (Womelsdorf, Johnston, Vinck, & Everling, 2010; van Noordt, Desjardins, Gogo, Tekok-Kilic, & Segalowitz, 2017). Most interestingly for our purpose, theta phase has been related to the amount of peri-saccadic mislocalization, suggesting it as a possible substrate for several peri-saccadic phenomena (McLelland, Lavergne, & VanRullen, 2016). In chapter VI we investigate if full field masking, assumed to trigger peri-saccadic mechanisms, leads to a distortion of relative time perception, another peri-saccadic illusion potentially caused by oscillatory processes.

1.4 Discrete Perception

Our everyday visual perception is usually experienced as a "continuous flow". However, people under the influence of certain psychedelic substances like LSD or those who suffer from akinetopsia (motion blindness) can experience it more

like a discrete series of static images (Dubois & VanRullen, 2011). This intriguing observation raises an interesting question. Can our visual experience generally be considered continuous and certain substances artificially discretize it? Or is our visual experience generally discretized and certain substances break the neural mechanism that hides the empty spaces in-between from conscious perception? The theory of discrete perception explores this second idea, proposing that a discrete sampling mechanism governs the temporal structure of our conscious visual perception (VanRullen & Koch, 2003; VanRullen, 2016).

The question whether perception is discrete or continuous outdates the use of EEG or the knowledge about brain rhythms. First considered by William James in 1890 the theory gained popularity when the first EEG recordings were performed and it became obvious that the brain is a highly rhythmic organ (Berger, 1931; Johnson & Henley, 2013). The first hypotheses were strongly influenced by the emergence of the cinema, leading to the assumption that visual sampling mechanisms with fast enough sampling rates would appear to be continuous, just like observed with the "novel" opto-mechanical projectors used at the time (Pitts & McCulloch, 1947; Harter, 1967). One of the most prominent concepts, that of the "perceptual moment" was promoted by Stroud, and describe a basic interval of time within which all events are subjectively perceived as co-temporal (Stroud, 1956). Stroud's ideas formed the basis of the modern theory of discrete perception.

Modern discrete sampling in the visual system can loosely be understood in analogy to a digital camera that collects a certain number of frames per second. The idea is that the brain periodically divides the visual input into discrete windows or "perceptual moments" (VanRullen, 2016). Two stimuli that would fall into a single perceptual moment would therefore be perceived as occurring simultaneously, while two stimuli in separate subsequent perceptual moments would be perceived as sequential (Figure 4). A recent upsurge of psychophysiological and electrophysiological studies have investigated discrete perception in the context of the alpha rhythm (VanRullen & Koch, 2003; Busch et al., 2009; Lőrincz et al., 2009; Haegens et al., 2011; Vijayan & Kopell, 2012; Samaha & Postle, 2015). One of these studies demonstrated that participants with faster alpha rhythms showed higher visual temporal resolution in a two-flash fusion task (Samaha & Postle, 2015). Similarly, when entraining a slightly faster or slower alpha rhythm (IAF $\pm$ 2 Hz), using visuo-auditory entrainment, percep-

tion could be sped up or slowed down in a segregation/integration task (Ronconi, Busch, & Melcher, 2018). Aiming at implicating the occipital alpha rhythm in a causal manner, we demonstrated that visual entrainment at 10 Hz leads to a periodic modulation of temporal perception in the flash lag effect (FLE) (Chota & VanRullen, 2019). The flash-lag effect is a visual illusion that has been suggested to arise from discrete sampling in the visual system (Chakravarthi & Vanrullen, 2012; Schneider, 2018).

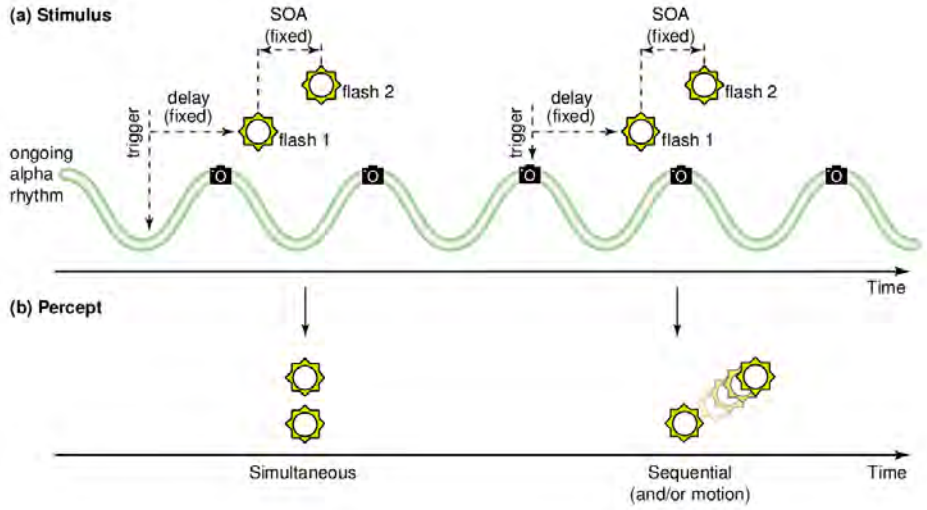

Figure 4. *Alpha Phase and perception of relative timing.* **A.** Relative timing between alpha phase and the appearance of two sequential flashes with fixed SOA. Beginning and end of discrete perceptual moments are indicated by camera symbols. Note that in the first case the two flashes fall into the same perceptual moment whereas in the second case the flashes fall into two separate perceptual moment. **B.** Two stimuli that fall within the same perceptual moment are perceived as occuring simultaneously whereas two stimuli in successive perceptual moments are perceived as sequential. Figure modified from VanRullen (2003)

It is believed that discrete sampling is serving two primary roles. One is the the reduction of complexity and the other is to facilitate communication in the brain (VanRullen & Koch, 2003; Vanrullen & Dubois, 2011). Complexity reduction is always a trade-off between resources and information.

Dense Sampling Method

The dense sampling method is a behavioral method that allows the researcher to probe the behavioral correlates of dynamic brain processes over time. In the course of this project I made extensive use of this method because it lends itself nicely to investigate oscillatory processes. Usually oscillatory phase is arbitrary at the onset of a trial. The key challenge therefore lies in resetting the phase of the oscillation that is assumed to influence behavior periodically. This reset can be done via visual or auditory stimuli or with TMS pulses. A phasic reset is performed at the beginning of every trial. In the illustration below we see that the phase reset causes the peak of the oscillation to always be at the same time relative to trial onset. Over the course of many trials we can now probe all possible positions and reconstruct the dynamic influence that the hidden underlying process has on behavior.

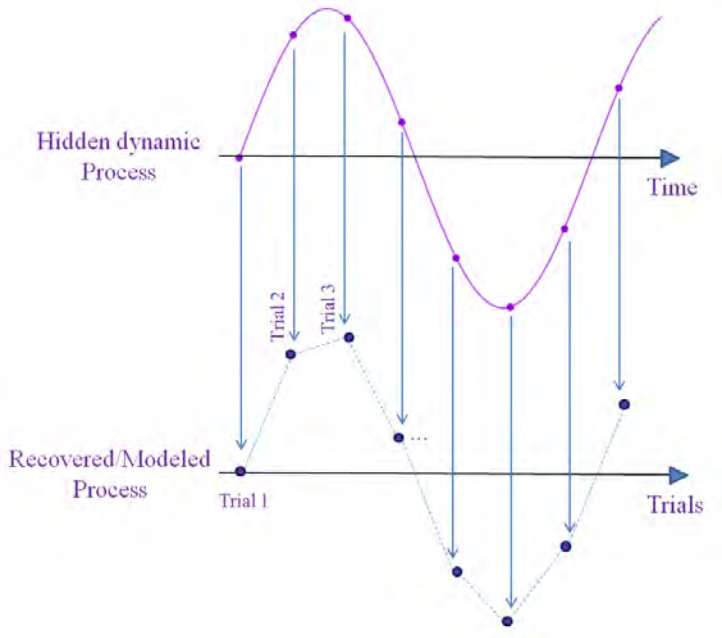

The dense sampling method is especially useful to investigate fast dynamical cognitive processes that exceed the number and frequency with which human participants can report perception within a single trial. On the downside this method usually requires an extensive number of trials, increasing the length of experiments.

Fast sampling rates might require the brain to make more computations in a shorter amount of time (Schroeder & Lakatos, 2009). Slow sampling rates might deteriorate perception too severely for efficient interaction with the environment. Facilitation of communication is assumed to be at least partially allowed by synchronizing the phase of two brain regions, therefore aligning phases of excitation and inhibition and maximizing information flow (Fries, 2015). This process, while most likely periodic, is very well compatible with a continuous rhythmic form of information processing and does not require strictly discrete frames. Neural communication however is much more complex than just to optimize information flow between regions. Stimuli that are processed in different brain regions, potentially different modalities need to be compared, an endeavour that is immensely complicated by neural communication delays. On top of that a promising new model for brain functioning, that has emerged in the form of hierarchical predictive coding, runs into similar difficulties (Rao & Ballard, 1999). In it's simplest form a predictive coding model is constantly trying to make sense of it's environment by comparing bottom-up evidence with top-down predictions. If the two do not match then the residual error is propagated up the hierarchy. This process is assumed to run in parallel on all hierarchical layers. Evidently this requires a fine mechanism that allows predictions and evidence to find each other in neural space-time. Discretizing input into quanta might be an elegant solution to create defined "feature" packages that can be compared. Moreover by concentrating processing to certain phases of the oscillation the brain creates a defined temporal structure that reduces temporal uncertainty, therefore allowing more precise timing e.g. of top down predictions (Hogendoorn & Burkitt, 2019). The perceptual echoes described in chapter IV have been implicated in predictive coding processes and might be reflective of the propagation of top-down and/or bottom up information along the visual hierarchy, potentially aiding this matching problem in the light of neural time delays (Alamia & VanRullen, 2019).

In the chapter on alpha oscillations we described how the phase of alpha oscillations relates to excitability fluctuations. This feature of alpha phase is an important one to consider because it introduces a potential alternative explanations for the findings in integration/segregation tasks. Alpha phase might modulate task performance not via changes in temporal perception but by decreasing visibility of one of two stimuli. In this way alpha phase would still periodically modulate time perception but via different secondary mechanisms.

We will refer to this account as the "soft" version of rhythmic perception. Separating "hard" and "soft" accounts of rhythmic perception necessitates intricate task design that controls for fluctuations in visibility. We describe such a design in chapter III. Our approach was successful and together with the previous literature, supports the idea that the visual system discretely samples the visual scene at a 10 Hz rhythm analogous to the "hard" version of periodic perception (VanRullen, 2016).

1.5 Rhythmic entrainment and phase resets

Now that we have discussed the relationship between behavioral and neuronal oscillations we need to tend towards the directionality of this relationship, that is, what is the causal link between them. Most of the above mentioned studies do not provide evidence on the question if the neural oscillations actually cause the periodicities in behavior. Manipulating stimuli and investigating how brain rhythms change does gives us causal evidence only in one (complex but rather unsurprising) direction. To proof if the neural oscillations are the underlying cause of perceptual and behavioral findings we need to manipulate the oscillations themselves and observe if perception and behavior changes.

TMS

Transcranial Magetic Stimulation is a non-invasive brain stimulation technique. By running a strong biphasic pulse through a form-of-eight coil we can generate a directed magnetic field. When placed on top of the scalp the magnetic field generates a current flow in the superficial parts of the brain which in turn depolarizes cortical cells and causes action potentials. The exact way in which TMS interferes with the brain is unknown, it is however assumed that it targets mostly cortical pyramidal cells. TMS not only lets us target very specific brain regions but also gives us precise temporal control over the stimulation pattern. Recently investigators have started to apply multiple pulses with fixed frequency to measure the brains response to rhythmic input.

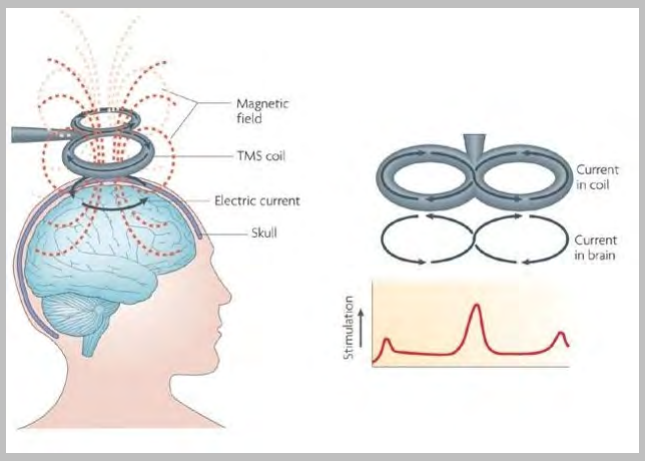

I used rhythmic TMS in chapter II to entrain alpha oscillations. Often TMS is used in combination with preceding structural fMRI scans to determine the exact location of the brain to which the coil should be aligned. It is possible to circumvent these extra measurements by using a phosphene mapping procedure: By stimulating the brain over primary visual areas it is possible to elicit visual sensations at specific locations in the visual field. This allows the investigator to map the stimulated location on the scalp to the reported location on the screen and enables precise positioning of the experimental stimulus over the stimulated area. Reproduced from Spronk (2011).

One prominent way to interfere with oscillatory brain activity is to reset the

phase of an ongoing oscillation and therefore control the phase in the subsequent time windows. This can be done with single impulses of visual stimulation or TMS in accordance with the following principle: Hypothetically if the stimulation is strong enough it depolarizes and homogenizes a subset of the affected neural population (Box "TMS") (Savers, Beagley, & Henshall, 1974; Makeig et al., 2002; Klimesch, Sauseng, Hanslmayr, Gruber, & Freunberger, 2007; Romei, Gross, & Thut, 2012). If the neurons involved are intrinsically oscillatory then also their oscillatory phase is reset (Paus, Sipila, & Strafella, 2001; Fuggetta, Fiaschi, & Manganotti, 2005; Rosanova et al., 2009; Herring, Thut, Jensen, & Bergmann, 2015). Over the course of many trials in an experimental setup we can use this to create more or less equal conditions, with respect to the oscillatory phase, in each trial. We assume that this mechanism at least partially underlies our observations in chapter V and VI. Although this method is very useful it also comes with its limitations. It offers no control over which oscillation we want to phase-reset. This however might be an advantage if one does not want to have prior assumptions on the frequency. Another problem is that single pulses might not be sufficiently strong to reset a behaviorally significant subset of the population. These issues can be resolved by applying multiple pulses as described in the next paragraph.

Another method to interfere with brain oscillations is through rhythmic stimulation. Presenting visual stimuli or applying rhythmic TMS pulses at specific frequencies is assumed to directly interfere with the corresponding frequency band. This effect, presumably a result of multiple successive phase resets, can lead to power increases in the respective frequency band (Figure 5) (Herrmann, 2001; Schwab et al., 2006; Spaak et al., 2014; Helfrich et al., 2014). Furthermore we can observe that the increase in power outlasts the stimulation period and critically these short lived effects are behaviorally significant. Entrainment at 10 Hz has been shown to decrease target detection rates, an observation that is frequently linked to high alpha power (Romei et al., 2010; Thut et al., 2011). However we can not only investigate the resulting changes in oscillatory power but we can also probe the effect of phase with this method. Probing different time-points after entrainment reveals fluctuations in target detection and temporal perception (Ronconi & Melcher, 2017; Ronconi et al., 2018). I make use of this method in chapter II and III. In chapter IV we use tactile stimulation to probe entrainment effects in the somatosensory system.

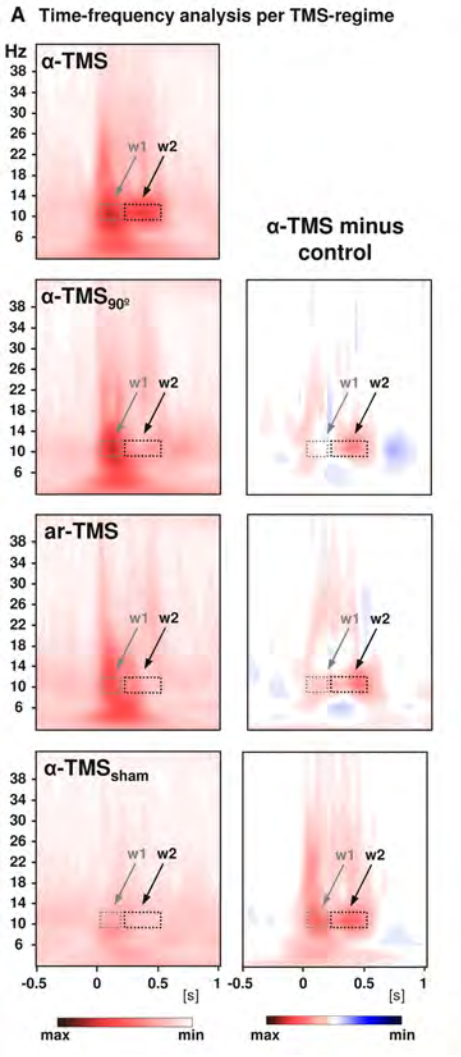

Figure 5. *Rhythmic TMS stimulation at 10 Hz leads to Alpha entrainment.* Alpha TMS was applied perpendicular to a target gyrus (Row 1). The time-frequency representation shows increased alpha power compared to baseline in the 300 ms window following stimulation. Row 2,3 and 4 are direct comparisons between the main condition (Row 1) and control conditions in which the coil was rotated by 90 degrees (Row 2), a-rhythmic TMS was applied (Row 3) or the tms mode was set to inactive. We can observe that broad band activity emerged for all active conditions during stimulation (w1). Contrasts (second column) show that lasting alpha oscillations are only present in the main condition (w2). Figure adopted from Thut (2011).

1.6 Main Research Questions

Oscillatory activity seems to have profound effects on multiple aspects of our perception and might be strongly involved in the way we sample our visual environment. Many of these relationships however are poorly understood, specifically in their causal-directional nature. This poses a problem since a purely correlational link between perception and brain states does not allow us to in-

fer if the two are functionally linked at all. It might simply be the case that oscillations arise as a irrelevant by-product of other cognitive processes, as a mere epiphenomenon. This theoretical possibility is demonstrated in a recent publication by Alamia et. al. who implemented a simple predictive coding inspired network with biologically plausible time constants (Alamia & VanRullen, 2019). The network uses inhibitory feedback to predict the activity of lower layers in a recursive manner. Most importantly the network is not constructed to make use of rhythmic processing to solve the task. When stimulated with random noise sequences however we can observe strong oscillatory activity with frequencies dependent on the choice of time constants. The oscillations in this specific implementation of the network correlate with the input sequence but do not serve any functional purpose. Hypothetically we could expand this idea to the whole brain since the generation of oscillatory activity is very easily accomplished e.g. using inhibitory feedback (Wang, 2010). So how can we know if a certain brain rhythm is actively involved in solving a specific task instead of being an epiphenomenon? In order to answer this question we need to be able to directly modulate rhythmic activity and observe the changes that occur in perception and behavior. As described above, non-invasive stimulation techniques like TMS or rhythmic visual stimulation, and even random noise stimulation have proven useful tools to manipulate brain rhythms.

In this thesis, I make use of these non-invasive methods to investigate the causal role of neural oscillations in temporal sampling mechanisms. The original manuscripts in chapter II and III are dedicated to perceptual sampling in the alpha band. Early behavioral studies have found that the minimal delay between two offset stimuli to induce a perception of motion was around 100 ms (Wertheimer, 1912; Anstis, 1978). It was logically followed that the duration of the frame that allowed for integration of two stimuli and their relative timing was around 100 ms. If stimuli were closer together, then relative timing could not be discerned. The alpha band became a interesting subject in explaining how the brain might implement such frames because it naturally cycled every 100 ms (Valera et al., 1981). Several decades of research later the alpha band is still an interesting candidate proposed to implement discrete windows in vision so that visual information is periodically compressed at a rate of approximately 10 Hz. (VanRullen, 2016). While we have many correlational studies showing it's relationship to temporal perception, there is still no clear evidence that alpha actively implements a mechanism to discretely sample visual input (Chakravarthi

& Vanrullen, 2012; Samaha & Postle, 2015). The matter is further complicated by the findings that alpha phase modulates cortical excitability (Busch et al., 2009; Haegens et al., 2011; Dugué et al., 2011). This observation had led to the distinction between "hard" and "soft" version of discrete perception, where the hard version refers to true modulations of time perception and the soft version refers to indirect modulations of time perception through excitability fluctuations (e.g. occlusion of one stimulus). In chapter II and III we therefore set out to test if rhythmic stimulation, via visual entrainers or TMS at 10 Hz, could modulate the alpha rhythm in such a way that perception of relative timing could be changed. More specifically we stimulated at an alpha rhythm and probed temporal perception at different phases of the entrained oscillation. If specific phases of the alpha cycle mark the beginning of discrete frames then behavior should be dependent on the phase were stimuli were presented. Importantly we aimed at controlling for the previously described effect of excitability to ensure that our findings support the "hard" version of discrete perception.

Besides the behavioral oscillations investigated in chapter II and III there are also neural signatures that hint at the intrinsic periodicity with which sensory cortices collect information. When presented with random noise luminance sequences the visual system responds with long lasting reverbrations at 10 Hz (VanRullen & Macdonald, 2012). These reverbrations, revealed by cross-correlating input sequences with the concurrent EEG signal, have been termed perceptual echoes. An especially stunning feature of these echoes is that they suggest that the visual system periodically "re-activates" the 10 Hz component of the stimulation sequence for up to 1 second. Since alpha oscillations usually de-synchronize very consistently in response to visual stimulation (Klimesch, Sauseng, & Hanslmayr, 2007) the echoes indirectly implicate alpha in active stimulus processing. However, few studies have provided concrete insights into the functional role of these echoes (Chang, Schwartzman, VanRullen, Kanai, & Seth, 2017). It has been proposed that perceptual echoes reflect a mechanism by which the brain transforms a continuous visual input stream into periodically structured activity (Schwenk, VanRullen, & Bremmer, 2020). The cross-correlation between EEG and white noise,(which per definition containing equal power in all frequency bands) produces the Impulse Response function of the brain, in other words the echoes reflect the function that the brain applies to the incoming signal. Thus one interpretation is that the brain filters the visual input at 10 Hz which is very similar to periodic sampling at 10 Hz.

Other sensory modalities have been hypothesized to sample their input in a similar fashion compared to the visual system. Beta oscillations in the somatosensory system have been demonstrated to modulate temporal integration performance in a periodic fashion (Baumgarten, Schnitzler, & Lange, 2015). If beta oscillations serve the same function in the visual as compared to the tactile domain then we should expect to find perceptual echoes in the tactile domain as well, although at the beta frequency. Extending the existence of perceptual echoes to other modalities would provide evidence that 1. these other modalities also process information periodically and 2. that they utilize similar neural mechanisms for this purpose. In the original manuscripts in chapter IV I investigated if we can find perceptual echoes in the tactile domain.

The periodic sampling mechanisms of the brain seem to be dissociable into a more low-level perceptual and a more high-level attentional sampling mechanism. Attentional sampling is assumed to be more flexible, task dependent and has been hypothesized to be caused by theta rhythmic activity in PFC. Providing support for these findings in humans would help us to identify the oscillatory mechanism that is responsible for behavioral attentional fluctuations found in many studies. The original manuscript in chapter V presents a study in which we replicate behavioral findings of the macaque-study in humans.

Which location in the visual field attentional sampling mechanisms collect information from depends strongly on the position of our eyes. Saccades and attentional sampling need therefore be highly coordinated. One way to synchronize these two systems is through oscillatory activity. It has been proposed that saccades, and surprisingly also strong visual transients, can reset the phase of theta oscillations which in turn allow for well timed processing of relevant stimuli. If this mechanism indeed relies on rhythmic activity then we should be able to disrupt it and observe corresponding errors in attentional sampling. The original manuscript in chapter VI investigates which effects strong visual disruptions have on the perceived relative timing of two stimuli.

During my doctorate I sought to answer the following research questions:

1. Is the occipital alpha rhythm causally involved in discretely sampling vi-

sual information? (**chapter II and III**)

2. Is there a link between oscillatory activity and rhythmic sampling in the somatosensory system?(**chapter IV**)

3. Can we manipulate theta rhythmic activity to modulate attentional sampling? (**chapter V and VI**)

Chapter 2

Visual Entrainment at 10 Hz Causes Periodic Modulation of the Flash Lag Illusion

The following chapter contains the original manuscript that appeared as: Chota, Samson, and Rufin VanRullen. "Visual Entrainment at 10 Hz causes periodic modulation of the Flash Lag Illusion." Frontiers in neuroscience 13 (2019): 232.

2.1 Abstract

It has long been debated whether visual processing is, at least partially, a discrete process. Although vision appears to be a continuous stream of sensory information, sophisticated experiments reveal periodic modulations of perception and behavior. Previous work has demonstrated that the phase of endogenous neural oscillations in the 10 Hz range predicts the "lag" of the flash lag effect, a temporal visual illusion in which a static object is perceived to be lagging in time behind a moving object. Consequently, it has been proposed that the flash lag illusion could be a manifestation of a periodic, discrete sampling mechanism in the visual system. In this experiment we set out to causally test this hypothesis by entraining the visual system to a periodic 10 Hz stimulus and probing the flash lag effect (FLE) at different time points during entrainment. We hypothesized that the perceived FLE would be modulated over time, at the same frequency as the entrainer (10 Hz). A frequency analysis of the average FLE time-course indeed reveals a significant peak at 10 Hz as well as a strong phase consistency between subjects (N = 25). Our findings provide causal evidence for fluctuations in temporal perception and indicate an involvement of occipital alpha oscillations.

2.2 Introduction

It has been suggested that perception may be a periodic process (VanRullen, 2016). The detection probability of near-threshold stimuli has been shown to oscillate between 5 and 15 Hz in vision (Busch et al., 2009). Reaction times are governed by similar periodic fluctuations in the 10 Hz range (Callaway & Yeager, 1960; Başar, Başar-Eroglu, Karakaş, & Schürmann, 2001). While it was theorized that the endogenous alpha oscillations of the brain might give rise to these periodicities, their functional relevance is an ongoing enigma. One possible functional role for these neural rhythms is that of a periodic sampling mechanism (VanRullen & Koch, 2003; Busch et al., 2009; Lőrincz et al., 2009; Haegens et al., 2011; Vijayan & Kopell, 2012; Samaha & Postle, 2015; VanRullen, 2016): in order to reduce the complexity of the visual stream, the brain is repeatedly dividing the incoming visual information into temporal chunks or windows; these chunks are then passed on for further processing and subsequently made consciously available. Few studies have explicitly tested the periodicity of temporal perception (and thus, the more conservative or "hard"

definition of discrete perception). Samaha and Postle demonstrated that the individual alpha peak frequency is predictive of the performance in the two-flash-fusion paradigm (Samaha & Postle, 2015). Opposite phases of the alpha rhythm are related to perception of synchronicity and a-synchronicity, respectively (Valera et al., 1981; Milton & Pleydell-Pearce, 2016). Of high importance for this study are the findings by Chakravarthi and VanRullen (2012), relating the perceived flash lag duration to the phase of endogenous alpha oscillations using EEG.

In this study we were interested in providing causal evidence for a periodic modulation of time perception. To our knowledge only one study has succeeded in this so far. In a recent publication by Ronconi et al. (2018) it was shown that visuo-auditory entrainment at the individuals alpha frequency + or -2 Hz was able to modulate the integration or segregation of two stimuli in close temporal proximity. In this study we seek to provide an important addition to these findings by demonstrating a causal influence of alpha on the perception of time, using a well investigated visual illusion, the flash lag effect (FLE).

Discrete sampling in the visual system has previously been hypothesized to underlie the FLE (Chakravarthi & Vanrullen, 2012; Schneider, 2018). In the FLE a stationary object is shortly presented ("flashed") alongside a moving object. Although the position of both objects is identical at the onset of the flashed, stationary object, observers systematically judge the flashed object to be lagging behind (Figure 1A). In the past years a new hypothesis regarding the FLE has been suggested, most prominently by Schneider (2018). He suggests that the FLE and other related illusions are a natural result of a discrete periodic sampling process. The theory states that visual information is collected over the time course of a so called "perceptual moment." While information is collected continuously, the position of the object is registered only at the end of the perceptual moment and at its last known position. We can imagine a scenario where the static object is flashed right at the beginning of the perceptual moment (Figure 1A). The moving object would then move on for a specific period, until the end of the perceptual moment, at which the position of both objects is registered. In case A the perceived offset between moving and static object would be maximal. On the contrary, if the static object is flashed right at the end of the perceptual moment, the moving object would not move any further before the positions are registered, and the perceived offset would be

minimal (Figure 1B). Based on the findings that the average perceived FLE is around 50 ms, with a standard deviation of 50 ms, the duration of a perceptual moment should be around 100 ms, which was verified by Schneider who investigated a large FLE dataset by Murakami (2001).

In this account, whether a long (Figure 1A) or short (Figure 1B) flash-lag illusion occurs on a given trial is mainly determined by the phase of the discrete sampling cycle at the moment of the flash onset. As this phase is generally unknown to the experimenter, the trial-to-trial variability in the illusion strength is often interpreted as noise. Some studies, however, have directly measured this phase with EEG, and verified that it influenced the flash-lag magnitude (Chakravarthi & Vanrullen, 2012). Here, our aim was to causally modulate the phase of the discrete sampling cycle by modulating the luminance of an annulus that surrounded a clock stimulus, and to prove that this phase had a causal influence on the flash-lag illusion. The FLE was randomly probed at 120 consecutive time points over the course of the entrainment (Figure 2). A frequency analysis of the average time course revealed a modulation of the perceived FLE duration at 10 Hz. We conclude that the visual stimulus entrained the discrete neural sampling mechanism, leading to a periodic modulation of the FLE.

2.3 Materials and Methods

2.3.1 Participants

Twenty five participants (aged 18–30, 13 females) with normal or corrected to normal vision participated in the experiment. Informed consent forms were signed before the experiment. The experiment was carried out in accordance with the protocol approved by the Centre National de la Recherché Scientifique ethical committee and followed the Code of Ethics of the World Medical Association (Declaration of Helsinki).

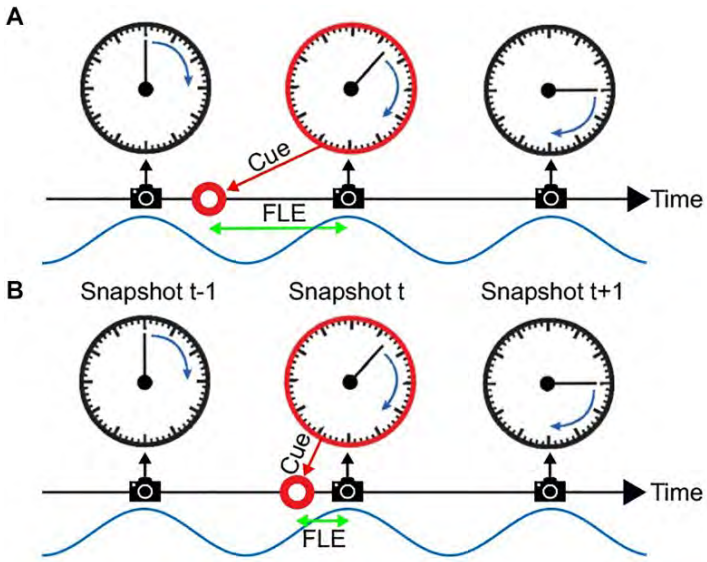

Figure 1. *The flash lag illusion as a consequence of discrete sampling.* Following the hypothesis of Schneider (2018), the visual system samples the visual scene, here a clock with rotating clock hand, during reoccurring intervals ("perceptual moments," indicated by spaces between camera symbols). The end of these perceptual moments or "snapshots" (camera symbols) marks the registration of the stimulus position [the orientation of the clock hand and the flashed cue (red circle)]. The stimuli are registered at the last known position. This is always the correct position for the clock hand, since it is moving at a fixed speed and constantly updated, but not for the transient red cue since the presentation dates back in time, and instantaneous updating cannot occur. Hence, a systematic lag of the red cue is perceived, its magnitude depending on the relative onset between cue and snapshot (camera symbol). In Panel A the red cue is presented very early in the perceptual moment. The temporal distance between the cue presentation and the end of the snapshot is large, leading to a long perceived flash lag. In Panel B the red cue is presented very shortly before the end of the perceptual moment. A short amount of time passes until the stimulus position is registered, and the perceived flash lag is brief.

2.3.2 Protocol

Stimuli were presented at a distance of 57 cm with a LCD display (1920 × 1080 resolution, 120 Hz refresh rate) using the Psychophysics Toolbox (Brainard, 1997) running in MATLAB (MathWorks). Stimuli consisted of a central fixation dot (diameter = 0.3˚), a central clock stimulus (radius = 2˚) with a black border (width = 0.3˚), 60 evenly spaced clock markers (12 with length = 0.4˚,

48 with length = 0.3°) and a rotating clock hand (length = 0.7°). The gap between the clock hand and the clock border was 1.3° and between clock hand and long clock marker 0.9°. The entrainer annulus and the clock hand were separated by 1.5°. The clock was surrounded by an entrainer annulus (outer radius = 11.5°, inner radius = 3.5°). Stimuli were presented on a gray background.

Trials started with the fixation point on the screen (Figure 2A). Participants initiated the trial via button press. Directly after the button press the entrainer annulus as well as the clock stimulus appeared on the screen with the clock hand rotating with 1 rotation/s. The luminance of the entrainer annulus was modulated sinusoidally at 10 Hz with the luminance ranging from 0 to 255 (0.68 to 100.8 cd/m2). At a random time point between 1000 and 2000 ms (SOA window) a cue was presented (the frame of the clock stimulus turned red) for 66 ms (eight frames). Afterward the clock hand continued rotating until the 3000 ms mark was reached. After a delay of 1000 ms an identical clock with a static hand was presented. The participant could rotate the clock hand with the arrow keys to indicate the perceived location of the clock hand at the time point of Cue onset. The Cue onset was randomly chosen from a discrete uniform distribution of the 120 SOAs between 1000 and 2000 ms. Participants each performed 480 trials resulting in 4 responses per SOA. Participants were instructed to maintain central fixation during the 3 s window when the clock was on the screen. The starting position of the clock hand was randomized between subjects but was kept constant for a single subject.

2.3.3 Control Experiment

We conducted a control experiment to verify that the observed modulation was due to neural entrainment and not simply due to the luminance of the annulus. A new set of participants (N = 25) conducted a similar experiment where the luminance of the annulus was kept constant throughout the trial. Instead of testing all 7 luminance values we tested the most extremes ones (black and white) as well as 50% luminance (gray) at which the annulus is indistinguishable from the background. In the original experiment 40 trials were collected for each of the two extreme luminance values and 80 trials for the 50% luminance per participant. In the control experiment we collected 40 trials for each of the three luminance values resulting in 120 trials per subject. To compare the perceived FLE between the luminance values a one-way-ANOVA was conducted.

2.3.4 Data Analysis

Attributing one SOA (frame 1 to frame 120) to every position of the clock hand we can define the FLE duration as the temporal distance (in frames) between the actual onset of the Cue (position of the clock hand when clock border turns red) and the orientation of the clock hand that the participant indicated. Note that we define SOA as the temporal distance to the onset of the central 1 s window, within which the Cue could appear. We restricted our analysis on responses that were within 3.5 times the standard deviation of each individual participant (mean: 290.2 ms, SEM: ±22.3 ms) before or after the actual Cue onset. Single trial responses were averaged over the respective SOA (4 per SOA, 120 SOAs). The resulting time course represents the average FLE as a function of time for one individual. The individual time course was then down-sampled from 120 to 60 Hz. To eliminate effects of the position of the clock hand on the flash lag illusion, we fitted a 1 Hz sinus function and subtracted it from the individual time course. The frequency of the fit was determined by assuming that any effects stemming from the clock hand position should influence the flash lag illusion at a frequency identical to the revolution frequency 1 Hz. We then normalized the data by applying a moving z-score window of length 116 ms. A 116 ms window (7 SOAs) of the original data was z-scored and the central value was saved in a separate array. The window was then shifted by 16 ms (1 SOA) and the process was repeated resulting in one normalized time course per subject. We validated in a separate re-analysis that the length of the window did not affect our findings. Window lengths of 60 ms up to 208 ms lead to comparable modulations at 10 Hz.

Individual time courses were then averaged and analyzed in the frequency domain using FFT. 60 SOAs at 60 Hz allowed for a Nyquist frequency of 30 Hz. Only frequencies from 1 Hz to 2/3 of the Nyquist frequency (1 to 20 Hz, 20 values) were considered. The complex FFT coefficients were squared to obtain oscillatory power at each frequency. To statistically test if the power at 10 Hz is significant we calculated 5000 surrogates by shuffling the SOA-labels between trials, and repeating all analysis steps for each surrogate as explained above (60 Hz down-sampling, 1 Hz detrending, normalization). The original power spectrum was then compared to the surrogate distribution and p-values were corrected for multiple comparisons using the False Discovery Rate. Individual Phase angles were extracted from the 10 Hz component of the FFT of the down-

sampled and normalized time-courses. Rayleigh's test for non-uniformity was used to statistically test if individual phases were significantly coherent.

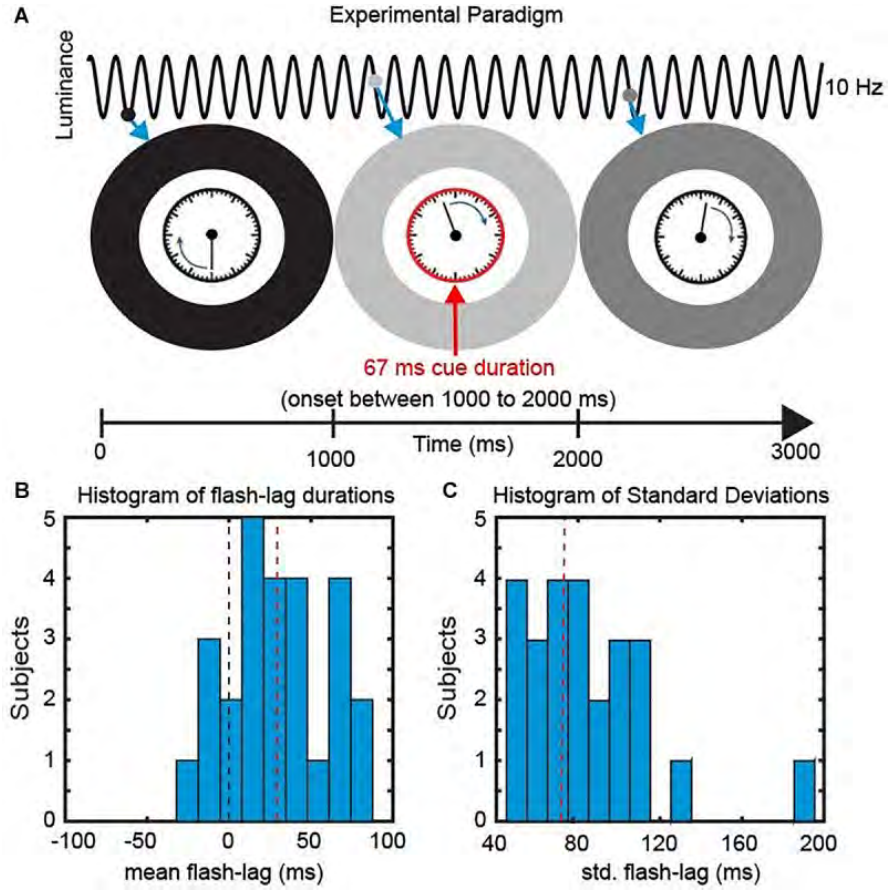

Figure 2. *Experimental Paradigm.* **(A)** We presented a clock consisting of a static frame and a rotating clock hand for 3000 ms. The clock hand was rotating at one revolution per second and was surrounded by an entrainer annulus that periodically changed its luminance (from white to black) with a frequency of 10 Hz. At a random time point, within the central 1000 ms, a cue was presented in the form of the clock frame flashing red for 67 ms. Subsequently Participants reported the orientation of the clock hand at the onset of the cue. **(B)** Behavioral Data. The mean perceived FLE duration was 32.4 ms (SEM across subjects: 6.48 ms). **(C)** The mean std. across trials was 75.4 ms (SEM across subjects: 6.42 ms).

2.4 Results

In the current study, we investigated the causal influence of a periodic entrainer on the perceived FLE duration. We presented participants with a clock stimulus containing a clock hand revolving at 1 Hz. The clock stimulus was surrounded by an entrainer annulus that changed its luminance from black to white periodically (following a sine function) at 10 Hz. At random SOAs we presented a cue by turning the frame of the clock red. Participants were then instructed to indicate the position of the clock hand at the onset of the Cue.

The mean FLE duration (misperception in milliseconds) across observers was 32.4 ms (±6.48 ms, SEM) (Figure 2B). Across trials the perceived FLE had an average standard deviation of 75.4 ms (±6.42 ms, SEM across subjects) (Figure 2C). Large standard deviations have been previously reported and have been shown to be unaffected by low level stimulus features (Linares et al., 2009; Chakravarthi and VanRullen, 2012). We were specifically interested in explaining this variability over trials in the context of a discrete sampling framework.

2.4.1 Visual Entrainment Modulates the Perceived FLE

In order to verify an effect of the visual entrainment on the perceived FLE we calculated the average FLE time-series over individuals across the 120 SOAs. The original FLE time-series were down-sampled from 120 to 60 Hz, de-trended by subtracting the 1 Hz Fourier component and normalized using a moving z-score, before averaging (window length 116 ms. See "Materials and Methods" section). Initial inspection of the time course (Figures 3A,B) indicates a strong oscillatory component, coupled with the background luminance modulation, in the 10 Hz range. To quantify this, we performed a frequency analysis on the preprocessed FL time-series. The resulting power spectrum revealed a dominant oscillation at 10 Hz (Figure 3C). To statistically test the significance of this peak we created 10.000 surrogates by shuffling the 120 SOA-bin labels within subjects and recalculating the power spectrum. P-values were computed as the percentile of the mean power values within the bootstrapping distribution. This allowed us to test the null-hypothesis that the power spectrum of the average FLE time course does not show a peak at a specific frequency. All preprocessing steps were kept identical for the surrogates. The FLE time course oscillatory power at 10 Hz was significantly higher compared to the surrogate distribution

(Figure 3C, p = 0.028, FDR corrected). Further peaks at 2 Hz as well as 4 Hz were significantly higher than the surrogate distribution. These oscillatory components might reflect slower attentional or strategic effects that have been shown to influence performance at low frequencies (Wyart et al., 2012). As we only manipulated the 10 Hz component via flicker stimulation, we elected to focus on this component.

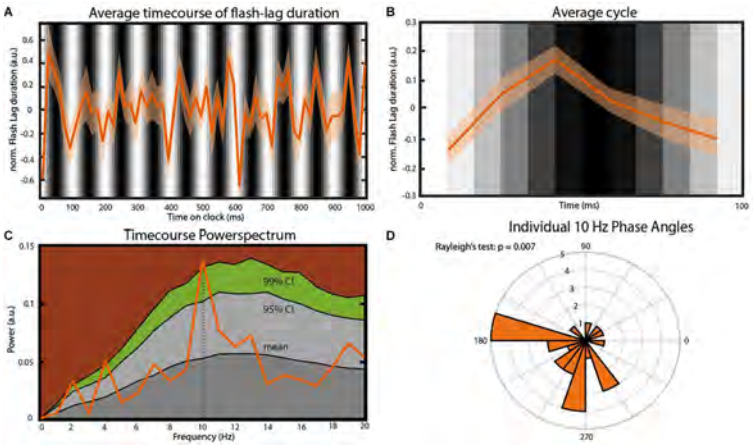

Figure 3. *Main findings.* **(A)** Average time course of FLE (N = 25). Before averaging the individual time courses were down-sampled from 120 to 60 Hz, detrended by subtracting the 1 Hz Fourier component and normalized using a moving z-score (window length 116 ms. See "Materials and Methods" section). The gray bars in the background indicate the luminance of the entrainer annulus at the moment of cue presentation. Transparent area shows the inter-subject SEM for the respective time point. **(B)** Average cycle of the oscillation observed in **(A)**. Background Gray-scale bars indicate the luminance of the annulus at cue onset. Note that due to the down-sampling of the time course the six points of this average cycle always fall between two consecutive luminance bars. **(C)** power spectrum of the average FLE time-course. The peak at 10 Hz was statistically compared to a surrogate distribution (10.000 surrogates) and was significant after correcting for multiple comparisons (p = 0.004, FDR-corrected: p = 0.028). Colored areas: Dark gray, mean of the surrogate distribution; Light gray, 95% confidence interval; Green, 99% confidence interval; Brown, >99% confidence interval. **(D)** Rose plot of the 10 Hz phases angles of individual FLE time-courses. The Rayleigh's test of non-uniformity reveals a significant phase coherence between individual 10 Hz phases (p = 0.007).

We also analyzed the phase-consistency of the 10 Hz oscillation across subjects. The complex FFT coefficients at 10 Hz were extracted to calculate individual phase angles. We then compared these angles using Rayleigh's test for

non-uniformity testing the null hypothesis that the phase angles are randomly distributed. Phase angles were significantly clustered (Figure 3D, $p < 0.05$).

2.4.2 Control for Annulus Luminance

Figures 3A,B show that bright luminance values tend to induce lower FLE values compared to dark luminance values. In accordance with our hypothesis, we interpret this effect as a result of the entrainment of the discrete sampling mechanism to the rhythmic luminance modulation. However, an alternative interpretation could be that the luminance of the background (even when it is not rhythmically modulated) has an effect on FLE. In order to control for the possible confound that the modulation in perceived FLE was caused merely by the luminance values of the annulus rather than neural entrainment caused by the dynamics of the stimulus, we conducted a control experiment (N = 25). The experimental parameters were kept identical to the dynamic entrainment condition with the exception of the annulus, which had a static luminance of 0% (black), 50% (gray) or 100% (white) throughout the trial. We statistically compared the perceived FLE in the three static luminance conditions using a one-way ANOVA (Figure 4). No significant difference in perceived FLE was observed between luminance conditions [$F(2,2955) = 1.616$, $p = 0.19$]. We conclude that the luminance of the entrainer is not the main factor that explains the observed FLE modulation in the main experiment. Instead, it is likely that the rhythmic modulation of this luminance played a key role via rhythmic entrainment, in line with our hypothesis.

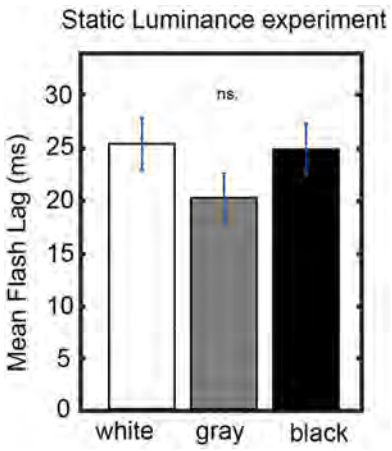

Figure 4. *Control experiment.* Static luminance annuli were used to measure the effect of background luminance on the perceived FLE. The task paradigm was kept constant to that of the main experiment with the exception of the static annulus luminance. We did not find a significant effect of annulus luminance on the perceived FLE between any luminance conditions (one-way ANOVA, $F(2,1977) = 0.02$, $p = 0.98$).

2.5 Discussion

In this study we tested the causal influence of a visual entrainer at 10 Hz on the flash lag illusion. We found that the perceived FLE duration was periodically modulated at the entrainer frequency of 10 Hz and that these oscillations in the individual FLE time-series were strongly phase coherent between subjects. The oscillatory fluctuation in the perceived temporal offset between the moving and flashed object in the flash lag illusion is a direct demonstration of a rhythmic modulation of time perception. Our findings therefore provide strong causal evidence for the "hard" theory of discrete perception.

Our experiment was based on the discrete sampling hypothesis of perception (Valera et al., 1981; VanRullen & Koch, 2003; Busch et al., 2009; Lőrincz et al., 2009; Haegens et al., 2011; Vijayan & Kopell, 2012; Samaha & Postle, 2015; VanRullen, 2016), which claims that the visual system periodically divides incoming visual information in discrete chunks. In the context of the flash lag illusion, visual information is assumed to be periodically collected over the course of a fixed time frame, sometimes called a "perceptual moment," at the end of which the last known positions of the objects are registered (Schneider, 2018). If two objects are presented, one static and flashed and another moving continuously, a systematic offset between real and registered position is introduced, depending on the relative timing between presentation of the static object and the end of the perceptual moment (Figure 1).

The idea of a discrete sampling mechanism in vision affecting temporal perception has enjoyed a recent upswing in interest. Most recently it was shown that audio-visual entrainment at a participant's individual alpha frequency influences performance in a visual integration/segregation task (Ronconi et al., 2018). Similarly, the phase of alpha oscillations can predict performance in a synchronous/asynchronous task (Valera et al., 1981; Milton & Pleydell-Pearce, 2016). Furthermore the frequency of individual alpha oscillations has been related to the participant's two-flash fusion threshold, suggesting that visual systems with faster alpha rhythm sample the visual scene more frequently (Samaha & Postle, 2015). The above findings forward the existence of a certain integration window in the visual system within which information is merged. The fact that these windows can be dynamically modulated by rhythmic stimulation in psychophysical experiments as well as the correlational evidence provided by

electrophysiological measurements hint at a neuro-oscillatory origin in the 8 to 12 Hz range, the alpha rhythm. Our findings fit well in this context, by providing causal evidence that a prominent temporal perceptual illusion can be dynamically modulated under the assumption of this discrete sampling mechanism.

What is the physiological explanation for our findings? The phase of alpha oscillations has been shown to be predictive of cortical excitability (Busch et al., 2009; Dugué et al., 2011), of neuronal firing rates (Lőrincz et al., 2009; Haegens et al., 2011; Vijayan & Kopell, 2012) as well as of the amplitude of gamma oscillations (Osipova, Hermes, & Jensen, 2008; Voytek et al., 2010). As these neural signatures have been frequently implicated in neuronal processing it seems therefore logical that visual processing is concentrated on specific reoccurring intervals. The brain might use these naturally occurring periodicities, in the form of oscillations, to reduce the complexity of incoming information by compressing it into discrete packages. This compression might come at the cost of a reduced temporal resolution, leading to systematic errors in the perceived timing of stimuli as shown in this study (Schneider, 2018).

While our experimental paradigm was successful in eliciting the flash lag illusion, the mean perceived lag (32.4 ms) and the variation within participants (mean std: 75.4 ms) was different compared to some previous studies (Eagleman & Sejnowski, 2000; Murakami, 2001; Kerzel, 2010; Schneider, 2018). We attribute this discrepancy mainly to the paradigm that was applied in this experiment. Previous experiments have typically used only two visible stimuli to assess the FLE. In our paradigm multiple reference objects (i.e., minute markers) are on the screen that may aid the correct localization of the stimuli. An almost identical paradigm using the same clock stimulus was used by Chakravarthi and VanRullen (2012) and a similar mean FLE (27 ms) was observed, supporting this account. The mean std. across trials found here is somewhat closer to what has previously been reported. We think that the increase in variability might be a result of the highly dynamic entrainer annulus which might have had a distracting effect on attention. Without further experiments, however, we will not be able to explain these discrepancies fully. In the future it could be helpful to use individual EEG recordings to tailor flicker stimulation parameters for single individuals.

Two important questions remain unanswered by our findings. First of all we only tested one specific frequency for the visual entrainment. While the alpha band has been previously related to the flash lag illusion (Chakravarthi & Vanrullen, 2012) and visual entrainment seems to be most effective at the brains endogenous alpha frequency (Herrmann, 2001), we cannot exclude the possibility that entrainment at a different frequency could lead to a similar modulation of the FLE (see also: Keitel et al., 2014). In order to address this question, this experiment should be repeated in the future, using different frequencies for entrainment. Second, it is unclear if a periodicity of the entraining stimulus is necessary. In our case it is unlikely but imaginable that transient annuli of white (or black) could be interpreted as single events by the brain, and lead to a subsequent dynamic modulation of the FLE. If this FLE modulation by each white (or black) transient was fast enough, this would become apparent as a 10 Hz oscillation in our FLE time-series. Unfortunately the two possibilities are close to impossible to disentangle, because single impulses, visual or applied with TMS, are often sufficient to elicit alpha oscillations as measured by EEG, and in turn would rhythmically influence the perceived FLE, which would also be consistent with our theory (VanRullen & Macdonald, 2012; Herring et al., 2015).

Last we would like to mention that the idea of discrete perception is not entirely undisputed (Fekete, Van de Cruys, Ekroll, & van Leeuwen, 2018; White, 2018). While our findings indicate an involvement of the occipital 10 Hz rhythm, the range of frequencies at which perception was found to fluctuate varies between studies (White, 2018). Additionally, the effect of alpha phase on perception is not found systematically, e.g., in one study it was reported only when alpha power was high (Mathewson et al., 2009). Furthermore the reported effects of phase are often very small, which makes it difficult to convincingly conclude that perception is subject to discrete frames (Milton & Pleydell-Pearce, 2016). We hope that our findings contribute to resolve these mysteries.

2.6 Conclusion

In this study, we successfully demonstrated that visual entrainment at 10 Hz leads to a periodic modulation of the FLE at an identical frequency. Furthermore this modulation was evident in most subjects, demonstrated by a strong inter-individual phase coherence of the individual FLE time courses. Our find-

ings cannot be explained by static luminance states of the entrainer annulus, which we verified in a separate control experiment. In conclusion, we were able to provide causal evidence for the existence of a discrete sampling process in the visual system that gives rise to the flash lag illusion and can be dynamically modulated using visual entrainment. Our findings are in support of a "hard" version of discrete perception (whereby oscillations modulate not only sensory excitability, but also time perception), and hint at an involvement of the endogenous alpha rhythm of the brain.

Getting closer to the source: From rhythmic visual stimulation to direct magnetic entrainment.

Visual Entrainment is efficient and easy to implement experimentally. While it clearly influences the alpha rhythm, it comes with intrinsic limitations. The occipital cortex serves many more functions than complexity reduction in time. It is impossible for us to control or measure all of the processes that get initiated when we present our entrainment sequences. We can therefore not unequivocally attribute our observations of perception to the changes in the alpha rhythm as compared to all other potentially influenced processes. We need a way to influence the alpha rhythm at it's source with the recruitment of as few other visual processes, like memory or attention, as possible.

In our previous study we presented our perceptual probes during ongoing visual entrainment. This makes it potentially more likely that we probe secondary perceptual processes, directly following the entrainer, that are not intrinsically linked to the alpha rhythm. True entrainment is often required to be demonstrated as oscillatory activity that outlasts the entrainment period. Presenting stimuli outside of the actual entraiment window will therefore strengthen our confidence in an actual causal relationship to the alpha rhythm.

In the following study we addressed, among other things, both of these problems in a TMS-entrainment study.

Chapter 3

Occipital Alpha-TMS causally modulates Temporal Order Judgements

The following chapter contains the original manuscript that appeared as: Chota, Samson, Rufin VanRullen, and Phillipe Marque. "Occipital Alpha-TMS causally modulates Temporal Order Judgements: Evidence for discrete temporal windows in vision." bioRxiv (2020).

3.1 Abstract

Recent advances in neuroscience have challenged the view of conscious visual perception as a continuous process. Behavioral performance, reaction times and some visual illusions all undergo periodic fluctuations that can be traced back to oscillatory activity in the brain. These findings have given rise to the idea of a discrete sampling mechanism in the visual system. In this study we seek to investigate the causal relationship between occipital alpha oscillations and Temporal Order Judgements using neural entrainment via rhythmic TMS. We find that certain phases of the entrained oscillation facilitate temporal order perception of two visual stimuli, whereas others hinder it. Our findings support the idea that the visual system periodically compresses information into discrete packages within which temporal order information is lost.

3.2 Introduction

A large body of literature investigates the effects of alpha amplitude on perception, linking high alpha power to high inhibition. More specifically, alpha power has been shown to increase in task irrelevant areas, whereas it decreases in task relevant areas, demonstrating its role in spatial attention (Sauseng et al., 2005; Kelly et al., 2006; Foxe & Snyder, 2011). Alpha oscillations play an even more dynamic role in the context of temporal attention, decreasing/increasing its amplitude at the moment when a target/distractor is expected (Rohenkohl & Nobre, 2011; van Diepen et al., 2015). On an even finer temporal scale we find that the phase of ongoing oscillations in the 5-15 Hz range influences perception. Busch et al. and Mathewson et al. (2009) demonstrated that the phase of occipital alpha oscillations is predictive of stimulus detection performance, implying that excitability in the visual cortex oscillates at around 7-10 Hz (Busch et al., 2009; Mathewson et al., 2009). These findings have been replicated several times using rhythmic entrainment at 10 Hz via periodic visual stimuli or alpha-TMS (Mathewson et al., 2010; Romei et al., 2010; Thut et al., 2011; Spaak et al., 2014; Dugué & VanRullen, 2017). Interestingly the ongoing fluctuations of the occipital alpha cycle also influence temporal perception periodically, giving rise to the idea that alpha implements discrete perceptual windows in vision, vaguely similar to the frames of a camera.

More precisely the idea of a strictly discrete sampling mechanism (or "hard"

version of discrete temporal perception (DTP)) states that the brain periodically divides the visual input into discrete windows or "perceptual moments" (VanRullen & Koch, 2003; Busch et al., 2009; Lőrincz et al., 2009; Haegens et al., 2011; Vijayan & Kopell, 2012; Samaha & Postle, 2015). Hypothetically two stimuli that fall within one perceptual moment are perceived as occurring together whereas two stimuli falling in separate moments are perceived as occurring in succession. Recently the idea has gained renewed support by psychophysiological and electrophysiological studies linking it more directly to the occipital alpha rhythm (VanRullen, 2016). It was shown that participant's individual alpha peak frequencies are predictive of performance in a two-flash fusion task (Samaha & Postle, 2015). Following these lines it was demonstrated that visuoauditory entrainment at the individual alpha frequency ± 2 Hz could facilitate or impair performance in a temporal segregation/integration task (Ronconi et al., 2018). Further evidence comes from studies investigating the flash-lag effect (FLE), a visual illusion that has been suggested to arise from discrete sampling in the visual system (Chakravarthi & Vanrullen, 2012; Schneider, 2018). We demonstrated that visual entrainment at 10 Hz leads to a periodic modulation of temporal perception in the FLE (Chota & VanRullen, 2019). Given that alpha cycles most likely modulate cortical excitability it is critical to separate the effects of visibility fluctuations from the effects of discrete windows on time perception. The former can be thought of as a "soft" version of DTP, giving rise to fluctuations solely due to differences in excitability/visibility i.e. by suppressing one of two stimuli and therefore indirectly biasing relative timing perception. The latter can be thought of as a stricter "hard version" of DTP, implemented by discrete perceptual windows. A key aspect in the studies described above (Chakravarthi & Vanrullen, 2012; Ronconi et al., 2018; Chota & VanRullen, 2019) is that there is not only a fluctuation of perception (detection probabilities, perceived intensities), which is predicted by the soft version of DTP, but also a fluctuation of time perception itself (relative timing, temporal integration/segregation) which is the key prediction of the hard version of DTP. Building on top of the previous findings we set out to causally link the "hard" version of DTP closely to the occipital alpha rhythm as well as to separate observed effects from "soft" modulations of excitability. We tested this hypothesis causally by utilizing TMS to manipulate the occipital alpha rhythm and probed temporal order judgments (TOJ) at different phases of the entrained oscillation.

3.3 Materials and Methods

3.3.1 Participants

25 participants (aged 18-31, 9 females) with normal or corrected to normal vision enrolled in the experiment. 7 participants had to be excluded during the first phosphene localization session because of their inability to see TMS-induced phosphenes, leaving 18 participants for the complete experiment and the final analysis. Note that this number of subjects excluded for this reason is very common in the TMS literature. Dropout rates of 40% due to inability to perceive phosphenes (at medial stimulation intensities) are commonly reported. Informed consent forms were signed before the experiment. The experiment was carried out in accordance with the protocol approved by the Centre National de la Recherche Scientifique ethical committee and followed the Code of Ethics of the World Medical Association (Declaration of Helsinki).

3.3.2 TMS apparatus, parameters and phosphene localization

The TMS stimulation was performed using a Magstim Rapid2 stimulator of 3.5 tesla, producing a biphasic current. At the beginning of the first session participants were tested on their ability to detect TMS-induced phosphenes. TMS stimulation was initiated at 55% of the maximum stimulator output applying 7 pulses at 20 Hz over occipital cortex. At the beginning of each phosphene localization trial participants were asked to fixate a central cross. Participants closed their eyes without changing the direction of their gaze. TMS was applied, participants opened their eyes and used the mouse to draw the outline and location of the perceived phosphene onto the screen. If no phosphene was perceived the coil position or stimulation intensity were changed manually and the procedure was repeated. When a reliable phosphene was found the coil was fixated using an armed pedestal. We successfully elicited phosphenes in 18 out of 25 subject in the right (N = 9) or left (N = 9) visual field (Figure 1). Later, we used the phosphene location to place stimuli and scale them according to the cortical magnification factor (see section Stimuli below). Using a two-down one-up staircase procedure, we then determined the individual phosphene perception intensity threshold. Mean phosphene perception intensity threshold was 54.3% of maximum stimulator output. During the experimental TMS sessions we adjusted the TMS intensity to 75% of the individual phosphene perception

intensity threshold (no subject reported perceiving a phosphene during the test trials).

3.3.3 Stimuli

Stimuli were presented at a distance of 57 cm with a LCD display (1920 x 1080 resolution, 120 Hz refresh rate) using the Psychophysics Toolbox (Brainard, 1997) running in MATLAB (MathWorks). Stimuli consisted of a central fixation cross (diameter = 0.3˚), a square placeholder (black, 4˚*4˚), Gabor patches (Stim A and Stim B) of two orientations (45˚ and 135˚, diameter = 3˚, spatial frequency = 1.076 cycles/degree) as well as a mask in the form of a plaid (diameter = 3˚), (Figure 2A). We included a masking stimulus in order to prevent subjects from using the persistence or the afterimage of Stimulus B to solve the TOJ task. Stimulus A will always be referring to the first stimulus of the sequence, whereas Stimulus B or "target" will be referring to the second stimulus of the sequence, irrespective of their orientation. During the task Stimulus A and B were presented in quick succession and participants gave Temporal Order Judgements by identifying the orientation of stimulus B. Additionally we included a single stimulus condition where only one stimulus (Stimulus A or Stimulus B) was presented. Participants reported these trials using a third button. The single stimulus condition was included in order to control for the possibility that TMS entrainment could lead to a significant decrease in stimulus visibility for one of the two stimuli (A or B). In that case we would expect an increase in single stimulus reports. We will show later in the behavioral results that this was not the case.

The experiment consisted of a training condition and a TMS condition. We included a rather extensive training session in order to minimize any potential practice effects that could influence our TMS sessions and to reduce potential biases towards stimulus visibility, as we will explain later. The training condition was run with the parameters described above. The location of placeholder and stimulus sequence was fixed in the lower right or left visual field with equal probability (eccentricity 7˚). The stimulus parameters in the TMS condition were identical to the training condition except for the size and position of the stimuli and placeholder which were adjusted based on the phosphene location acquired during the phosphene localization described in the previous paragraph. The location of the stimuli was chosen to be within the reported phosphene area,

and as close to the position of the training stimuli as possible (Figure 1). This ensured that stimuli in the TMS condition were not presented further than 7° visual angle from the position of the training stimuli in 96% of trials to keep training and TMS conditions comparable. The stimuli were scaled based on their eccentricity according to cortical magnification (Horton and Hoyt, 1991) in order to match the cortical representation of the stimulus to the actual cortical stimulation site during TMS. For example, the stimulus diameter measured 3° at 7° eccentricity and 3.78° at 10° of eccentricity. The contralateral stimulus position was determined by flipping the ipsilateral position around the central y-axis. Left and right stimulus trials were matched pseudo-randomly. Stimuli were presented on a gray background.

We modulated the contrast of our stimuli in a subset of trials. This was done for two reasons. First of all, it allowed us to control for the potential effects of TMS on the visibility of the stimuli. We hypothesized that any detrimental effects of TMS on visibility should be maximal when target contrast is minimal. More specifically, this potential confound should manifest as a reduction in performance for stimuli that were presented on the hemisphere contra-lateral to TMS, with high contrast stimuli being least and low contrast stimuli being most affected. As we will show later in the Results section, this was not the case. Second, by having stimuli vary in contrast, we aimed to discourage participants from basing their TOJ judgments on visibility (e.g. always judging the most visible stimulus as occurring first or last), by making stimulus visibility inconsistent across trials while at the same time providing feedback. Therefore, even if the entrainment oscillatory phase should affect visibility, participants are actively encouraged to neglect visibility cues and base their decision purely on the perceived temporal order. For this second reason we decided to include several intermediate contrast conditions to better simulate perceptual ambiguity and increase the sense of unreliability of stimulus visibility. 5 Contrast conditions were used (Figure 2C): Normal (100% contrast for A and B), low contrast 10% (Stimulus A: 90% contrast, Stimulus B: 10% contrast), low contrast 90% (Stimulus A: 10% contrast, Stimulus B: 90% contrast), low contrast 25% (Stimulus A: 75% contrast, Stimulus B: 25% contrast), low contrast 75% (Stimulus A: 25% contrast, Stimulus B: 75% contrast). Condition names (e.g. low contrast 75%) refer to the contrast value of the second stimulus of the sequence (Orientation of Stimulus B which had to be identified in the TOJ task) and will be used for later reference. Low percentage values represent low contrast

or small difference to background luminance. The percentage values represent the Michelson contrast, defined as the ratio between the minimal/maximal luminance value of the stimulus and the gray background ((max. Luminance – min. Luminance)/(max. Luminance + min. Luminance)).

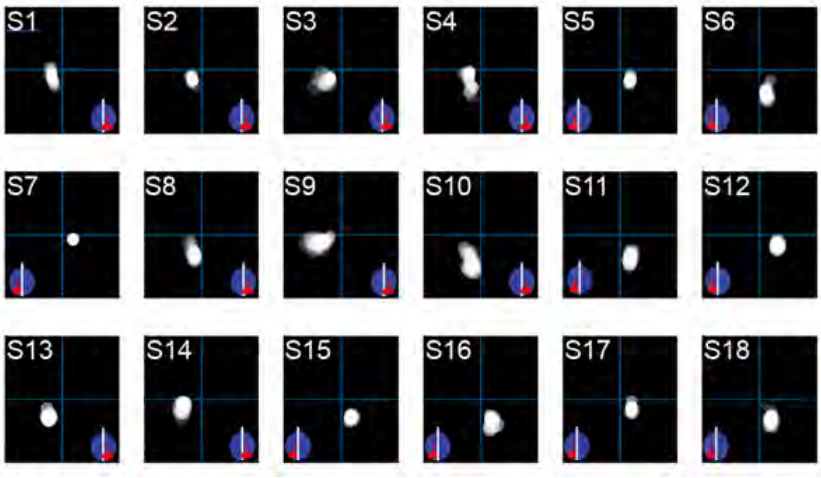

Figure 1. *Stimulus locations for all subjects.* The stimulus locations during the TMS blocks were determined during the phosphene localization. Participants had their eyes closed and received 7 TMS pulses at 20 Hz either over left or right occipital cortex. The red coil symbol over the blue head inset indicates the hemisphere of stimulation. The mouse was used by the subject to draw the outline of the perceived phosphene on the screen. Stimuli (here represented as superimposed white disks) were positioned inside the phosphene regions and scaled according to the cortical magnification factor (Horton and Hoyt, 1991). Note that due to slight changes in head position, the location of the phosphenes could change during the experiment. We re-localized phosphenes and adjusted the stimulus position at the beginning of every block.

3.3.4 Experimental Protocol

On the first session only, participants performed an extensive pre-training consisting of 12 Training Blocks (23 trials each). Training blocks were identical to the TMS blocks with few exceptions. No TMS-pulses were applied during training and the placeholder as well as sequence presentation was in the lower right or left (equally balanced) visual field. Participants received positive or negative feedback in the form of the fixation cross turning green or red. One goal of the Training Blocks was to prevent participants from basing their TOJ judgements

on the visibility of stimuli by making the contrast maximally uninformative as described above. Furthermore, it served to keep performance on a steady level by providing frequent feedback to the participant. In the training blocks 44.3% of trials were low contrast trials, 22.3% were single stimulus trials and 33.3% were normal contrast trials.

Afterwards subjects performed the main experimental procedure, which was repeated on session 2 and session 3. In the main experimental procedure participants performed 19 blocks (15 TMS blocks, 5 Training blocks) with 23 trials per block (In the last TMS block only 20 trials were collected). 3 TMS blocks were interleaved with 1 Training Block. Over the course of 3 sessions this resulted in 1035 trials in the TMS and 345 trials in the training condition per subject (50% trials contralateral to TMS, 50% trials ipsilateral to TMS). Per SOA and per visual field 57 trials were collected. Before each of the 45 TMS blocks participants performed a phosphene localization to make sure that the coil position had not changed and the correct cortical area was stimulated. Trials started with the central fixation cross and the placeholder on either side of the screen (Figure 2 A). The placeholder served as a cue to indicate location of the stimulus sequence with 100% cue validity. This served to avoid potential attentional confounds by always directing attention to the precise location of the upcoming stimuli. Participants initiated the trial via button press. 1000 ms after the button press 5 TMS pulses (100 ms between pulses) were administered over the course of 400 ms. Starting with the last TMS pulse, after a variable delay (25 – 158 ms in steps of 16.7 ms) the stimulus sequence was presented inside the square placeholder. The orientation of Stim A and Stim B was pseudo-randomly chosen every trial (45° and 135° or vice versa).The presentation length for Stim A, Stim B and the mask was 42 ms each. The ISI between Stim A and Stim B was 16 ms. The ISI between Stim B and the mask was slightly longer with 24 ms. During Piloting we observed a forward and backwards masking effect on the second stimulus which we compensated by shifting the onset of the mask to a later time-point. This was done to equalize visibility between Stim A and Stim B which we verified during piloting in 4 subjects. After a delay of 1000 ms participants reported either the orientation of Stimulus B (arrow key left or right) or reported perceiving a single stimulus (arrow key up). Trials were randomly chosen from the normal condition (66.3% probability) [Stim A (normal contrast), Stim B (normal contrast), Mask], low contrast condition (22.3% probability) [Stim A (low contrast), Stim B (low contrast), Mask] or a single stimulus condition (11.3% probability) [Stim A (normal contrast), omitted,

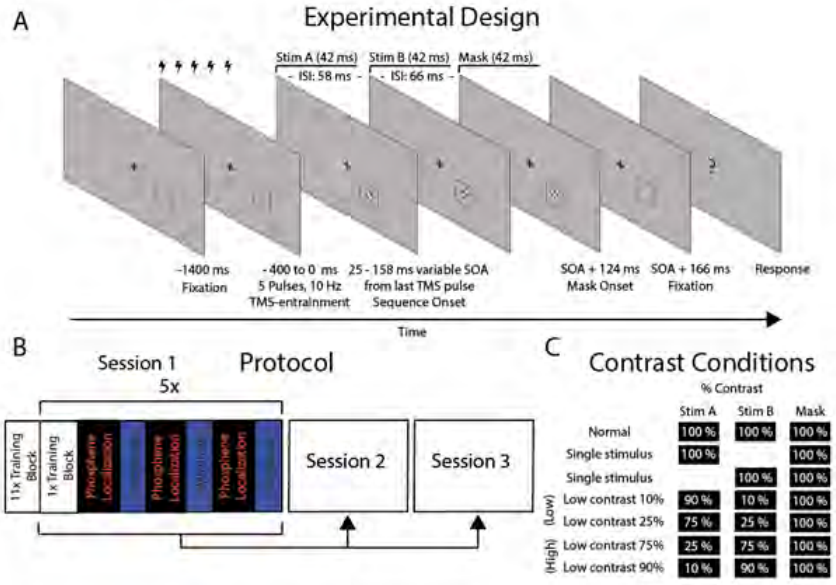

Figure 2. *Paradigm.* **A.** Experimental Design. Participant's initiated trials via button press while fixating at a central fixation cross. After 1000 ms 5 TMS pulses at 10 Hz were administered. We probed TOJ performance at nine time points between 25 ms and 158 ms after the last TMS pulse. This was done by presenting a sequence of two gabor patches with different orientation (Stim A and Stim B, 45˚ or 135˚, stimulus length: 42 ms, ISI 58 ms), followed by a mask to prevent stimulus persistence or long afterimages. Participants had to identify the orientation of the second stimulus which was different on every trial. Alternatively participants could report (using a different key) a single stimulus condition where either the first or second stimulus was omitted (see C.). In the TMS Blocks no feedback was provided. **B.** Protocol. The experiment was performed on 3 separate days within 5 days. On the first session only, participants performed an extensive training consisting of 253 trials without TMS, with feedback and with a predefined stimulus location. Afterwards the main experiment was performed consisting of 5 repetitions of the Block sequence indicated in the figure. These 5 repetitions were repeated on session 2 and 3. **C.** In order to control for an effect of TMS on the visibility of the stimuli we used 5 different contrast conditions. In a subset of trials the contrast of the stimuli in the sequence was separately reduced to either 10%, 25%, 75% or 90%. The contrast of the Mask was identical in all conditions. Additionally we included a single stimulus condition where one stimulus was omitted.

Mask] or [omitted, Stim B (normal contrast), Mask] (See Figure 2C). During the phosphene localization and the experiment, the participants head was fixed between a chinrest and the TMS coil, leading to a stable position. In total, a

maximum of 2215 TMS pulses were administered per session.

3.3.5 Data Analysis

We analyzed the data collected during the training blocks and the TMS-blocks separately. The 11 pre-training blocks at the beginning of session 1, which were included to prevent visibility biases, were not included in the analysis because of potential practice effects. Only training blocks that were collected during the main experimental procedure (interleaved with the TMS blocks) are included in this analysis (3×5 blocks of 23 trials per subject).

Training Blocks mean performance

Due to the significantly smaller number of trials collected in the training blocks compared to the TMS-blocks we did not analyze the time course of TOJ performance during training but looked at the overall performance for all 6 conditions (normal contrast condition, 4 low contrast conditions, single stimulus condition). The 4 low contrast conditions (Figure 2C) were merged into two groups based on the contrast of the stimulus B (target), separating them into a low target contrast group (Stimulus B contrast 10% and 25%) and high target contrast group (Stimulus B contrast (75% and 90%). Note that the major aim of including several fine grained contrast conditions in the first place was to counteract potential visibility biases, by preventing subjects from relying on visibility instead of TOJ. The separation based on Stimulus B contrast was done to control for possible effects of TMS on Stimulus B (target) visibility which should be maximal for the low contrast stimuli (for which orientation was reported) in the low target contrast group. Mean performance (Hits/Misses) was averaged within each subject for 1. normal contrast, 2. low target contrast (low contrast 10%, low contrast 25%), 3. high target contrast (low contrast 75%, low contrast 90%) and 4. single stimulus conditions separately. For the low contrast conditions we acquired 41.9 trials (low target contrast) and 42.2 trials (high target contrast) on average per subject. For the normal contrast and the single stimulus conditions on average 81.3 and 29.5 trials were collected per subject. The behavioral performance for each condition during training was quantified using a repeated measures ANOVA.

TMS Blocks

Analysis of mean performance

The analysis of the mean performance for the 6 conditions (normal contrast condition, 4 low contrast conditions, single stimulus condition) was done similarly to the analysis in the previous section by merging low contrast conditions into 2 groups (low target contrast, high target contrast). Mean performance per subject in the resulting 4 conditions and for each visual field (contraTMS and ipsiTMS) was analyzed using a repeated measures ANOVA.

Analysis of TOJ time-series

For our main results, the effect of TMS on subsequent TOJ-performance was analyzed as a function of the delay between the last TMS-pulse and presentation of the first stimulus of the sequence. Since the other contrast conditions only served to ensure that participants engaged in unbiased TOJ judgments Oonly the normal contrast condition (66.3% of trials) was included in this analysis. We removed all responses where subjects erroneously reported single stimuli (5.4%), counting only left/right responses (making chance performance 50%).

We probed TOJ performance at 9 time points (SOA's) after TMS (25 ms, 41.7 ms, 58.3 ms, 75 ms, 91.7 ms, 108.3 ms, 125 ms, 141.7 ms, 158.3 ms). On average 712.5 trials (24.2 SEM) were collected per subject. Performance (Hits/Total number of trials) was averaged within each subject at each of 9 SOA's for stimuli presented contralateral and ipsilateral to TMS respectively. The resulting time series were normalized by subtracting the mean and averaged over subjects, resulting in a grand average contralateral (contraTMS) and ipsilateral (IpsiTMS) time series.

In an additional analysis the individual 133 ms long TOJ time-series were subtracted on a subject by subject basis in order to calculate the difference waves between the two conditions. These difference waves were averaged resulting in the grand average difference wave (contraTMS minus ipsiTMS). Time-series were zero-padded to a length of 6 times the original window length (6*133.3 ms) and analyzed in the frequency domain using FFT (frequency resolution 1.1 Hz). 9 SOA's at 60 Hz allowed for a Nyquist frequency of 30 Hz. The complex FFT coefficients were squared to obtain oscillatory power at each frequency. To statistically test if the time-series contain significant oscillatory power we calcu-

lated 1.000.000 surrogates by shuffling the SOA-labels between trials for every subject, and repeating all analysis steps for each surrogate. The original power spectrum was then compared to the surrogate distribution and p-values were corrected for multiple comparisons using the False Discovery Rate. The FFT revealed a peak at 10 Hz for contraTMS and a peak at 7.8 Hz for the ipsiTMS condition.

Phase Analysis

For the phase analysis, we therefore decided to extract individual phase angles from the center frequency 8.9 Hz component of the FFT of the down-sampled and normalized contraTMS and ipsiTMS time-courses as well as the contraTMS minus ipsiTMS difference wave. Individual contraTMS and ipsiTMS phase angles were subtracted (contra minus ipsi, pairwise subtraction) to investigate the phase relationship in individuals. Rayleigh's test for non-uniformity was used to statistically test if individual phases were significantly coherent.

3.4 Results

In this study we seek to provide causal evidence for the hard theory of discrete perception. Specifically we aim to show that discrete perception entails a periodic compression of time information. Our hypothesis therefore states that within a perceptual moment, perception of the temporal order of events is impaired. To test this hypothesis we entrained participants' alpha oscillations using 10 Hz-TMS over early visual areas. We probed TOJ performance, an index of perception of relative timing, at different phases of the entrained oscillation after stimulation. A significant oscillatory component at 10 Hz at the entrained location (as measured by a frequency analysis on the average TOJ time-course) would suggest a rhythmic modulation of time perception.

3.4.1 Mean performance and low contrast control conditions

Mean performance in the normal and low contrast conditions was compared between Training blocks (no-TMS) and TMS blocks. During Training the mean performance across subjects and visual fields was 63.14% (±3.5% SEM) for the normal condition, 56.4% (±4.4% SEM) for the low target contrast condi-

tion, 63.1% (±3.4% SEM) for the high target contrast condition and d'=0.69 (±0.117% SEM) for the single stimulus condition. In the TMS blocks the mean TOJ performance across observers in the normal contrast condition was 64.4% (± 2.6% SEM) for stimuli contralateral and 62.4% (± 2.5% SEM) for stimuli ipsilateral to the cortical entrainment site. For the single stimulus condition d' was 1.61 (± 0.083% SEM) for stimuli contralateral and d' = 1.59 (±0.106% SEM) for stimuli ipsilateral to the cortical stimulation site. In the low target contrast condition average performance was 63.6% (±3.3% SEM) for the contraTMS condition and 57.4% (±3.7% SEM) for the ipsiTMS condition. Last, in the high target contrast condition performance was 65.8% (±3% SEM) for the contraTMS and 62.1% (±1.8% SEM) for the ipsiTMS condition.

To investigate if TMS or contrast asymmetries had a detrimental phase-independent effect on performance when stimulus visibility is low, both TMS blocks and Training blocks were analyzed using a repeated measures ANOVA with factors TMS (TMS versus Training), hemisphere (contra versus ipsilateral to TMS) and contrast (normal, low target contrast, high target contrast, single stimulus). We were particularly interested in 1. verifying that TMS did not cause any phase-independent decreases in task performance, as this would indicate that changes in excitability (here not via phase fluctuations but e.g. via increases in alpha power) could potentially deteriorate orientation identification and 2. to verify that asymmetries in stimulus contrast did not impair TOJ performance, as effects of rhythmic entrainment might lead to asymmetries in orientation perception and thus might influence TOJ performance.

Next we also investigated the relative number of single stimulus responses for all conditions. We hypothesized that if TMS leads to an occlusion of a single stimulus this should be apparent in an increase in the ratio of single-stimulus responses. Moreover this should especially be the case for stimuli presented contralateral to TMS. The repeated measures ANOVA revealed a main effect of contrast ($F(3,51) = 71.1$, $p < 0.005$) but not of TMS ($p = 0.12$) or hemisphere ($p = 0.69$). Post hoc tests revealed significantly different ratios of single stimulus reports between all contrast conditions (Normal contrast: 5.4%, high target contrast: 10.9%, low target contrast: 28.8%, single stimulus condition: 51.9%, $p<0.05$ respectively). This finding comes as no surprise and shows that our contrast manipulation successfully created distinct levels of target visibility. Importantly however no interaction effect between TMS and hemisphere (p

= 0.2), TMS and contrast (p = 0.73) or TMS, contrast and hemisphere (p = 0.1) was found, indicating that TMS did not lead to a higher number of single stimulus responses. To avoid confusion, we would like to mention again that, although an increase in single stimulus responses should lead to a decrease in overall performance, the results of both ANOVA's are not contradictory, since in the first ANOVA the single-stimulus reports were removed in all but the single stimulus condition.

We interpret the above presented findings as evidence that TMS did not have a general, time-unspecific effect on stimulus detection or orientation identification, which could have indirectly led to a modulation of TOJ performance, but rather modulated perceived relative timing of the stimuli. Similarly we can conclude that severe asymmetries in stimulus contrast, potentially causing difficulties in orientation detection, do not lead to differences in TOJ performance and cannot cause modulations in performance.

3.4.2 Alpha-TMS leads to periodic modulation of TOJ performance

In order to verify that TOJ performance was rhythmically modulated by alpha-TMS we calculated the average TOJ time-series over individuals. This was done by calculating the average performance p(correct—2 stimuli) for each of the 9 SOA's. Performance was analyzed separately for sequences presented contralateral (contraTMS) and ipsilateral (ipsiTMS) to alpha-TMS. Only normal contrast trials (66.3% of all trials) were included in this analysis, in order to discard any possible influence of contrast differences on stimulus visibility. For this analysis we excluded trials in which participants reported only a single stimulus: when both stimuli are visible, we can reasonably assume that subjects' reports reflect their perceived temporal order, as per the task instructions.

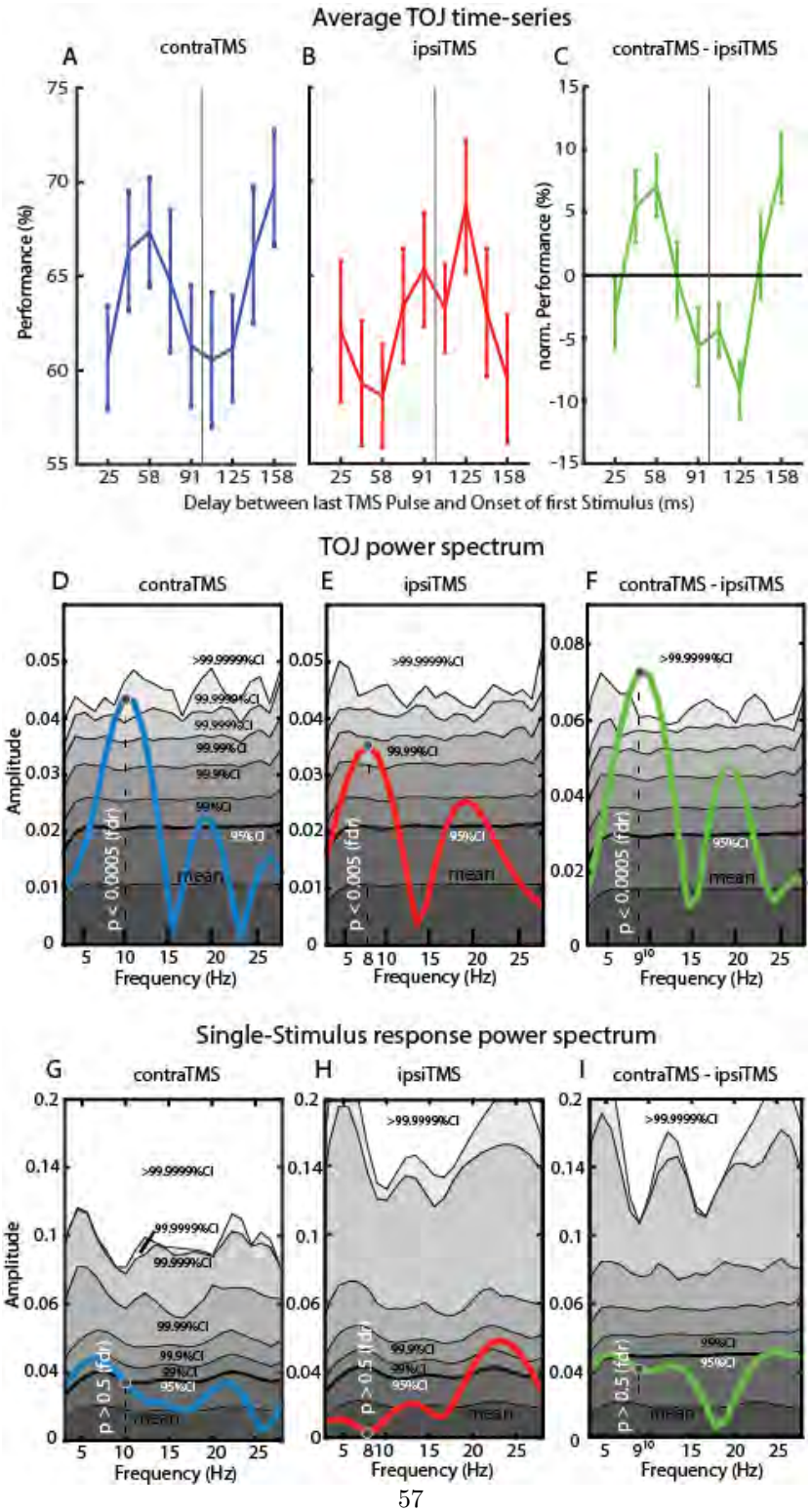
Average TOJ time-series
A
contraTMS
B
ipsiTMS
C
contraTMS - ipsiTMS
Performance (%)
norm. Performance (%)
Delay between last TMS Pulse and Onset of first Stimulus (ms)
TOJ power spectrum
D
contraTMS
E
ipsiTMS
F
contraTMS - ipsiTMS
Amplitude
Frequency (Hz)
p < 0.0005 (fdr)
mean
Single-Stimulus response power spectrum
G
contraTMS
H
ipsiTMS
I
contraTMS - ipsiTMS
p > 0.5 (fdr)

Figure 3. *Main findings.* **A.** Average TOJ time-series (N = 18) for stimuli presented contralateral to TMS. Error bars represent standard error of mean. The vertical gray line indicates the hypothetical time point of the next TMS pulse if the entraining sequence had continued. **B.** TOJ time-series for ipsilateral stimuli. **C.** Difference wave between contraTMS and ipsiTMS time series. **D.** Power spectrum of the contraTMS time-series. We compared the peak at 10 Hz to a surrogate distribution (1.000.000 surrogates) which revealed a significantly higher power at this frequency compared to other frequencies after correcting for multiple comparisons ($p = 0.00006$, FDR-corrected: $p = 0.005$). Colored areas: Dark gray: Mean of the surrogate distribution; Light gray: 95% Confidence Interval; 99% CI; 99.9% CI; 99.99% CI; 99.999% CI; 99.9999% CI; White: >99.9999% CI. **E.** Power spectrum of the ipsiTMS time-series. We observed a relatively strong oscillatory component at around 8 Hz. Analogous to (D) we analyzed oscillatory power at 8 Hz and found significantly more power compared to the surrogate distribution ($p = 0.00038$, FDR-corrected: $p = 0.0039$). **F.** Power spectrum of the contraTMS minus ipsiTMS time-series. Oscillatory peak was at 9 Hz and showed significant power ($p < 0.0005$, FDR-corrected: $p = 0.0005$). Note that 9 Hz oscillatory power was 71% higher in amplitude compared to the 10 Hz oscillation in the contraTMS condition, indicating an anti-phasic relationship. **G,H,I**. Same as D,E,F but for the time-series of single-stimulus reports p(single-stimulus report — 2 stimuli). No significant oscillatory peak was observed in contraTMS or ipsiTMS conditions and neither in contraTMS minus ipiTMS time-series compared to the surrogate distribution at our frequencies of interest (5-15 Hz, FDR-corrected: $p > 0.5$ respectively).

TOJ time-series were normalized by subtracting the individual mean before applying the FFT. Figure 3A shows the original, un-normalized time-series. Initial inspection of the time course for contraTMS indicates a strong oscillation in the TOJ performance lasting for more than 158 ms. To quantify this effect we performed a frequency analysis on the average TOJ-time -series. The resulting power spectrum revealed a dominant oscillation at 10 Hz (Figure 3D). For statistical validation of this peak we created 1.000.000 surrogates by shuffling the 9 SOA-bin labels within subjects and recalculated the power spectrum of the resulting TOJ time series. P-values were computed as the percentile of the mean power values within the bootstrapping distribution. This allowed us to test the null-hypothesis that the power spectrum of the average TOJ time-series does not show a peak at a specific frequency. The TOJ time-series power at 10 Hz was significantly higher compared to the surrogate distribution (Figure 3D, 10 Hz: $p = 0.00006$, FDR corrected). We analyzed the ipsiTMS TOJ time-series in an identical fashion. Initial inspection indicated a slightly weaker oscillation

peaking at a lower frequency of 8 Hz (Figure 3B). The frequency analysis and statistical analysis of the ipsiTMS time-series showed significantly more power compared to the surrogate distribution (Figure 3E). Power peaked at 8 Hz ($p = 0.0039$, FDR corrected) but was still significant at the entrainment frequency of 10 Hz ($p = 0.015$, FDR corrected). Additionally, a visual inspection of the individual TOJ time-series revealed clear peaks in 16 out of 18 subjects in the 6.6 to 12.2 Hz range (mean 9.8 Hz, SEM ± 0.51).

To test if the oscillation in the ipsiTMS time-series is caused by a non-specific effect of TMS on both hemispheres, we tested whether oscillations in contra and ipsilateral TOJ time-series were consistent in phase. We therefore subtracted ipsiTMS time-series from the contraTMS time-series for each subject individually. Should both fluctuations in the time-series be caused by the same non-specific effect of TMS they should cancel out and the resulting contraTMS minus ipsiTMS time-series should show reduced amplitude. On the contrary, the resulting difference wave showed markedly higher fluctuations (71% increase in range) compared to the contraTMS time-series. By performing another frequency analysis, this time on the contraTMS minus ipsiTMS time-series, we could attribute this increase to a strong oscillatory component in the 9 Hz range (Figure 3F, 9 Hz: $p < 0.00005$, FDR corrected). The increase in oscillatory power in the difference wave is likely a result of subtracting two oscillations that share a common (or neighboring) frequency but are in anti-phasic relationship.

As a control analysis we investigated if alpha-TMS leads to a periodic modulation of the ratio of single stimulus responses. To exclude the possibility that certain phases of the entrained alpha oscillation lead to perceptual occlusion of one or both stimuli, and in turn might periodically modulate the ability to perform temporal order judgments, we repeated the above presented analysis on the ratio of single stimulus responses p(single-stimulus report — 2 stimuli). This ratio can be considered a measure of excitability/visibility as it indicates how often participants reported a single stimulus when actually two stimuli were presented, thus presumably missing one stimulus due to occlusion. All analytic and statistical parameters were kept identical. The frequency analysis of contraTMS and contraTMS minus ipsiTMS revealed no peaks in oscillatory power that were significantly higher compared to the surrogate distribution (Figure 3 G,I; 5 to 25 Hz: $p > 0.5$ respectively, FDR corrected). We observed a signif-

icant peak at 24 Hz in the ipsiTMS time-series (Figure 3 H; p = 0.048, FDR corrected). Since this oscillatory component was far away from our frequency of interest 10 Hz and not significant in any other control condition we did not investigate it further. Given that single-target reports were not modulated at 10 Hz we conclude that modulations of excitability cannot explain the modulation of TOJ performance.

In addition to the results of our various control analyses we would like to address a final potential confound to which our attention was drawn during the review process. As mentioned previously, even if both stimuli have been detected, failure to identify the orientation of one (or both) of the stimuli could potentially bias TOJ performance in a phase-dependent manner. On the one hand this situation might arise if the first or the second stimulus falls into the "excitability trough" (note that due to the SOA of 58 ms this means that the other stimulus necessarily falls into the preceding or following excitability peak). On the other hand it might arise if the two stimuli fall evenly on the left and right side of an excitability peak or trough (an "equilibrium configuration") and both suffer from a relative decrease in orientation identification compared to the excitability peak. These 2 cases (peak/trough configurations and equilibrium configurations) might affect orientation identification to the same extent, in which case we would not expect to see resulting fluctuations in performance. If they differ however, e.g. if the orientation of stimuli in equilibrium states is harder to identify, then we would expect a drop in performance two times per cycle (when the stimuli fall on both sides of the peak and again when they fall on both sides of the trough). Importantly, this should manifest not as a 10 Hz oscillation but as a 20 Hz oscillation in our behavioral time-course. In fact we did observe a slight modulation at 19 Hz in our behavioral time-course (Figure 3). However this oscillatory component did not reach statistical significance (p = 0.11). We conclude that while excitability fluctuations might slightly modulate performance (at 20 Hz) they cannot explain the 10 Hz peak, which is better explained by discrete temporal windows in vision.

3.4.3 10 Hz Phase analysis

To test if the oscillations observed in both hemifields are in anti-phase we analyzed the 9 Hz phase angles of the ipsiTMS and contraTMS time-series (Figure 4A) as well as the difference wave across subjects. The frequency of 9 Hz was

chosen because it lies right within the frequency ranges of the contra and ipsilateral peak components and both time series show highly significant power at this frequency (contraTMS: $p = 0.00017$; ipsiTMS: $p = 0.0039$). Additionally we performed a pair wise subtraction of the individual contraTMS and ipsiTMS phase angles (phase domain difference) to test if a possible anti-phasic relationship is visible on the single subject level. The complex FFT coefficients at 9 Hz were extracted to calculate individual phase angles (Figure 4B). We then compared these angles using Rayleigh's test for non-uniformity testing the null hypothesis that the phase angles are randomly distributed. Phase angles were significantly clustered in ipsilateral as well as contralateral TOJ time-series (Figure 4B, contralateral: $p = 0.000062$, ipsilateral: $p = 0.0017$). We were further interested in the phase relationship between 9 Hz oscillations in contraTMS and ipsiTMS time-series (time domain difference). To test the two sets for phase opposition we subtracted the phase angles for each subject and performed Rayleigh's test for non-uniformity on the resulting phase differences. Phase difference angles were significantly clustered at 180 degrees, indicating anti-phasic oscillations at opposing hemispheres (CI lower bound: 120.5 degrees, upper bound: 199.8 degrees, mean: 160.2 degrees, $p < 0.01$). The difference wave was analyzed in an identical fashion as contraTMS and ipsiTMS time-series, showing highly significant 9 Hz phase clustering ($p=0.000001$).

3.5 Discussion

We tested the influence of alpha-TMS on subsequent temporal order judgments at varying SOA's. 5 Pulses at 10 Hz were administered over left or right occipital cortex. alpha-TMS was intended to entrain alpha-oscillations in a local neural population. We probed temporal order perception of two Gabor patches, at the spatial location presumably affected by the TMS entrainment, at 9 SOA's between 25 ms and 158 ms after the last TMS-pulse. Behavioral performance at every SOA was averaged to obtain a 133 ms long TOJ time-series. The frequency analysis of the TOJ time-series contralateral to TMS revealed a strong oscillation at our entrainment frequency of 10 Hz. We found no evidence of potentially confounding effects of excitability fluctuations on TOJ in our control conditions. In line with previous accounts of discrete perception we hypothesize that the rhythmic modulation in TOJ was caused by a TMS-evoked entrainment of occipital alpha-oscillations. The phase of alpha-oscillations has previously been

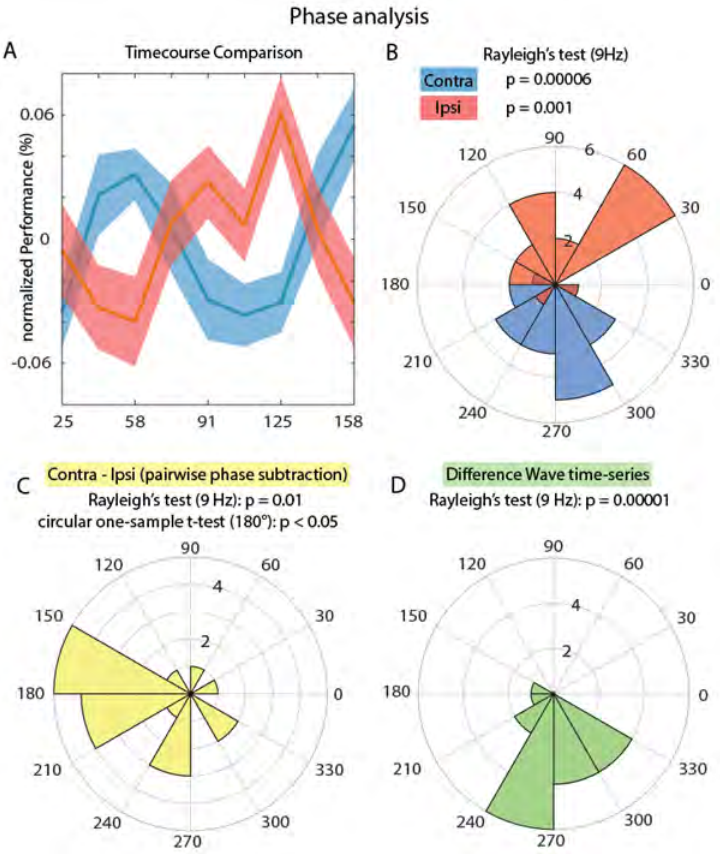

Figure 4. *9 Hz Phase Analysis.* A. Time Course of normalized contraTMS (stimulated hemifield) and ipsiTMS (non-stimulated hemifield) time courses for direct comparison. Note the clear antiphasic relationship between the two. B. 9 Hz phase angles of contraTMS (blue) and ipsiTMS (red) time-series. Rayleigh's test reveals significant phase clustering for both conditions. C. Pairwise subtraction of 9 Hz contraTMS minus ipsiTMS phase angles (phase domain difference). Phase angles were significantly clustered around 180 degrees indicating an antiphasic relationship between individual contraTMS and ipsiTMS time-series. D. 9 Hz Phase analysis of the difference wave (contraTMS minus ipsiTMS, time domain difference). Phase angles were significantly clustered.

related to so-called "perceptual windows" that serve to discretize visual input into compressed packages. Here we specifically tested the hypothesis that this compression leads to a deterioration of temporal order information. Depending on the relative timing to the last TMS pulse (SOA) the two stimuli fall either in the same or separate perceptual windows, leading to decreased or enhanced

TOJ performance respectively. Our findings are in line with a "hard" theory of discrete perception suggesting that temporal order information is limited within perceptual windows. We provide causal evidence for an involvement of occipital alpha-oscillations in this process.

Correlational evidence for an involvement of the occipital alpha-rhythm in the discretization of visual input is frequent (Valera et al., 1981; VanRullen & Koch, 2003; Lőrincz et al., 2009; Busch et al., 2009; Haegens et al., 2011; Vijayan & Kopell, 2012; Samaha & Postle, 2015; Milton & Pleydell-Pearce, 2016; VanRullen, 2016). Yet it was not clear if the alpha-rhythm merely modulates excitability, leading to continuous fluctuations in visual performance or if it implements discrete non-overlapping perceptual windows. It is important to note that fluctuations in performance do not need to be all-or-none to support the "hard" version of temporal perception. All-or-none effects can rarely be expected due to noise in the phase entrainment and phase measurement methods or due to inter-individual differences in oscillatory frequency and optimal phase. We argue that it is sufficient to show that temporal perception itself fluctuates and that these fluctuations cannot simply be explained by changes in excitability (e.g. stimulus detection), leaving discrete temporal windows as the most plausible explanation.

Recent work shows that the alpha-rhythm can be causally modulated via visual entrainment, leading to fluctuations in temporal parsing performance (Ronconi et al., 2018; Chota & VanRullen, 2019). While these studies help to link alpha-oscillations and perception, they are limited since a visual entrainer passes various processing stages e.g. the LGN before arriving at V1. The LGN is hypothesized to project not only to V1, but also directly to higher cortical areas like V2 and V3 (Schmid et al., 2010). Strictly speaking every possible target of visual entrainment could serve as a potential source for the behavioral observations previously reported (Mathewson et al., 2010; Spaak et al., 2014; Ronconi et al., 2018; Chota & VanRullen, 2019). TMS allows for a direct and relatively localized interaction with endogenous cortical rhythms and is especially efficient at 10 Hz, even when individual alpha-peak frequencies differ (Romei et al., 2010; Thut et al., 2011). Furthermore phosphene-based TMS localization procedures have been successful in modulating rhythmic behavior (Romei et al., 2010). As the target of our entrainment is confined to the early occipital cortex we can say with relative certainty that the occipital alpha-rhythm gives rise to the per-

ceptual effects demonstrated in this study. We therefore provide a direct link between occipital alpha-oscillations and temporal order judgements. Former experiments have mostly used integration versus segregation tasks (IvS), i.e. the two-flash fusion paradigm, to quantify temporal parsing performance (Valera et al., 1981; Samaha & Postle, 2015; Ronconi et al., 2018). These tasks present two stimuli in quick succession and subsequently probe participants' temporal segregation abilities (simultaneous vs. non-simultaneous, one vs. two). However, perceptually it is principally sufficient to detect changes in luminance over time, irrespective of the stimulus characteristics. Flicker fusion experiments show that temporal changes can be detected at far higher frequencies than 10 Hz (Simonson & Brozek, 1952). TOJ's however require precise perception of temporal relationships between individual stimuli and cannot be solved purely by identifying transient changes in luminance. We therefore suggest that TOJ is better suited to investigate the effect of alpha-phase on temporal perception.

While the effect of alpha-TMS on the contralateral visual field was somewhat expected, we were surprised to find a TMS-evoked oscillatory pattern also in the ipsilateral visual field. The ipsiTMS time-series showed a relatively weaker amplitude, oscillated at around 8 Hz and fluctuated in antiphase compared to its contralateral counterpart for at least 160 ms. It is unlikely that the magnetic field of the TMS-pulse directly interacted with the contralateral hemisphere because first, all subjects reported phosphenes only contralaterally, and second, TMS pulses seemed to have opposing effects depending on the stimulus location. Previous work has shown that alpha-TMS can affect target detection performance in the visual field contra- and ipsilateral to the entrainment site, possibly through a transcallosal "push-pull" effect (Romei et al., 2010). Our findings suggest that alpha-phase is modulated by this network effect, potentially releasing one hemisphere from inhibition when the other hemisphere enters a state of inhibition. One possible interpretation of the frequency difference is that the ipsilateral oscillation reflects a slower attentional rhythm that is usually placed in the 3 to 8 Hz range, potentially lower than our frequency analysis allows us to investigate (VanRullen et al., 2007; VanRullen, 2013; Fiebelkorn & Kastner, 2018; Fiebelkorn et al., 2018). Another possibility is that the change in frequency relates to differences in alpha-power between hemispheres. As mentioned before a push-pull effect might lead to a significant reduction in 10 Hz power in the ipsilateral hemisphere (Romei et al., 2010). Since this oscillatory frequency is likely relevant for stimulus processing the brain might hypotheti-

cally try to compensate by modulating excitability at a lower frequency.

The phase of alpha-oscillations is predictive of cortical excitability (Busch et al., 2009; Dugué et al., 2011), of neuronal firing rates (Lőrincz et al., 2009; Vijayan & Kopell, 2012; Haegens et al., 2011) and of the amplitude of gamma oscillations (Osipova et al., 2008; Voytek et al., 2010). As these neural signatures have been implicated in neuronal processing it seems logical that visual processing is concentrated on specific reoccurring intervals. The brain might use these naturally occurring periodicities, in the form of oscillations, to reduce the complexity of incoming information by compressing it into discrete packages. Our findings suggest that this compression results in the loss of temporal relationship between two stimuli. Note that the visual system is very robust to subsampling in the 100 ms range (VanRullen, Zoefel, & Ilhan, 2014), presumably because visual information is highly redundant, allowing the visual system to reduce complexity via periodic discretization without losing too much relevant information.

In this study we successfully demonstrated that TMS entrainment at 10 Hz leads to a causal rhythmic modulation of temporal order judgements. This modulation was evident in the majority of subjects, shown by a strong inter-individual phase coherence in individual TOJ time-series. Furthermore we found that ipsilateral TOJ time-series were modulated in antiphase to their contralateral counterparts; this cross-hemispheric effect is unlikely to be caused directly by the TMS, but may result from a secondary trans-callosal pathway. We hypothesize that the visual system periodically discards temporal order information in order to reduce the complexity of incoming visual information. Further, we hypothesize that this mechanism is implemented by occipital oscillations in the alpha-range.

3.6 Conclusion

In this study we successfully demonstrated that TMS entrainment at 10 Hz leads to a causal rhythmic modulation of temporal order judgements. This modulation was evident in the majority of subjects, shown by a strong inter-individual phase coherence in individual TOJ time-series. Furthermore we found that ipsilateral TOJ time-series were modulated in antiphase to their contralateral

counterparts; this cross-hemispheric effect is unlikely to be caused directly by the TMS, but may result from a secondary trans-callosal pathway. We hypothesize that the visual system periodically discards temporal order information in order to reduce the complexity of incoming visual information. Further, we hypothesize that this mechanism is implemented by occipital oscillations in the alpha-range.

Different senses, common mechanisms: Rhythmic reverbrations in the somatosensory system.

We know now that the alpha rhythm plays an important role in the visual system. Our previous two experiments have shown that oscillations play a causal role in perception and that one of their functional roles might be the reduction of complexity in time. Not only the visual system is confronted with this challenge but other senses, e.g. the tactile system as well. To investigate if these systems use similar mechanisms to solve similar problems we need to find out if they express comparable dynamics in response to stimulation.

However the question gets more complicated if we take into account that the structural make-up of different sensory systems varies. In addition, the problems that they need to solve might conceptually be similar but practically our sensory systems receive very different types of information that require different computations. The same process in one sensory domain might look very differently in another domain.

One way to disentangle which processes express in which way is to find simple baseline measures that give us an idea of the basic dynamic principles of different cortical architectures. One such principle is the idea of the natural resonance frequency. Similar to physical objects, cortical areas tend to respond to certain frequencies more strongly than to others. In the visual system this frequency is assumed to be in the 10 Hz range. In somatosensory areas we expect it to be in the beta band around 25 Hz. These resonance frequencies could be indicative of basic computations that happen in respective regions and allow us to relate other neural signatures or behavioral fluctuations to them. In the next chapter we follow this approach by investigating the tactile IRF and comparing it to the somatosensory resonance frequency using a somatosensory steady state evoked potential paradigm.

Chapter 4

Random Tactile Noise Stimulation reveals periodic Reverbrations in the Somatosensory System

The following chapter contains an original manuscript in preparation: Chota, Samson, Rasa Gulbinaite and Rufin VanRullen. "Random Tactile Noise Stimulation reveals periodic Reverbrations in the Somatosensory System."

4.1 Abstract

The brain is an intrinsically rhythmic organ. Different brain regions express different oscillatory profiles that can be coarsely classified by frequency and are assumed to result from inhibitory circuits on a local and cortico-cortical network dynamics on a global scale. Moreover different brain regions exhibit enhanced responses when presented with rhythmic stimuli at specific frequencies, supporting the idea that different networks have different resonant frequencies. Since these resonant frequencies are a result of several underlying factors determined by function and makeup of the respective region, investigating them will provide valuable information about the regions fundamental properties. Here we apply tactile broadband stimulation to participants' index fingers and measure the resulting impulse response function over somatosensory areas. We find that the impulse response function does not follow a regular ERP shape but has a strong oscillatory component at around 25 Hz suggesting that the somatosensory system reverberates information periodically, similar to the visual system.

4.2 Introduction

Neural oscillations are ubiquitous in the brain and are assumed to serve several fundamental functions (Buzsaki, 2006). While their functional role is still poorly understood, recent work has helped in developing tools that enable us to directly modulate these rhythms and observe changes in neural dynamics and behavior (Thut et al., 2011). Along these lines Steady State Evoked Potential (SSEP) methods have proven valuable to investigate the oscillatory properties of the visual system and the somatosensory system (Regan, 1977). Periodic stimulation of sensory systems leads to a frequency specific response that is maximal at the resonance frequency of the respective cortical region. Previous work has identified the resonance frequency of the visual system to be around 10 Hz, linking it closely to endogenous posterior alpha oscillations (Berger, 1931; Herrmann, 2001; Vialatte, Maurice, Dauwels, & Cichocki, 2010). Similar evidence for the tactile domain is more sparse but places the resonance frequency of the somatosensory system in the beta band (21 to 27 Hz) (Snyder, 1992; Tobimatsu, Zhang, & Kato, 1999; Muller, Neuper, & Pfurtscheller, 2001). Functionally the "visual" occipital alpha and the "somatosensory" fronto-parietal beta band behave similarly in that they de-synchronize before and during visual stimulation, motor execution and tactile stimulation respectively (Pfurtscheller & Lopes da

Silva, 1999; Ploner, Gross, Timmermann, Pollok, & Schnitzler, 2006; Kilavik, Zaepffel, Brovelli, MacKay, & Riehle, 2013). Recently VanRullen et. al. have shown that visual random noise stimulation leads to an up to 1 second long reverberation of visual information in occipital regions at 10 Hz. The neural signature was thus coined "perceptual echo" (VanRullen & Macdonald, 2012) and represented intriguing evidence that alpha power might increase in response to visual stimulation. The peak frequency of individual participant's echoes was strongly correlated with their alpha peak frequency during rest, hinting at a common generative neural mechanism. Importantly the random noise sequence was unbiased in its frequency content, supporting the claim that the visual system selectively reverberates the 10 Hz component of its input. Although the functional role of the perceptual echoes has up until now not been clearly identified, they strongly highlight the intrinsically alpha-periodic properties of the visual system. The question remains if the perceptual echoes are unique to the visual system or if we can find them in other modalities. Doing so would strongly suggest that they reflect a common basic computing signature of sensory processing areas and implicate them in an active role in stimulus processing. In this study we aim at investigating the relationship between tactile perceptual echoes and Somato-sensory steady state responses (SSSEP) in 18 human subjects (8 females). SSSEP's were probed at multiple frequencies between 12 and 39 Hz using a tactor device and extracted using a spatiotemporal source separation method. Perceptual echoes were calculated by cross-correlating tactile white noise input sequences, applied with a tactor to the right index finger, with the corresponding EEG signal. We find that the Somatosensory System reverberates the white noise input sequence at 25 Hz similar to the perceptual echoes in the visual domain. Furthermore tactile perceptual echoes and SSSEP's showed a significant correlation in peak frequency. Our findings support the claim that perceptual echoes are a signature of fundamental processing in the visual and in the tactile domain and closely relate to the resonance frequency of the somatosensory system.

4.3 Materials and Methods

4.3.1 Participants

18 participants (aged 22-41, 8 females) with normal or corrected to normal vision enrolled in the experiment. 1 participant had to be excluded due to excessive

movement artifacts in the EEG recordings, leaving 17 participants for the complete experiment and the final analysis. Informed consent forms were signed before the experiment. The experiment was carried out in accordance with the protocol approved by the Centre National de la Recherché Scientifique ethical committee and followed the Code of Ethics of the World Medical Association (Declaration of Helsinki). Subjects were compensated with 10 Euro/hour.

4.3.2 Protocol

Participants performed a practice session to become acquainted with vibrotactile stimulation and target detection task. We used a self-build tactor device that was driven by an audio amplifier. The practice session consisted of 5 trials of steady state stimulation (150 Hz carrier wave with constant frequency sine-wave signal). All steady state stimuli contained a target in the form of a frequency reduction by 15% for 1 second (127.5 Hz). After the practice session participants were first presented with 200 pulse stimuli (200 ms duration, 150 Hz vibration) separated by an ITI of 1-1.5 sec. Thereafter participants completed 616 experimental trials: 400 trials of white noise sequences and 216 trials of steady state stimulation. White noise sequences were created by randomly modulating the amplitude of a 150 Hz carrier wave. The random amplitude modulation was generated using a white noise signal and normalizing the amplitude of its Fourier components before applying an inverse Fourier transform. The random amplitude modulation was applied to the 150 Hz carrier wave in such a way that its amplitude was changed on a cycle by cycle basis (every 6.6 ms). Steady state stimuli were created by amplitude-modulating a 150 Hz carrier frequency with a constant frequency sine-wave signal. In total we used 18 stimulation frequencies covering the beta frequency range (14-30 Hz) and a few frequencies below and above: 12 to 20 Hz in steps of 2 Hz, 21 to 30 Hz in steps of 1 Hz, and 33 to 39 Hz in steps of 3 Hz. Each frequency was presented on 12 trials. 20% of all trials (White Noise and Steady State) contained a target in the form of 15% (127.5 Hz) decrease in carrier frequency for 1 second. Trial length was 6.7 seconds (6.6625 s, 301000 samples). Experimental trials were divided into 8 blocks. To make sure that participants could not perform the target detection task by using auditory information (vibrotactile electromagnetic solenoid-type stimulators make a faint yet audible sound), they were using earplugs.

4.3.3 Data acquisition and preprocessing

We recorded participants EEG using a 64 channel ActiveTwo Biosemi system. Two additional electrodes placed on the outer eye canthi recorded horizontal and vertical eye movements. Data analysis was performed in Matlab using the Fieldtrip toolbox. The EEG data was bandpass filtered between 1 and 20 Hz and line noise was removed using a DFT-filter (50, 100 and 150 Hz). Thereafter the data was epoched for SSEP, White Noise and ERP trials separately. Muscle and eye-movement related artifacts were first removed manually. Then we performed an ICA on the datasets separately to remove remaining artefactual components.

ERP analysis

Event related potentials were calculated by averaging epochs from 400 ms before stimulus presentation to 600 ms after stimulus presentation. Absolute baseline correction was applied by subtracting the average from the 400 to 0 ms pre-stimulus time-window of the single trial ERP's.

Impulse Response Functions

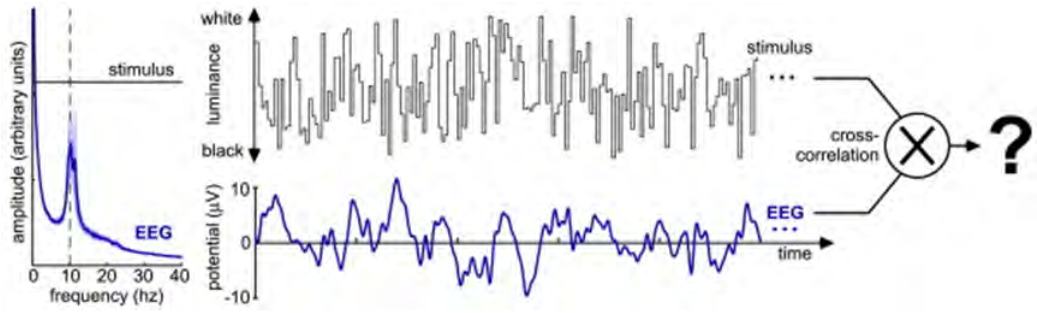

Figure 1. *Cross Correlation Procedure.* The cross-correlation between white noise sequence and EEG epoch results in the Impulse Response function, the brain response to a single Impulse. Theoretically this IRF should be similar to a low frequency ERP, however the IRF was shown to have strong oscillatory power in higher frequencies.

Impulse response functions (IRF) were calculated by cross-correlating the z-scored single-trial EEG signal with the white noise sequence presented at that particular trial. EEG trials were downsampled to 160 Hz before cross-correlating (Figure 1). The surrogate echoes were computed similarly by cross-correlating the EEG signal with the white noise signal of a different trial. All stimulus time

points were entered in the cross-correlation except the first 500 ms and the last 1000 ms to avoid influences of the ERP. The cross-correlation was calculated for lags between -300 ms and 500 ms as follows:

$$IRF(t) = \sum_{T} stim(T).eeg(T+t)$$

With *stim* and *eeg* denoting standardized stimulus sequence and corresponding standardized EEG signal respectively.

Steady State Evoked Potentials

Frequency-specific SSSEP responses were obtained using a spatiotemporal source separation method called rhythmic entrainment source separation as described in (Cohen & Gulbinaite, 2017)

IRF and ERP Time Frequency/Power Analysis

Power and time-frequency analyses for IRF's and ERP's were performed using multitaper time-frequency transformation using Hanning tapers based on multiplication in the frequency domain. We analyzed frequencies from 2 to 50 Hz in steps of 1 Hz. TFR's were calculated using an adaptive time-window encompassing 4 cycles of the respective oscillation. The length of the beta component of the IRF was analyzed in a similar fashion using an adaptive time-window that encompassed 1-cycle of the corresponding frequency. Powerspectra were calculated using fast fourier transforms.

4.4 Results

In this study we were interested in verifying the existence of perceptual echoes in the tactile domain as well as in comparing them to SSSEP's. Participants were stimulated at their right index finger using a Tactor device. SSSEP's were acquired by presenting 6.7 second long carrier waves that were amplitude modulated at 18 different frequencies covering the beta band. Random stimulation

sequences consisted of 6.7 second long white noise sequences, amplitude modulated in a similar fashion. To compute Impulse Response functions the white noise sequences were cross-correlated with the corresponding EEG signal of that trial. We extracted SSSEP's using spatial filters that were constructed using generalized eigenvalue decomposition.

4.4.1 Random Noise Stimulation reveals oscillatory Impulse Response Function

Cross correlating the white noise sequences with the EEG signal revealed a strong oscillatory component, similar to the IRF's found in the visual domain (Fig. 2). Initial visual inspection of the average IRF and it's TFR showed that these reverbrations were present for lags up to 200 ms and had strong oscillatory power in the beta band compared to the surrogate distribution. The oscillatory peak was around 20 Hz. This served as a qualitative confirmation of the existence of perceptual echoes in the tactile domain.

The impulse response functions were analyzed quantitatively by averaging them across trials for each channel on a subject by subject basis. Time Frequency representations were calculated for each subject and for each channel on the trial-averaged IRF's. Figure 3 A shows the group level TFR of the IRF averaged over all subjects and channels. The time-frequency representation revealed strong power in the beta range for positive lags. Based on visual inspection of the TFR we defined the time and frequency window of interest between 0 and 200 ms and 15 and 35 Hz. The power in our two time-frequency windows of interest was averaged and plotted topographically (Figure 3 B). We observed the highest power over left parietal and frontal channels. Average power was statistically compared between surrogates and IRF's. The surrogates were computed by cross-correlating the white noise input sequences with the EEG signal from a random trial. The t-test (alpha = 0.005) revealed 19 channels in which beta power was significantly higher in the IRF compared to the surrogate. These channels were defined as our channels of interest for the estimation of the beta peak frequency and for the comparison with ERP's. The power spectrum (Figure 3C) was calculated based on our channels, time and frequency of interest. The oscillatory peak of the grand average was 22 Hz.

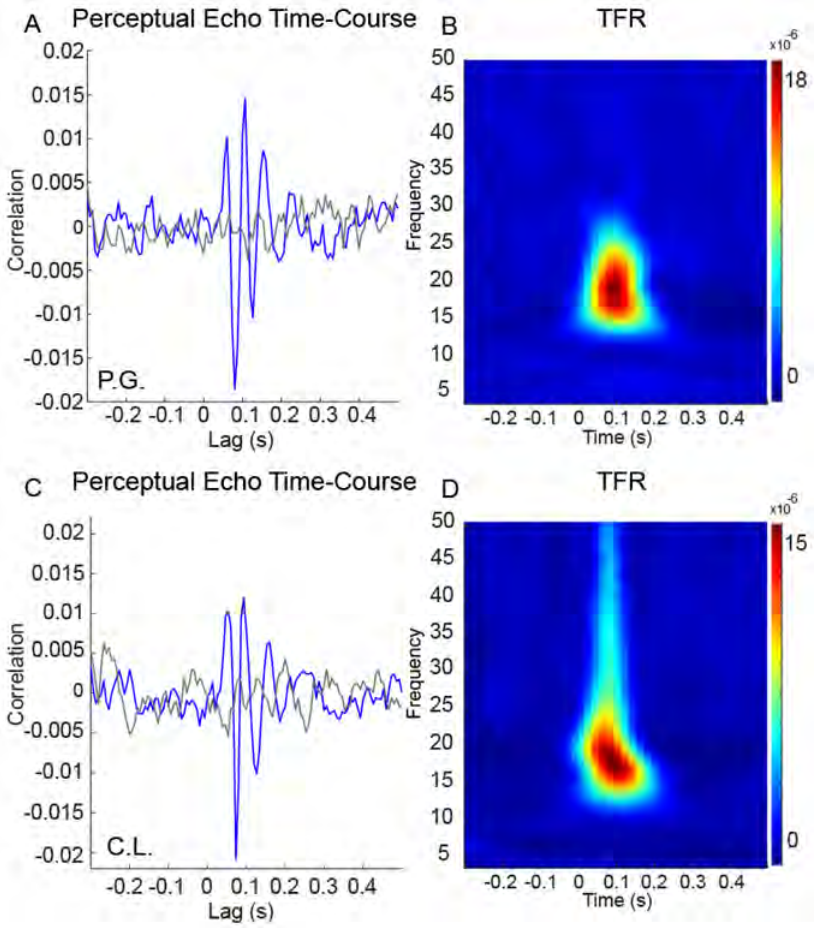

Figure 2. *Two representative IRF's with corresponding TFR.* **A**. Perceptual Echoes were calculated by cross-correlating tactile white noise sequences with the recorded EEG signal. **B**. Time frequency representation of the single subject IRF over channel CP5. **C**,**D**. Same as A,B but for separate subject.

Visual perceptual echoes can be observed for a maximum of up to 1 second (on average 4 to 5 alpha cycles). We were interested if the short duration of the tactile echoes (200 ms), relative to the visual echoes was related to the difference in oscillatory frequency between tactile and visual IRF's. We therefore quantified the length of the echoes by calculating a 1-cycle TFR. Power

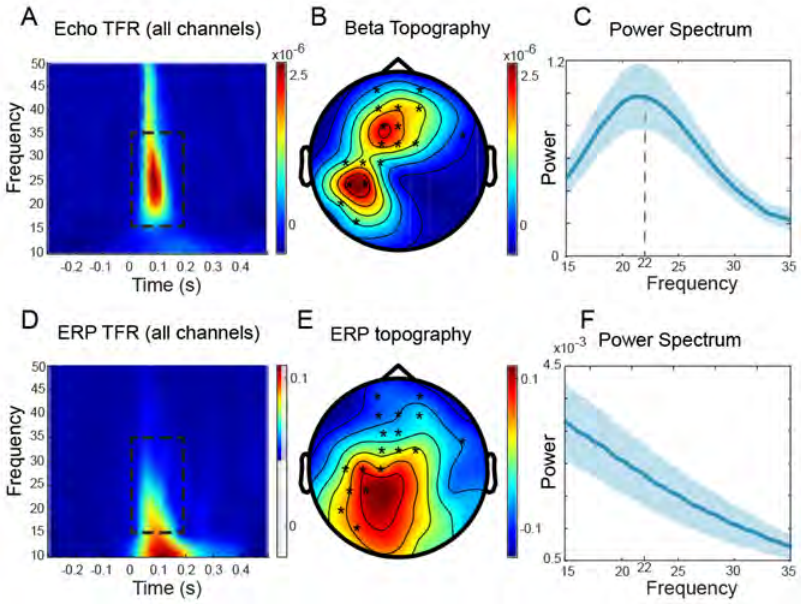

Figure 3. *Echo ERP comparison.* **A**. Time Frequency representation of IRF averaged over all channels. Oscillatory power was strongest in the 12 to 35 Hz range between 0 and 200 ms. We selected this frequency band and time window as our frequency and time of interest. **B**. Topography of the beta power distribution (12 to 35 Hz) between 0 and 200 ms (black dashed box). A left-frontal and a left-parietal beta power hotspots emerge in proximity to the somatosensory cortex. Statistical analysis revealed 19 channels with higher beta power compared to the surrogate IRF. These channels served as our channels of interest. **C**. Average power spectrum of the IRF for our channels of interest (determined from B). The oscillatory peak was found at 22 Hz. **D**. Time frequency representation of ERP's averaged over all channels. In contrast to the IRF no comparable oscillatory component was identified in the beta band. Low frequency oscillations can be observed as expected from classical somatosensory ERP's. **E**. Topography of the ERP waveform. **F**. Average power spectrum of the ERP for significant channels from B. Identical to the IRF analysis the power spectrum was calculated for the time window from 0 to 200 ms (black dashed box) between 15 and 35 Hz. No oscillatory peak can be observed in the beta range.

envelopes were extracted at the individual peak frequencies. IRF length was determined as the time point where the power reached below 10% of the peak power. These echo lengths were then normalized for the adaptive FTT window length by subtracting half a cycle of the respective frequency. E.g. to the echo length of subject AS (0 ms to below 30% of peak = 260 ms) at the individual

frequency of 23 Hz was added half a cycle of the 23 Hz oscillation 17.4 ms. for a total length of 277.4 ms. Spearman correlation between the echo length and the echo frequency revealed no significant relationship between length and frequency (Figure 5B, $p < 0.05$) indicating that echo length is independent of frequency. Based on the raw estimated 1-cycle fft echo durations and the corresponding peak frequency we estimated that tactile echoes lasted for an average of 4.1 cycles (SEM +- 0.51) comparable to visual perceptual echoes. To highlight the unique oscillatory dynamics of the IRF we directly compared their frequency content to traditional somatosensory ERP's. Figure 3D shows the average time-frequency representation of the ERP's of all channels. In contrast to the IRF we find no increase in beta oscillatory power but characteristic low frequency components that are usually found in ERP's. Also the topography of the ERP amplitude differs from the beta topography of IRF's (Figure 3 E). Last we investigated the ERP power spectrum (Figure 3 F) for the time-frequency window in which we found the strongest beta increase in the IRF (Figure 3 A,D, black dashed box). No peak in the beta range is observed for the ERP. These findings support the claim that perceptual echoes, as in the visual domain, are not simply evoked potentials but characterize unique oscillatory dynamics in response to white noise input.

4.4.2 Steady State Stimulation evokes maximal response at 25 Hz

Similar to the visual perceptual echoes the tactile IRF's appear to oscillate at an endogenous frequency of the somatosensory system. We were interested in verifying that the echoes reflect the natural frequency of the tactile domain which has previously been shown to lie between 21 and 27 Hz (Snyder, 1992; Tobimatsu et al., 1999; Muller et al., 2001). In order to do so we applied tactile stimulation at multiple frequencies. We then correlated the peak frequencies acquired from the SSSEP with the individual peak frequency of the echo. SSSEP's were extracted using a spatiotemporal source separation method previously described in (Cohen & Gulbinaite, 2017). The spatial filters acquired using Generalized eigenvalue decomposition (GED) were mapped onto source space using a model brain (Figure 4 A). Spatial filters were applied to the raw data to extract the SSSEP signal with the best signal to noise ratio for every frequency. Figure 4 B

shows the brains frequency response for every input frequency. We can see that stimulation frequencies in the beta band (20 to 30 Hz) led to strong frequency responses in the EEG signal at similar frequencies (Figure 4C). The mean peak response frequency was 25 Hz. These findings verify previous accounts, placing the resonance frequency of the somatosensory system in the 25 Hz beta range (Snyder, 1992; Tobimatsu et al., 1999; Muller et al., 2001).

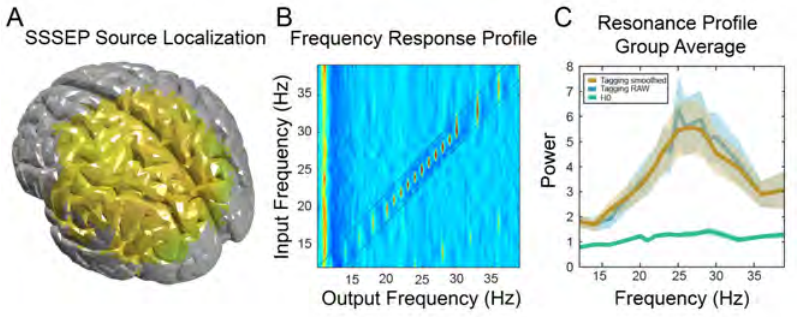

Figure 4. *SSSEP analysis.* **A**. We used Generalized Eigenvector Decomposition to generate spatial filters to extract the SSSEP signals. The Model brain shows the average over individual filter weights. **B**. Average Input-Output frequency spectrum. Input frequencies are along the y-axis and Output frequencies along the x-axis. Hot colors indicate stronger responses at the respective frequency. We observe strong oscillatory responses for the input frequencies in the beta band. **C**. Average resonance profile of frequency responses. Blue: Raw resonance profile of GED signal. Brown: Smoothed resonance profile of GED signal. Green: resonance profile for GED noise.

4.4.3 Relationship between SSSEP's and Perceptual Echoes

We were specifically interested in investigating how the SSSEP signals relate to the tactile IRF's. We therefore compared the peak frequency in the SSSEP's, defined as the frequency at which the strongest oscillatory response is observed, with the peak frequency of individual IRF's. We used the channels of interest as well as the previously defined time frequency window to extract the peak frequency of individual tactile perceptual echoes. Power spectra were calculated for each channel of interest per subject. The channel with the highest power between 15 and 35 Hz was selected and the peak frequency was extracted. The average peak frequency based on this "best channel" approach was 22.7 Hz (std:

+-2.52). SSEP peak frequencies where then correlated with IRF peak frequencies. Spearman correlation revealed a significant positive relationship between IRF peak frequency and SSSEP peak frequency (Figure 5A, $p < 0.05$).

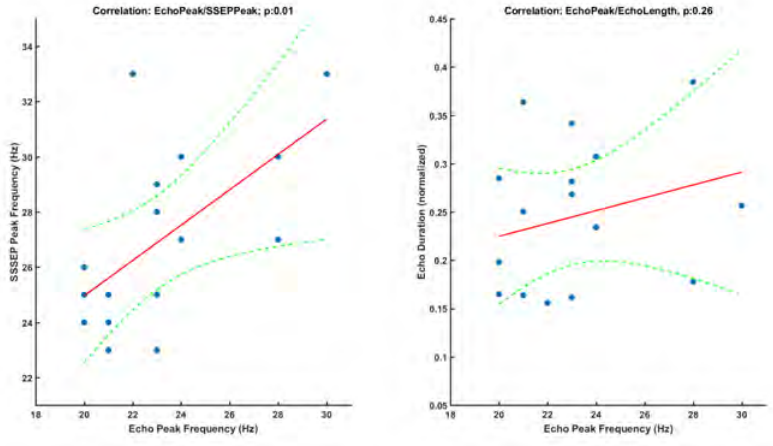

Figure 5. *Correlation analysis.* **A**. Pearson correlation between IRF peak frequency and SSEP peak frequency. We observed a positive correlation for the peak frequencies of both neural signatures indicating a common neural generation mechanism ($p < 0.05$). **B**. Pearson correlation between IRF peak frequency and normalized IRF length. No significant correlation was observed between normalized echo length and echo frequency ($p>0.05$).

4.5 Discussion

Previously it has been shown that visual random noise stimulation leads to a unique oscillatory Impulse Response function (perceptual echo) revealed by cross-correlating the white noise sequence with the corresponding EEG trial (VanRullen & Macdonald, 2012). This white noise sequence had strong power in the alpha band which is frequently identified as the resonance frequency of the visual system (Herrmann, 2001). The findings were intriguing because alpha power is usually observed to de-synchronize in response to visual stimulation. The fact that they can increase during visual processing highlight alpha oscillations as active mechanism that plays a special role in the visual system. A remaining question is if the perceptual echoes constitute a more general oscil-

latory mechanism that can also be found in other modalities. We therefore set out to investigate if we find perceptual echoes in the tactile domain. Our research question was therefore 3-fold. 1. Can we find oscillatory IRF's in response to tactile white noise stimulation? 2. How do these IRF's relate to the resonance frequency of the somatosensory system? 3. Do the tactile perceptual echoes constitute traditional ERP's or are they a novel oscillatory signature? We found that perceptual echoes can be found at 22 Hz in the somatosensory domain. Furthermore their peak frequency correlates with the resonance frequency of the somatosensory system. Last we demonstrated that tactile IRF's show fundamentally different oscillatory dynamics compared to somatosensory ERP's and therefore present a unique oscillatory signature.

The cross-correlation between tactile white noise (WN) sequences and corresponding EEG signal revealed 200 ms long IRF's that showed strong power in the beta band (22 Hz). Theoretically the so-derived IRF should resemble a classical ERP since both signatures represent the brains response to a single Impulse. We found however that they differ drastically. The ERP shows mostly low-frequency deflections reflecting classical ERP components. The IRF showed very little low-frequency components but rather a burst of beta oscillations that lasted for about 4 cycles similar, to IRF's found in the visual system (VanRullen & Macdonald, 2012). This was only the case if the cross-correlation was calculated with the correct WN/EEG pair. No reverberation was observed in the surrogate echoes where WN/EEG pairs were shuffled. This demonstrates that the somatosensory system selectively reverberates the specific beta component that was present in the respective trial. Given that our WN sequences were per definition frequency neutral, we can infer that the beta band plays a special role in active stimulus processing in the tactile domain. Tactile stimulation or electrical stimulation of the median nerve is accompanied by two signatures in the SS-system. One is a classical somatosensory evoked potential consisting of low frequency deflections and the other is a suppression of mu and beta activity (Pfurtscheller, 1981; Pfurtscheller, Woertz, Müller, Wriessnegger, & Pfurtscheller, 2002; Cheyne et al., 2003; Gaetz & Cheyne, 2006). These observations have given rise to the disputed hypothesis that a decrease in beta power reflects an increase in excitability (Pfurtscheller & Lopes da Silva, 1999; Kilavik et al., 2013) whereas an increase in beta might reflect active inhibition (Solis-Escalante, Müller-Putz, Pfurtscheller, & Neuper, 2012). Given these postulations the oscillatory characteristics of the IRF's are rather surprising since

one would expect a decrease in beta power following stimuli, similar to the one observed in SS ERP's. While the ERP could be considered an Impulse response function as well there are some important differences between them and perceptual echoes. First of calculating the IRF using cross-correlation assumes that the underlying system implements linear transformations which is clearly not true for the brain. Non-linear relationships between WN and EEG will therefore not be captured. Second the cross-correlation is a measure of similarity between two signals over time whereas ERP's are measure of cortical activity. Nevertheless these differences it is not trivial to explain the discrepancy between the oscillatory dynamics between the two.

Similarly to alpha oscillations in the visual domain (VanRullen, 2016), beta oscillations have been suggested to implement discrete perceptual cycles in the tactile domain (Baumgarten et al., 2015). The idea of discrete perception has been studied mostly in vision but potentially represents a general cortical mechanism for complexity reduction and metabolic efficiency in all sensory modalities (Schroeder & Lakatos, 2009; Jensen, Gips, Bergmann, & Bonnefond, 2014). Discrete perception proposes that continuously inflowing information is discretized into separate perceptual moments, within which temporal information is discarded. Two stimuli that fall within one such cycle would therefore be perceived as simultaneous. In the visual domain perceived simultaneity was shown to be dependent on the phase of alpha oscillations whereas in the tactile domain perception was determined by the phase of low beta oscillations (Baumgarten et al., 2015; VanRullen, 2016). Importantly these observations propose an active role for beta oscillations in temporally organizing information. This is in line with our observation that Two recent studies have implicated the perceptual echoes in regularity learning and predictive coding processes. The repeated presentation of a single WN sequence leads to incremental increase in oscillatory alpha power in the corresponding IRF (Chang et al., 2017). This increase is persistent even when the repetition is intervened with a novel WN sequence. The authors hypothesized that, in line with the idea that the visual system dynamically encodes visual sequences, the perceptual echo is a signature of this regularity learning mechanism. The authors discussed the possibility that the echoes might reflect a rhythmic updating of predictions about expected stimulation patterns thus giving rise to 10 Hz oscillations. Along these lines it was demonstrated that a simple computational predictive coding model was able to display similar echoes that showed characteristics of travelling waves moving

along the visual hierarchy (Alamia & VanRullen, 2019). Their results were verified in human EEG echoes that showed similar travelling wave dynamics that altered their direction depending on if visual input was present or not. Together these results suggest that IRF's might reflect predictive coding processes that continuously generate and update predictions about incoming information at an alpha rhythm (Friston, 2005; Linares, Holcombe, & White, 2009; Clark, 2013; Seth, 2014). Their locus of generation might therefore lie in the interactions between different columns in the visual hierarchy hypothesized to implementing predictive coding computations, potentially through canonical microcircuits (Bastos et al., 2012).

Endogenous beta oscillations can be observed in the somatosensory system (SS) during rest (Crone et al., 1998; Fransen, Dimitriadis, van Ede, & Maris, 2016). Experiments using rhythmic stimulation at various frequencies have shown that the SS responds strongest to stimulation at beta frequencies (Snyder, 1992; Tobimatsu et al., 1999; Muller et al., 2001). Using a spatiotemporal source separation method we investigated the resonance frequency of the SS of individual subjects to replicate previous findings and enable a direct comparison to tactile IRF's. Confirming previous reports we found the mean resonance frequency to be 25 Hz. A statistical analysis revealed a significant positive correlation between individual SSVEP peak frequencies and individual IRF peak frequencies indicating similar underlying neural generators.

4.6 Conclusion

In conclusion we find that similar to the visual domain, perceptual echoes are a signature of the somatosensory system as well. This means that incoming temporal tactile stimulation sequences are reverberated in the beta band for 4 cycles. Perceptual echoes significantly correlate in frequency with the resonance frequency of the SS system pointing at a common generator. Our findings provide further evidence that the beta rhythm is actively involved in stimulus processing. This active participation might be explained by predictive coding processes that have been hypothesized to give rise to the IRF dynamics in vision.

Rhythms of the brain, rhythms of attention: How neural oscillations give rise to attentional selection.

The previous chapter provided us some insight into the oscillatory neuronal dynamics that govern the tactile domain. The next logical step would be to relate this oscillatory activity to behavior to get a better understanding on which exact functions they implement. The following chapter tackles this idea in the context of attentional sampling. Although not directly correlating behavior with oscillatory activity, the motivation for this project stems from a study investigating intracranial recordings in macaques that found exactly this kind of relationship. In their paper, Kienitz et. al. (2018) were able to show that theta oscillations might help the brain to select attended targets and inhibit stimuli that are unattended. They provided convincing behavioral data in support of their hypothesis.

Attentional selection in humans has previously been related to frontal theta oscillations but never has a causal link been established. Moreover the frontal theta oscillations do often not correlate well with behavioral measures of attention. Given the direct link between theta and attention on macaques we hope that by adapting an almost identical task design we could find similar patterns in humans. This would, although not strictly causal, make a strong point that the oscillations indeed implement attentional selection.

Chapter 5

Rhythmic fluctuations of saccadic reaction time arising from visual competition

The following chapter contains the original manuscript that appeared as: Chota, Samson, et al. "Rhythmic fluctuations of saccadic reaction time arising from visual competition." Scientific reports 8.1 (2018): 1-7.

5.1 Abstract

Recent research indicates that attentional stimulus selection could be a rhythmic process. In monkey, neurons in V4 and IT exhibit rhythmic spiking activity in the theta range in response to a stimulus. When two stimuli are presented together, the rhythmic neuronal responses to each occur in anti-phase, a result indicative of competitive interactions. In addition, it was recently demonstrated that these alternating oscillations in monkey V4 modulate the speed of saccadic responses to a target flashed on one of the two competing stimuli. Here, we replicate a similar behavioral task in humans (7 participants, each performed 4000 trials) and report a pattern of results consistent with the monkey findings: saccadic response times fluctuate in the theta range (6 Hz), with opposite phase for targets flashed on distinct competing stimuli.

5.2 Introduction

Many exploratory actions such as eye movements reveal a specific rhythmicity upon closer inspection. During overt saccadic exploration of the visual field, saccades occur approximately every 200 ms i.e. at 5 Hz (Otero-Millan, Troncoso, Macknik, Serrano-Pedraza, & Martinez-Conde, 2008; Hogendoorn, 2016; McLelland et al., 2016). Moreover, even in the absence of eye movements, target detection rates have been shown to vary as a function of the cue-target interval at a similar frequency. It has been proposed that these behavioral fluctuations emerge from rhythmic attentional processes in the theta range (VanRullen et al., 2007; Landau & Fries, 2012; Fiebelkorn et al., 2013; Holcombe & Chen, 2013; VanRullen, 2013; Song, Meng, Chen, Zhou, & Luo, 2014). Spatial covert attention paradigms have suggested that multiple objects in the visual field are rhythmically and sequentially sampled and that these attentional sampling rhythms are related to brain oscillations in the 4-8 Hz range (Busch & VanRullen, 2010; Dugué et al., 2015; Crouzet & VanRullen, 2017). In addition, causal evidence was provided by Dugué, Marque VanRullen (Dugué et al., 2011) who used non-invasive brain stimulation, demonstrating that stimulus processing is vulnerable to disturbances via single TMS pulses at constant intervals in the theta range.

In a recent study, Kienitz et al. linked theta oscillations in macaque V4 to an attentional sampling process (Kienitz et al., 2018). V4 has been previously

related to attention, e.g. via lesion studies (DeWeerd, Peralta, Desimone, & Ungerleider, 1999). Furthermore, sporadic theta oscillations have been measured in V4 as well as in inferotemporal cortex when the animals were viewing a single stimulus (Sato, Kawamura, & Iwai, 1980; Nakamura, Mikami, & Kubota, 1991; Sheinberg & Logothetis, 1997; Tamura & Tanaka, 2001; Lee, Simpson, Logothetis, & Rainer, 2005); when two stimuli were shown together, the competition between them resulted in intricate theta-band oscillatory phase relations between the corresponding IT neural responses (Rollenhagen & Olson, 2005). Building on these findings, Kienitz et al. (Kienitz et al., 2018) showed that the presence of two visual objects, one in the excitatory center ("object") and one in the inhibitory surround ("flanker") of a V4 neuron's receptive field (RF), resulted in theta-rhythmic multi-unit-activity (MUA). Furthermore, they showed that the saccadic reaction times to targets presented in either of the two stimuli were subject to similar fluctuations at 3-6 Hz. Most importantly, the phase of both RT time-series and MUA oscillations depended on the order of display onset between the object and flanker stimuli. The authors demonstrated that these theta-rhythmic fluctuations emerge from competitive receptive field interactions, and could at least partially underlie the rhythmic attentional sampling of multiple objects observed in numerous human studies (Busch & VanRullen, 2010; Dugué et al., 2015; Crouzet & VanRullen, 2017).

In the current study, we investigate this question in human subjects, using a behavioral spatial attention paradigm directly inspired by this monkey study (Kienitz et al., 2018). A central disk object and two bar flankers were presented in the periphery with asynchronous sequential onset (500 ms SOA), and remained on the screen while participants maintained fixation. After a varying SOA following the second stimulus onset, a target was presented either in the central object or the flankers. The subjects were instructed to perform a saccade to the target. Reaction times was investigated as a function of the SOA between the second stimulus and the target. As found in monkeys, the analysis of RT time-series revealed an oscillation at approximately 6 Hz; furthermore the phase of this oscillation was dependent on both the initial stimulus order (object- or flanker-first) and on the location of the target (object or flanker).

5.3 Materials and Methods

5.3.1 Participants

Seven volunteers (aged 19–25, 3 females, all right-handed) with normal or corrected to normal vision participated in the experiment. Informed consent forms were signed before the experiment. Te experiment was carried out in accordance with the protocol approved by the Centre National de la Recherche Scientifque ethical committee and followed the Code of Ethics of the World Medical Association (Declaration of Helsinki).

5.3.2 Protocol

Stimuli were presented at a distance of 50 cm with a cathode ray monitor (1280×1024 resolution, 85Hz refresh rate) using the Psychophysics Toolbox (Brainard, 1997) running in MATLAB (MathWorks). Eye movements were recorded and monitored online using an EyeLink 1000 Desktop Mount (SR Research). A 9-point calibration was performed before each block of trials. Throughout the Methods section we will explicitly note the differences with the monkey study by Kienitz et al. (Kienitz et al., 2018). If no mention is provided, task parameters at hand were kept identical.

Stimuli consisted of a fixation dot (central black dot, diameter=0.3˚; [0.07˚ in Kienitz et al. 2018]), the object (a black disk in the lower right part of the screen, 2˚ diameter, positioned 4˚ right and 2˚ down from fixation center [in Kienitz et al. 14 the disk was positioned, within the RF of a V4 neuron]) and the flankers (two bars above and below the disk, height=1˚, width=0.25˚, 1˚ gap between disk and each bar) (Fig. 1). Stimuli were presented on a gray background.

After a pseudo-random (400–800 ms [1000 ms in Kienitz et al. 2018]) interval during which participants maintained central fixation, the first stimulus of the sequence, either the Object or the Flankers, appeared. We introduced a variable delay in this pre-stimulus interval to counteract potential attentional effects that could be introduced by the predictability of the stimulus onset. The second stimulus (the Flankers if the Object was presented first and vice versa) was added to the display 500 ms later [Object was always presented first in Kienitz et al. 2018]. After another variable SOA (250 to 1250 ms, in steps of 12 ms [0 to 750 ms, in steps of 37.5 ms in Kienitz et al. 2018]) a small target (0.2˚

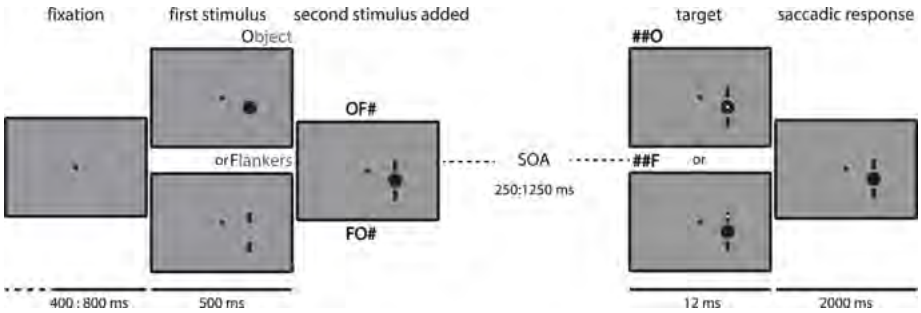

Figure 1. *Experimental Protocol.* Trials started with a fixation period during which participants maintained fixation for a variable delay between 400 and 800 ms. Following the fixation period the first stimulus (object or flanker) was presented for 500 ms after which a second object (flanker if object first (OFX) and vice versa (FOX)) was added. After a variable SOA of 250 to 1250 ms (in steps of 12 ms) a target was presented for 12 ms, either in the center of the object (XXO) or in the flanker (XXF). Participants were instructed to respond to the target with a saccade towards the stimulus in which it appeared.

diameter white dot) then appeared for a single frame (12 ms [8.3 ms in Kienitz et al. 2018]), either in the center of the upper flanker or the center of the disk object. In one out of 16 trials ([1 out of 3 in Kienitz et al. 2018]), no target was presented (catch trials). This reduction in the number in catch trials still allowed us to reliably control for non-target related saccades.

For consistency and clarity we will now refer to the four possible (non-catch) trial types as the conditions: OFO, OFF, FOO, FOF, where the 1st letter denotes the first stimulus onset (O for object, F for flanker), the 2nd letter corresponds to the second stimulus presented (identical notation), and the third to the stimulus in which the target appeared (identical notation) (See upper part of Fig. 2).

The timing of the target relative to the onset of the second stimulus (so-called stimulus onset asynchrony or SOA), was drawn from a uniform distribution with 85 steps from 250 to 1250 ms (corresponding to the refresh rate of the screen). The SOA tested on each trial was optimized online to equalize the number of trials obtained for each of the 85 SOA conditions: if a trial was not valid (see below), the same SOA value was more likely to be tested again.

The luminance of the target was adapted separately for each condition using a QUEST procedure (Watson & Pelli, 1983) so that each participant's detection

performance remained around 90%. We chose the 90% threshold in order to collect sufficient trials that could be entered in our analysis and at the same time require participants to pay attention. Because of the high number of trials, involving multiple sessions over several days, the luminance value defined by the QUEST procedure was adapted dynamically, based only on the last 40 trials.

Participants had to respond to the target by performing a saccade towards it. A saccade was considered valid if it landed in one of two 2° square boxes centered respectively on the object and upper flanker. Only valid saccades were included for further analysis. Reaction times (RT) were defined as the time between target onset and the time at which the eye position left a fixation region of 1° radius around the fixation point. Saccade durations were defined as the interval between the eye leaving the fixation region and the eye landing on one of the two boxes centered on object or flanker. To encourage participants to respond as fast as possible, online RT measurement were used and a message saying "TOO SLOW" was displayed if the RT of a given trial was above 2.5*SD from average (the average was calculated based only on valid trials (see below)). The experiment was stopped automatically when a participant obtained 4000 valid trials (split in blocks of 64). A trial was considered valid if (1) a target was presented, (2) the participant made a valid saccade to the correct location and (3) the RT was not an outlier (limits corresponding to 2.5*SD, updated online after each trial by considering all previous trials, even non-valid ones).

5.3.3 Data Analysis

During preprocessing, we removed all trials in which the saccade duration was above 70 ms, or the luminance value selected by the QUEST was outside the 2.5*SD limits (across all luminance values tested). For the RT analysis, we considered only trials in which a target was present (15 out of 16 trials) and the saccade was made to the correct location. This resulted in the inclusion of 72.67% of all trials on average (±5.62% standard error of mean across subjects).

To increase the number of trials per bin, SOA values were binned in groups of 3 (resulting in a change of effective sampling frequency from 85 Hz to 28 Hz). We validated in a separate re-analysis (not detailed here) that the exact position of the bin limits did not affect any of our findings. All the results were analyzed based on the binned SOA values. Single-trial RT values were then aggregated

for each condition and SOA bin, outliers were removed (values outside 2.5 SD around average), and averages computed to obtain RT time-series (average RT as a function of SOA) for each of the 4 types of sequences (OFO, OFF, FOO, FOF) and each subject.

We observed a strong negative trend in the RT time-series: early SOAs resulted in much slower RTs for most subjects. We attribute the slow RT decrease to the hazard rate although an additional forward masking effect could contribute to the early RT's (200 ms). To minimize the influence of these factors, RT time-series were de-trended using a second order polynomial (as is commonly done in most previous studies investigating oscillations of behavioral measures)

5.3.4 Frequency Analysis

RT time-series were analyzed in the frequency domain using both FFT and Hilbert methods. The 28 SOA values over a one second window allowed for a Nyquist frequency of 14 Hz. The complex FFT coefficients were squared to obtain oscillatory power at each frequency (Figs 2C,D and 3C,D).

5.4 Results

In the current experiment we investigated these fluctuations in a target detection task in humans, directly mirroring one part of the monkey study by Kienitz et al. (Kienitz et al., 2018). We presented a first stimulus, to which a second one was added (Fig. 1). A target was then presented in either of the two objects with many possible SOA's, spanning a 1000 ms interval in 12 ms steps. The participant was instructed to make a saccade to the target as fast as possible. We analyzed the reaction times as a function of the variable SOA. The dense temporal sampling of the target interval allowed us to quantify these behavioral modulations using frequency decomposition methods (Fourier and Hilbert transforms).

5.4.1 Fluctuations in RT time-series

To investigate rhythmic fluctuations in behavior, we performed a frequency analysis on the RT time-series for each condition separately. Although the average time courses (Fig. 2A,B) do not show evident oscillations (possibly due

to small differences in phase or frequency across subjects), the power spectra revealed a dominant oscillation at around 6 Hz for all conditions (Fig. 2C,D). To test if the observed peak at this specific frequency could be due to chance, we created 2000 surrogates by shuffling the 28 SOA-bin labels within subjects and within conditions and recalculating the power spectra. P-values were computed as the percentile of the mean power values within the bootstrapping distribution. This allowed us to test the null-hypothesis that all frequencies share similar power content. Both main data as well as the surrogates were de-trended. For all four conditions the observed spectral peak at 6 Hz proved to be significantly higher compared to the surrogate distribution (Fig. 2C,D; FOO: $p = 0.0045$, OFO: $p = 0.0012$, OFF: $p < 0.0005$, FOF: $p = 0.0255$). We observed additional significant peaks at 11 Hz (FOO: $p = 0.043$), 7 Hz (FOF: $p = 0.0185$), 14 Hz (OFF: $p = 0.0095$) as well as 1 Hz (OFF: $p = 0.003$; FOF: $p = 0.021$). As these additional effects were not consistent across the four conditions, we did not explore them further. The 6 Hz spectral peak, however, was present in all four conditions. Notably, the likelihood of all four conditions showing a significant peak at the same frequency would be extremely small under the null hypothesis: if the probability of one given frequency exceeding the statistical threshold is 0.05, then the likelihood of this event happening 4 successive times at the same frequency is 14 (frequencies) x 0.054 (conditions) = 0.0000875, i.e. $p < 0.0001$. We found no significant effect of stimulus sequence on the number of saccades during catch trials.

5.4.2 Opposed sequences reveal anti-phasic RT fluctuations

The spectral analysis illustrated in Fig. 2 reveals that all 4 experimental conditions display significant 6 Hz oscillations in behavioral RT time courses. Do all 4 oscillations share the same phase, or does the phase differ depending on task factors? In order to analyze potential differences in the phase of the observed oscillations, we subtracted the RT time-series of conditions that had identical target locations. These conditions differed only in the history of object and flanker presentation times. Stimulus competition normally begins when the second object appears on the screen; according to the idea of rhythmic attention sampling, this competition would initially be biased towards the second object (the last one to appear), then attention would move on to sample the first, and rhythmically alternate between them on subsequent cycles (Rollenhagen

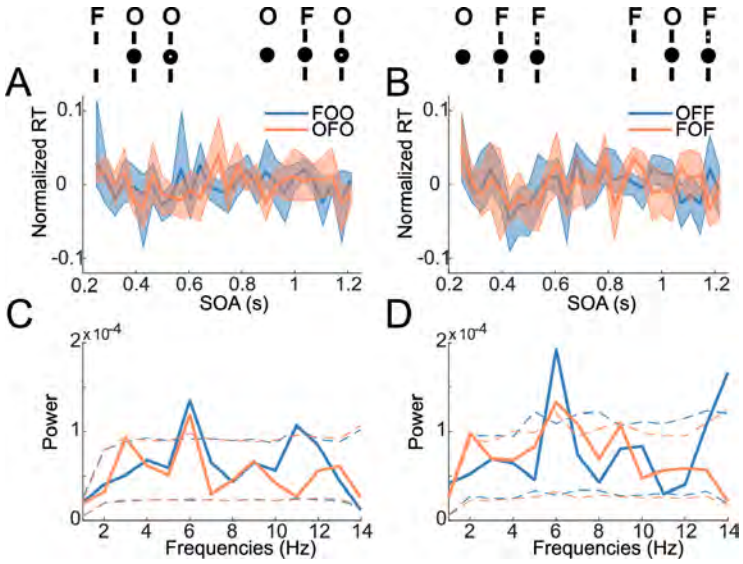

Figure 2. *Analysis of RT fluctuations for each condition.* The four conditions are illustrated at the top for reference; they vary based on the order of presentation of the stimuli (Object-first or Flanker-first) as well as the site of target presentation (Object, Flanker). (A,B) RT time-series averaged across subjects (error bars indicate bootstrapped 95% CI) for each of the four conditions, grouped according to the site of target presentation (Object in A, Flanker in B). (C,D) Average power spectrum across subjects for each of the four conditions (grouped as previously). Dotted lines indicate the bootstrapped 95% confidence interval under the null hypothesis that all frequencies have similar power. We observed a significant peak at 6 Hz for all four sequence types.

& Olson, 2005; Vanrullen & Dubois, 2011; Fiebelkorn et al., 2011; VanRullen, 2013). In other words, the phase of attention sampling (and thus the phase of behavioral RT oscillations, for a fixed target location) should be opposite for Object-first and Flanker-first sequences. Such an anti-phasic relationship should be visible as an elevated peak in the power spectrum of the difference in the RT time-series. Conversely, if oscillations for the two conditions shared the same phase, the subtraction should reduce the amplitude of the 6 Hz spectral peak.

As expected according to the rhythmic attention sampling idea, we observed an enhanced spectral peak at 6 Hz for both time-course subtractions (Fig. 3), indicating that the experimental conditions shared a frequency-specific oscillatory component, however with opposite phase for the two stimulation sequences.

For both comparisons, the amplitude of the 6 Hz peak in the subtraction was higher than that measured in either of the original signals (compare values in Fig. 3A,B with those in Fig. 2C,D), which is compatible with an anti-phase, but not an in-phase relation between the stimulation sequences. The significance of the 6 Hz peak (FOO minus OFO: $p < 0.001$, OFF minus FOF: $p < 0.001$, Bonferroni corrected) was confirmed by comparing it to a null hypothesis distribution, calculated by randomizing a subset of the target SOAs within subjects and between opposing sequences (FOO and OFO, OFF and FOF) 2000 times. The number of reaction times that were taken as the subset was determined by the total number of reaction times recorded for that specific SOA during the experiment, resulting in an identical number of trials per SOA in the original and randomized datasets. This method revealed an additional significant peak at 3 Hz ($p < 0.001$) for the FOO minus OFO condition, however markedly smaller than the peaks at 6 Hz.

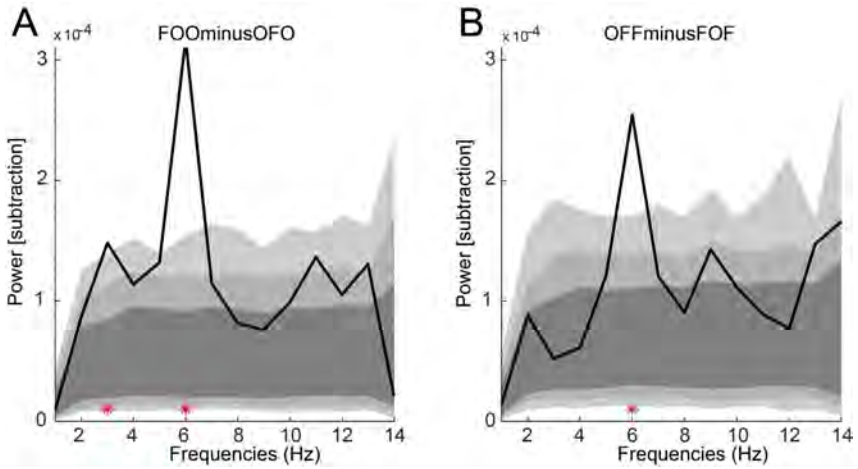

Figure 3. *Frequency Analysis of the difference in RT time series.* Comparison between conditions with identical target location (FOO vs. OFO in A, OFF vs. FOF in B). Light grey areas indicates the bootstrapped 99.9% CI (99% in darker grey, 95% CI in darkest grey). Red dots indicate frequencies with significantly higher power compared to a null hypothesis distribution calculated by randomizing the SOAs within opposing sequences.

5.5 Discussion

Our experimental paradigm was based on previous primate studies that investigated the oscillatory responses to competing stimuli (Rollenhagen & Olson, 2005; Kienitz et al., 2018). The paradigms used in these previous papers were as follows: A sequence of three stimuli was presented, Object followed by Flanker, or vice versa, followed by a target that could appear either in the Object or in the Flanker (Fig. 1). Firing responses of V4 and IT neurons selective for either of the stimuli (Object, Flanker) were recorded. The authors observed that firing rates oscillated at 4-5 Hz following stimulus presentation. Furthermore, if the neuron's "preferred" stimulus was presented second, the same oscillation was observed but in anti-phase (compared to the condition with "preferred" stimulus first). These oscillations were present but significantly weaker when only one stimulus was presented (even when it was the neuron's preferred stimulus). Finally, the Kienitz et al.14 study further revealed direct behavioral correlates of these oscillations, whereby rhythmic fluctuations of saccadic reaction times accompanied the firing rate oscillations. Altogether, these findings imply that the competition between visual neurons coding for distinct neighboring objects in the visual scene is modulated at around 4-5 Hz. The authors suggested that this modulation of competition might reflect a rhythmic attentional sampling mechanism, initiated by the sequential presentation of the two competing objects.

Here we investigated whether a similar mechanism could lead to behavioral theta-rhythmic fluctuations in humans. Using a similar experimental paradigm, we provided strong evidence that all four stimulus sequences (i.e., regardless of stimulus temporal order and target location) lead to rhythmic modulations in saccadic reaction times. Spectral analysis of the RT-time series revealed that 6 Hz is the dominant frequency of these fluctuations. We also confirmed that opposing sequences that differed only in the temporal order of the first two stimuli (Object-first or Flanker-first, keeping target location constant), induced fluctuations with opposing phase. This was shown by subtracting the two RT time-series followed by an examination of the spectral content of the difference wave. Our results are consistent with those of Kienitz et al., supporting the idea that an attentional sampling mechanism may underlie the theta-rhythmic fluctuations in behavior in monkeys and importantly extending them to humans.

An increasing number of studies have reported rhythmic fluctuations in perceptual performance. In the specific case of spatial attention, when multiple objects are presented on the screen, attention seems to alternatingly switch between the attended objects (VanRullen et al., 2007; Dugué et al., 2011; Landau & Fries, 2012; Fiebelkorn et al., 2013; VanRullen, 2013; Macdonald, Cavanagh, & VanRullen, 2014; Dugué et al., 2015, 2016). This alternation is assumed to be instantiated by a sequential attentional sampling process that leads to behavioral oscillations that are out of phase for the different attentional targets. A crucial element in the investigation of attentional processes is the relationship between behavior and neuronal processes. While it is difficult to investigate theta oscillations measured from single cells in humans, there are a number of electrophysiological EEG/MEG studies successfully relating theta rhythmicity in the human brain to attention. Busch VanRullen (Busch & VanRullen, 2010) investigated pre-stimulus oscillatory activity, by contrasting trials in which target detection was successful to unsuccessful trials. They found that the pre-stimulus phase in the theta band was predictive of stimulus detection, however only for attended stimuli, indicating that attentional sampling operates at around 7 Hz. Landau et al. (Landau et al., 2015) reported that pre-target gamma-band activity was modulated at 4 Hz when two stimuli were presented on the screen. Furthermore this modulation was predictive of task performance and provided important evidence for the hypothesis that the presentation of a relevant stimulus resets an ongoing attentional mechanism. These findings are especially relevant in the context of our study, since it is based on the assumption that the behavioral performance fluctuations are a result of a phase reset of an ongoing attentional oscillation by the stimulus onsets in the display sequence.

The above mentioned studies indicate that the pre-stimulus phase of theta oscillations can predict performance (Busch & VanRullen, 2010; Hanslmayr, Volberg, Wimber, Dalal, & Greenlee, 2013; Dugué et al., 2015). This raises the question of how ongoing and evoked (phase-reset) theta oscillations interact to influence task performance. Insight can be provided by the findings of Dugue et al. (Dugué et al., 2015): In their EEG experiment on visual search they observed pre-stimulus theta phase opposition between successful and unsuccessful search trials, together with stronger post-stimulus theta phase-locking as well as higher post-stimulus theta amplitude for successful compared to unsuccessful trials. This suggests that the pre-stimulus theta phase was indicative of both the post-stimulus EEG signal and of task performance; to account for this relation

between pre- and post-stimulus oscillations, they assumed that the presentation of a stimulus only leads to a partial phase reset of ongoing theta oscillations.

While our paradigm, closely resembling Kienitz et al. (Kienitz et al., 2018), was mostly concerned with covert attention, it remains unclear how our findings would translate to overt attention. Would we observe similar periodic fluctuations when observers are free to explore the visual scene? Interestingly eye movements occur approximately every 200-300 ms even in absence of a task, i.e. during free exploration (Otero-Millan et al., 2008). This rhythmicity is preserved if a target detection task is performed, in which participants can explore the visual scene freely (Hogendoorn, 2016). A crucial piece of evidence in the study by Hogendoorn is the fact that the phase of the behavioral oscillation did not change as a result of the saccade, indicating that the saccades may have been executed as part of an underlying attentional oscillation. One interpretation of these results is thus that a unique theta-rhythmic sampling mechanism could underlie both overt and covert forms of spatial attention.

Kienitz et al. (Kienitz et al., 2018) suggested that center surround interactions between neighboring stimuli in V4 might facilitate attentional stimulus selection. The fact that the excitatory center of V4-neurons found by Kienitz et al.14 showed maximal responses for stimuli measuring 2° of visual angle certainly restricts the conclusions that can be drawn in terms of larger objects or of wider distances. It is thus an open question how the brain could instantiate attentional selection among objects that are further spread across the visual field. Would this interaction still arise in V4, or in hierarchically higher areas with larger receptive field sizes spanning larger distances? It has been shown that similar behavioral competition can result in anti-phase theta-band rhythmic attentional sampling between two stimuli presented in opposite hemi fields (VanRullen et al., 2007; Landau & Fries, 2012; Fiebelkorn et al., 2013), and that corresponding neural correlates can be observed in visual cortex (based on MEG source reconstruction) (Landau et al., 2015). The precise neural source of this large-scale rhythmic attentional sampling, however, remains to be determined by direct electrophysiological experiments.

Our paradigm used 3 stimuli (one object and 2 flankers) of which 2 (the object and one flanker) were behavioral significant. It would therefore be highly interesting to investigate how attention behaves if the number of potential tar-

get positions is extended beyond 2. Similar experiments have been conducted by Holcombe and Chen (Holcombe & Chen, 2013) as well as Macdonald et al. (Macdonald et al., 2014). They suggest an attentional sampling mechanism with limited capacity, such that multiple objects are sampled less and less frequently with increasing numbers of objects. We intend to investigate this matter in future experiments.

5.6 Conclusion

In conclusion we provided new evidence for a sequential attentional sampling mechanism in the theta range (6 Hz) in humans. Our findings support those of Kienitz et al. (Kienitz et al., 2018), and demonstrate similar behavioral patterns in monkeys and humans. Our conclusions provide further insight into how the brain resolves potential competition by using attentional mechanisms to rhythmically select relevant stimuli.

Attention warps time: How saccadic mechanisms can influence Temporal Order Judgements.

In the previous chapter i presented findings that highlight the rhythmic nature of attentional selection. These findings allowed us to link attentional rhythms closely to neural oscillations. Importantly however we have only investigated covered attention until now, and have ignored saccades as a tool for attentional selection. Both of these systems need to be neatly orchestrated to provide us with a stable vision in the light of fast and frequent eye movements. The process implementing this function is referred to as saccadic remapping.

In order to perform successful saccadic remapping the visual system needs to detect the features and position of all relevant items in the visual field, then perform the saccade, and then match these items to the objects in the shifted visual field. We assumed that this process recruits attentional sampling that processes relevant objects in a sequential fashion. In the following paper we describe an experiment in which we activate saccadic remapping processes with a strong full field mask. Interestingly this leads to reversal of perceived order for two stimuli that were presented right before the mask. We hypothesize that this effect might be caused by the mask-induced interruption of theta rhythmic activity that sequentially samples stimuli for saccadic remapping.

Chapter 6

Full Field Masking Causes Reversals in Perceived Event Order

The following chapter contains the original manuscript that appeared as: Chota, Samson, et al. "Full Field Masking Causes Reversals in Perceived Event Order." Frontiers in Neuroscience 14 (2020): 217.

6.1 Abstract

We generally experience a stable visual world in spite of regular disruptions caused by our own movements (saccades, blinks) or by the visual input itself (flashes, occlusions). In trying to understand the mechanisms responsible for this stability, saccades have been particularly well-studied, and a number of peri-saccadic perceptual distortions (spatial and temporal compression, failure to detect target displacement) have been explored. It has been shown that some of these distortions are not saccade specific, but also arise when the visual input is instead abruptly and briefly masked. Here, we demonstrate that another peri-saccadic distortion, the reversal of the temporal order of a pair of brief events, may also be found with masking. Human participants performed a temporal order judgment task, and the timing of stimuli and mask was varied over trials. Perceptual order was reversed on 25% of the trials at the shortest stimulus to mask intervals. This was not merely a failure of target detection, since participants often reported these reversals with high subjective confidence. These findings update the constraints on models of stability around disruptions.

6.2 Introduction

Our visual system is continually challenged by disruptions, both in the form of externally imposed interruptions and internally generated saccadic eye movements. Characterizing the way that our brains build perceptual continuity in the face of these events can yield useful insights into the underlying mechanisms, as can the errors that are generated in the process.

Saccadic eye movements have been particularly well-studied in this regard, with several peri-saccadic illusory percepts characterized: displacement of an object during a saccade may go unnoticed ["saccadic suppression of displacement," (Bridgeman, Hendry, & Stark, 1975; Deubel, Schneider, & Bridgeman, 1996)] and both the spatial and temporal separation between briefly presented objects around saccade time is compressed (Ross, Morrone, & Burr, 1997; Lappe, Awater, & Krekelberg, 2000; Morrone, Ross, & Burr, 2005). These features were long identified with saccades and so were principally discussed within that context (Melcher & Colby, 2008). However, a number of studies have suggested that similar effects can be obtained during fixation if the visual scene is disrupted, by a saccade-mimicking shift of the stimuli (Mackay, 1970; O'Regan, 1984; Os-

tendorf, Fischer, Gaymard, & Ploner, 2006), or even by simpler manipulations such as flicker (Terao, Watanabe, Yagi, & Nishida, 2008) or a brief visual mask (Zimmermann, Born, Fink, & Cavanagh, 2014). This has led to the suggestions that these illusory percepts are not limited to saccades, but that the spatial and temporal compression may reflect more general mechanisms responsible for visual continuity in the face of disruptions (Zimmermann et al., 2014).

In the course of working with the masking paradigm used by Zimmermann et al. (2014), we noted another perceptual illusion: temporal reversal of a pair of brief visual events, that is, the later of two stimuli was perceived as occurring first. Again, a comparable illusory percept has previously been described for saccades (Morrone et al., 2005). To pilot our observation, we presented the demonstration video (Supplementary Video 1) as a repeated loop to 19 colleagues and found that 13 of them (including 4 out of 6 authors) reported seeing a temporal reversal (that is, they perceived the yellow probe as occurring before the red target).

During our pilot, the reports of mask-triggered, perceptual reversals were variable and did not reliably occur in every participant. When tested in the context of saccades, Morrone et al. (2005) reported a maximum reversal rate of almost 100 percent for their two participants as did Binda et al. (2009); however, further reports, also with saccades, suggest much lower probability of reversal perception on average (Kitazawa et al., n.d.; Kresevic, Marinovic, Johnston, & Arnold, 2016). In particular, Kresevic et al. (2016) found that just 7 of their 11 participants experienced robust occurrence of reversals with substantial interindividual variability in the proportion of reversals and the timing of the peak effect.

Here, we describe and formally test a masking procedure that yields this illusory reversed order percept in the majority (9 out of 14), but not all participants, and present results characterizing the temporal dynamics of the illusion (the effects of relative timing between the successive visual targets and the mask).

6.3 Materials and Methods

6.3.1 Participants

Fourteen participants (8 male) were tested, aged between 21 and 34 years old. All were naive to the goals of the experiment. All participants provided written informed consent. They were not preselected based on perception of the reversal in the demonstration video, and no authors were included. The experiment was carried out in accordance with the protocol approved by the Centre National de la Recherche Scientifique ethical committee and followed the Code of Ethics of the World Medical Association (Declaration of Helsinki).

6.3.2 Stimuli

The stimuli (Figure 1) comprised a fixation point, two briefly flashed objects at variable stimulus onset asynchronies (SOAs), and a full field mask, details as follows. Stimuli were generated using the Psychtoolbox extension (Brainard, 1997) for Matlab (Mathworks), and presented on a CRT monitor (100 Hz frame rate, 800 × 600 pixel resolution, 36.5 × 27.2 cm screen) at a distance of 57 cm from participants, who were seated with head position maintained at the center of the monitor by a chinrest. Stimuli were presented against a mid-gray background (CIE xyY 0.30 0.30 6.1). The fixation point was a black cross, situated toward the left of the screen (7.2˚ of visual angle from midline), at mid height, and was present continuously. The eccentric position of the fixation cross served to simulate conditions for an experiment with saccades toward the targets.

Two stimulus objects were presented to the right of the fixation point, also at mid screen height. The first, which we shall refer to as the "target," appeared with unpredictable timing relative to trial start (equal probability from 300 to 800 ms), for a duration of 50 ms. All other timings are described relative to target appearance. The target was presented 7.2˚ to the right of the fixation point, and comprised a red rectangle (CIE 0.54 0.32 4.65) with a 2-pixel wide blue border (CIE 0.18 0.15 1.8), the whole measuring 3˚ tall by 0.9˚ wide.

The second stimulus object, which we shall refer to as the "probe," was presented 2˚ to the right of the target, and with similar characteristics, except that the rectangle fill was yellow (CIE 0.41 0.48 11.6). The probe was presented for a duration of 20 ms, with variable SOA relative to the target across trials, from

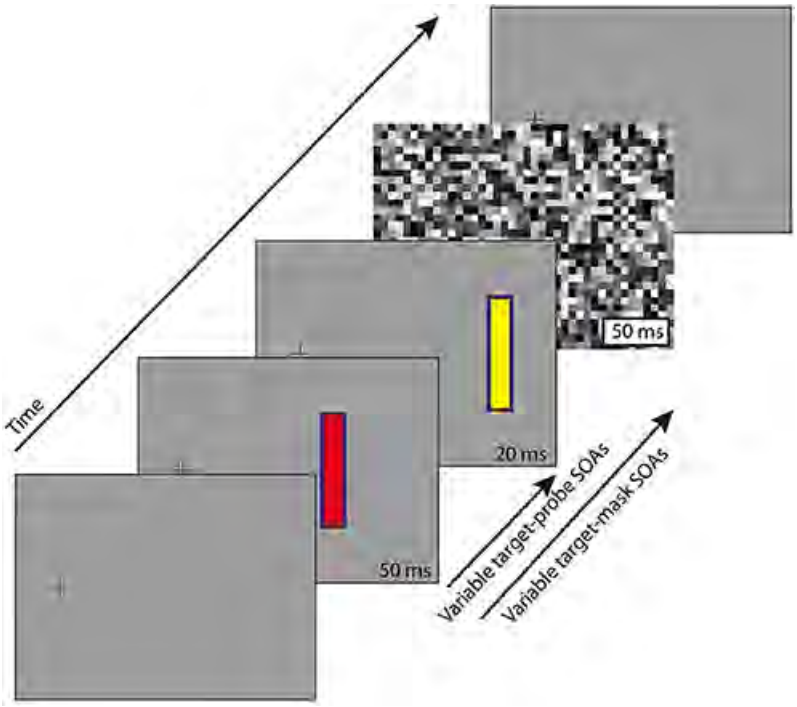

Figure 1. *Stimulus paradigm.* Participants maintained fixation on the black cross throughout. After a variable delay from trial start (300-800 ms), a target appeared (red, 50 ms duration), and with variable SOA around that (-20 to 160 ms) a probe (yellow, 20 ms duration). Note that the target and probe are at non-overlapping locations (see text for details). A full-field pixelated mask was presented (50 ms duration) at one of 3 delays after target onset: 50, 100, or 150 ms. There was also a no-mask control condition. For a demonstration of the illusion we refer to the video in the Supplementary Material.

20 ms before to 160 ms after, in 10 ms steps. The choice of SOA's and stimulus duration was determined by prior piloting to maximize illusory reversals.

The mask comprised a full-screen flash of pixelated white noise (see Figure 1), with square "pixels" measuring 1.1˚ each side, and each pixel taking a random luminance value (equal probability from minimum screen luminance, CIE 0.13 0.08 0.0, to maximum screen luminance, CIE 0.29 0.30 17.1). The mask was presented for a duration of 50 ms, with variable SOA relative to the target across trials, at 50, 100, or 150 ms. When mask and probe were simultaneously present, the probe was always drawn over the mask (that is, the mask did not directly conceal the probe).

There was also a control condition in which no mask was included. In total, 76 conditions (19 probe SOAs × [3 mask SOAs + 1 control]) were presented in random order, with 25 repeats of these blocks resulting in 1,900 trials per subject. All trials were collected over the course of 1–2 sessions per participant.

The participants' task on each trial was to report whether the target (red/leftmost) or probe (yellow/rightmost) appeared first, using a key press (target, "F"; probe "J"). If unsure, participants could indicate this (while still making a forced target/probe first choice) by using a different key pair (target, "G"; probe, "H"). Responses were not time limited, and the response key press launched the next trial. Pauses were included between blocks (terminated by the participant pressing the space key).

To enable readers to experience the illusion for themselves, we include a video of the stimulus paradigm (Supplementary Video 1), with timings that typically generate the illusion on a proportion of trials in most participants using a typical monitor with 60 Hz refresh rate: target duration 50 ms, target:probe SOA 117 ms, probe duration 17 ms, target:mask SOA of 150 ms, mask duration 50 ms, although note that the precise timings obtained will obviously depend on the video display equipment used.

6.3.3 Data Analysis

Data were analyzed and prepared for presentation using Matlab (Mathworks). For single participant performance data, we show the maximum likelihood estimate (mle) with 95% confidence intervals (CI; Clopper-Pearson method, Matlab binofit function). Where the difference from control performance is shown, we again show mle with 95% CI [Newcombe's CI, see (Newcombe, 1998; Brown & Li, 2005)]. For the group averages, we show the mean ± standard error (SEM; n = 14 throughout). Maximum likelihood estimates were calculated for each participant individually and then averaged to obtain mean and standard errors displayed in the group averages.

Statistical analysis of the group averages was calculated by performing t-tests for each Target:Probe SOA. P-values were corrected for multiple comparisons using False Discovery Rate (fdr). Statistical analyses of single participant data

was performed using a Chi-square test with Yates correction. For single participant statistical analysis, only the peak SOA's at 10 and 20 ms prior to mask (selected based on the group average) were included.

6.4 Results

For the control task with no mask (black curves repeated in each of Figures 2A–C), the psychometric function followed a predictable trend, with accurate reporting of "probe first" (yellow first) for early target-probe SOAs, and "target first" (red first) for late ($> 95\%$ accuracy for SOAs of <0 and >50 ms). Bearing in mind that the red target (50 ms duration) had a longer presentation time than the yellow probe (20 ms), the expected point of subjective simultaneity is at an SOA of 15 ms, assuming that perceptual timing for these brief stimuli is based on the midpoint of stimulus duration. This assumption appears to hold up as the data show a value of about 16 ms for subjective simultaneity (Figure 2A).

Figure 2A (red trace) shows the effect of including the mask 150 ms after the red target onset. For most target-to-probe SOAs, performance was unchanged from the control condition (black trace). However, when the mask closely followed the yellow probe (probe to mask intervals of 20 ms or less, SOA of 130 ms or more), the probe was erroneously perceived as occurring before the target on a about 25% of the trials, in spite of the long target to probe delay. We will refer to these perceptual errors as "temporal reversals." Figure 2B (green trace) shows that effects were similar for mask 100 ms after the red target onset, with temporal reversals observed for probe timing close to or during the mask, reaching over 30% reversals for the probe to mask interval of 10 ms.

Reversals were again observed for mask onset at 50 ms following the red target offset (Figure 2C). In this condition, it is clear that the reversals continue after the mask presentation. Note also that this early mask condition showed some reversals even when the yellow probe physically preceded the red target (the two leftmost tests at negative SOA in Figure 2B). In this case, the yellow probe was erroneously reported as following the red on about 10% of the trials. Importantly the mask did not have to temporally overlap with the probe in order to induce reversals: they could arise for probe onsets 30 ms or more before the mask onset (Figure 2B; again, note that probe duration was 20 ms) or after

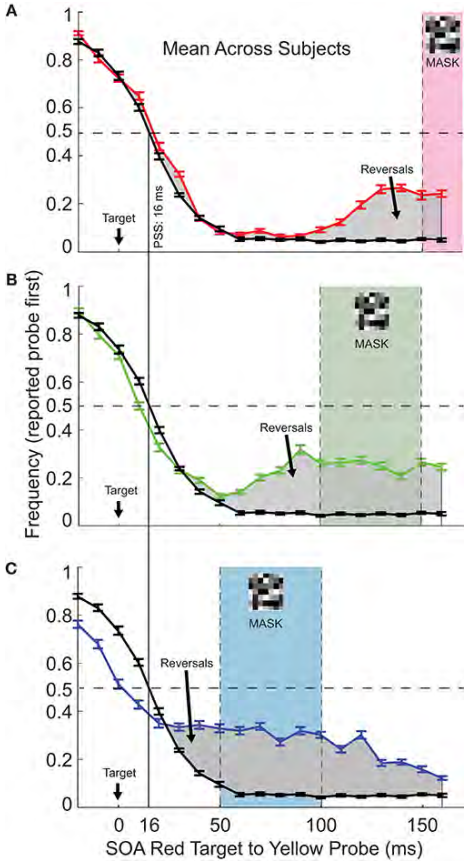

Figure 2. *The frequency of reporting probe first as a function of Target:Probe SOA and mask timing.* **(A)** The red curve shows mean performance (N = 14) for mask onset at 150 ms after the red target onset (mask timing indicated by the shaded area on the plot). The black curve, this plot and the following plots, shows performance in the control task, with no mask included. The vertical line indicates the Point of Subjective Simultaneity (PSS). For most probe timings, performance was unaffected by the inclusion of the mask. However, when probe onset was close to the time of mask onset, performance fell, that is, on a substantial fraction of trials, the probe was reported as occurring before the target, in spite of a >100 ms delay between them. Gray shaded areas indicate SOA's for which reversals were observed. **(B,C)** As for (A), except that the mask onset was at 100 ms (B) or 150 ms (C). Note that the same control curve is duplicated across plots for ease of reference. Error bars show ±1.0 SEM.

mask offset (Figure 2C).

Results compared to the control baseline with the data aligned to the mask onset are shown in Figure 3. T-tests on the group averages revealed several SOA's for which significantly more reversals were reported in all three mask conditions. Especially when probes were presented immediately prior to mask, reversals are frequently reported (students t-test, $p < 0.05$).

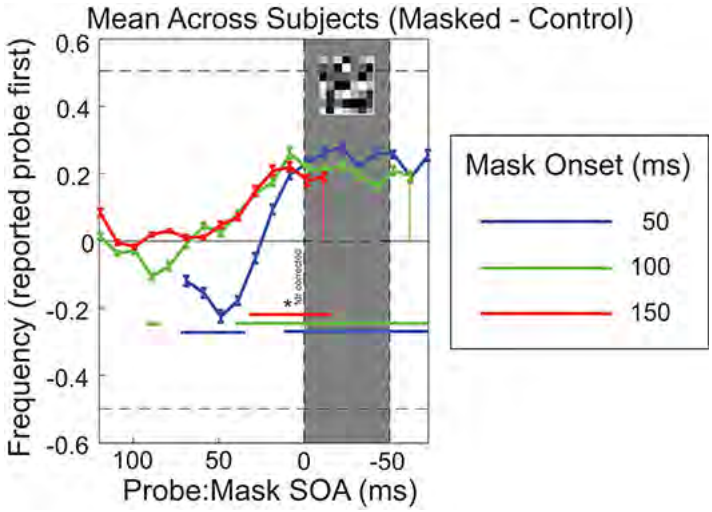

Figure 3. *Task performance aligned to mask onset.* Difference from control (no mask) performance (masked minus control). Mean result across participants (n = 14; error bars show SEM). Blue curves show results for mask onset at 50 ms, with mask timing indicated by the shaded gray area; likewise, green curves for mask onset at 100 ms, and red curves for mask onset at 150 ms. Blue, green and red horizontal bars denote the SOA's for which significantly more reversals were reported compared to 0 (students t-test, $p < 0.05$, false discovery rate correction).

6.4.1 Individual Differences

The individual results were quite variable. Five participants (Figure 4, S.B., M.A., M.M., S.C., L.T.) showed significant effects in all three masking conditions, with strong temporal reversals around mask timing for positive target:probe SOAs (Chi-square (with Yates correction, $p < 0.05$) tested on SOA 10–20 ms before mask onset). Four more participants (Figure 4, B.C., D.L., C.L., B.D.) showed a significant number of reversals in 2 out of 3 masking conditions. The remaining subjects showed significant reversals only in one (G.E.) or in none of the conditions (M.H., B.Z., J.K., B.H.).

We also observed some reversals for negative SOAs in the early mask condition in 10 out of 14 subjects. This was not unexpected since negative Probe:Mask SOA's in the early mask condition mimic the experimental parameters of positive Probe:Mask SOA's by simply swapping the timing of Probe and Target relative to the mask.

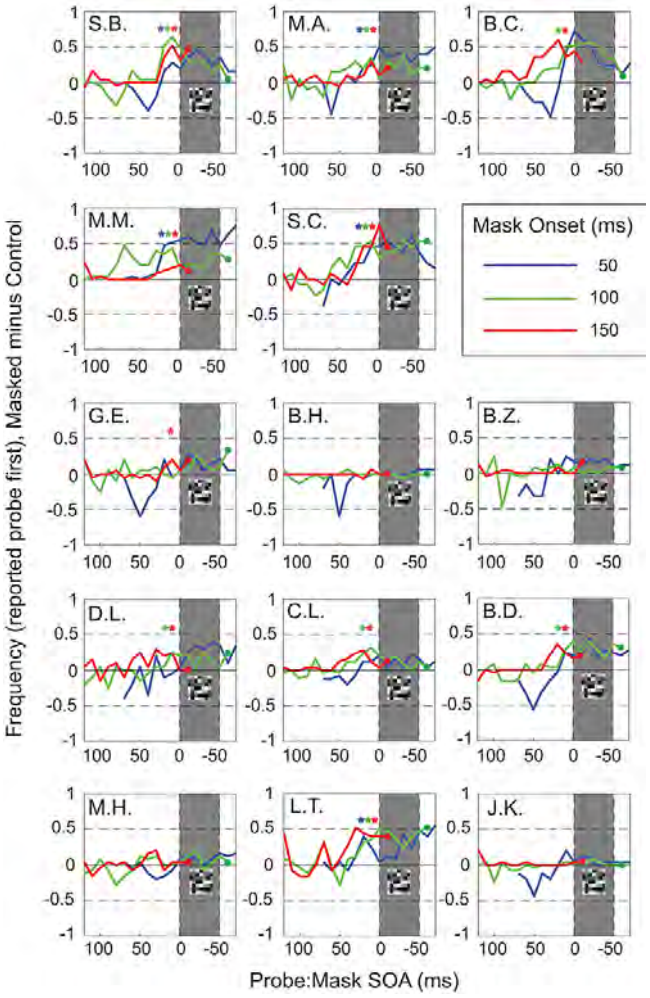

Figure 4. *Task performance aligned to mask onset (masked minus control).* Results for individual participants (mle). Blue curves show results for mask onset at 50 ms, with mask timing indicated by the shaded gray area; likewise, green curves for mask onset at 100 ms, and red curves for mask onset at 150 ms. Colored stars indicate significant increases in reported reversals compared to 0 (control/no mask) for blue (50 ms), green (100 ms), and red (150 ms) mask conditions at 10–20 ms before mask onset.

Participants were also required to include an indication of "high" or "low" confidence in their response on each trial (see Methods). High confidence trials indicate that participants clearly perceived the relative timing and detected both stimuli. Figure 5A shows that the analysis of only high confidence trials (78.7% of trials) resulted in a very similar pattern of temporal reversals over time, and only a slight reduction in the proportion of reversals reported. This shows that on trials where participants reported reversals, they most often had a clear subjective perception of both stimuli and their (illusory reversed) temporal order. Figure 5B shows the confidence ratings reported at the SOA's for which the strongest effects were observed (10–20 ms before mask, for every mask

condition, respectively). We separated subjects into two equal groups, one "frequent illusion" group, showing strong perceptual reversals and one "infrequent illusion" group, showing weak perceptual reversals. Separation was based on the frequency of reversals observed for SOA's prior to mask [10–20 ms, determined by a Chi-square test ($p < 0.005$)]. We did not find any significant differences in confidence ratings between the frequent reversal group (S.B., M.A., B.C., M.M., S.C., C.L., L.T.) and the complementary infrequent reversal group for any condition (students t-test) suggesting that differences in reported confidence do not suffice to explain perceived reversals.

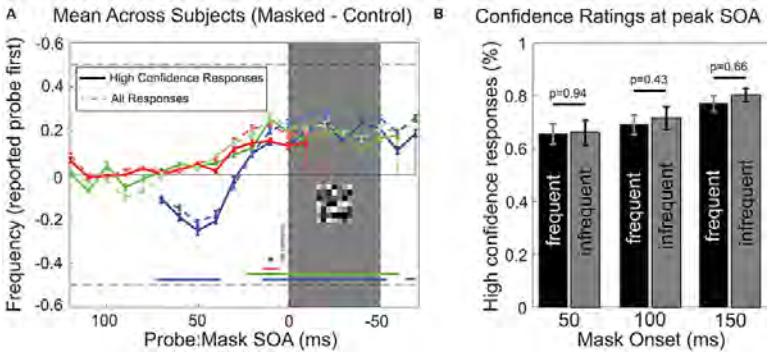

Figure 5. *Analysis of confidence ratings.* **(A)** Performance for high-confidence only responses. As Figure 3, except that only trials where participants responded with high confidence were included (mean across participants, ± SEM; n = 14). Faint dashed traces in the background show results for all trials for comparison. **(B)** Confidence ratings for the two SOA's for which reversals were reported most frequently [10 and 20 ms before MASK onset, see (A) for reference]. Participants were statistically divided into two equal groups, one "frequent illusion" (black bars) group and one "infrequent illusion" group (gray bars), based on the number of reversals that were observed for each subject for SOA's 10–20 ms before Mask [Chi-square test with Yates correction ($p < 0.005$)]. No significant difference in confidence was observed between subjects reporting frequent reversals and subjects reporting infrequent reversals for any mask condition (students t-test, $p < 0.05$). Error bars represent SEM.

6.5 Discussion

In this study, we have described a visual illusion whereby the temporal order of a pair of stimuli may be perceptually reversed when a visual disruption (full field mask) is presented.

This illusion resembles the phenomenon of temporal reversal previously described for events close to the time of saccades (Morrone et al., 2005; Kresevic et al., 2016). It has recently been shown that other visual phenomena, typically considered as "peri-saccadic," can also be produced by visual masking in the absence of saccades: spatial compression, temporal compression, and suppression of displacement (Zimmermann et al., 2014). Those results were taken to imply that the mechanisms underlying these phenomena might not be saccade specific, but rather reflect a more general mechanism to match corresponding visual objects across disruptions in space and time. Of course, despite the similarities between saccade- and mask-induced phenomena, the possibility remains that different or additional mechanisms are at play in the case of saccades. The present results contribute to this discussion as they show that yet another peri-saccadic phenomenon (temporal reversal) occurs for externally imposed visual disruptions.

While the original report of peri-saccadic temporal reversal presented data from a pair of participants who each experienced very robust reversals (approaching 100 percent of trials for optimal SOAs; (Morrone et al., 2005; Binda, Cicchini, Burr, & Morrone, 2009), more recent reports suggest much lower probability of reversal perception on average (Kitazawa et al., n.d.; Kresevic et al., 2016) similar to the levels we found here for mask-driven reversals. In particular, Kresevic et al. (2016) present individual data from 11 participants that emphasize the strong inter-participant variability in the perception of perisaccadic reversals: only 7 of their 11 participants experienced robust occurrence of reversals (greater than chance report level; around 80 percent reversals for each of those participants). Other participants reported 50 percent or lower reversals, and substantial variability in the timing of peak effect. The amplitude, time course and inter-participant variability of the effects are comparable for the saccade- and masking-triggered reversals. In particular, in the data of Kresevic et al. (2016), the peak timing for reversals was between 31 and 70 ms before the saccade onset (for 7 of 11 participants, including all of those with greater than chance levels of reversal). Since their two stimuli were separated by 50 ms, their peak effect occurred when the second stimulus appeared in the $\pm$20 ms around saccade onset. This is comparable to our observed probe to mask timing for the peak effect seen in Figure 3 where it is clear that most temporal reversals are perceived when the time of probe presentation is just before or overlaps with

the mask.

There are a number of suggestions for the origin of these temporal reversals, and here we will describe proposals arising from saccade and masking studies, as well as address possible confounds. First, it could be suggested that temporal reversals are simply an exaggerated version of temporal compression, that proportion of trials on which temporal compression was extreme enough to reverse the apparent order of stimuli. Both reversals and compression are found perisaccadically (Morrone et al., 2005; Binda et al., 2009) and with masking (Zimmermann et al., 2014). Binda et al. (2009) proposed that temporal compression could account for the perception of reversals in a temporal order. Briefly, the probability of observing a reversal under such a model depends on the overlap between two probability distributions, one each for the perceived timing of the "target" and the "probe." Reversals can occur within the overlapped regions and as compression pushed the distribution means together, the overlap increased, and according to the authors' model, so did the frequency of reversals. However, those results were for very short interstimulus intervals in the temporal order judgment task (8 or 20 ms) where there is clearly a large overlap between the distributions of the two judgments. This explanation cannot easily be extended to our data, with far longer intervals of up to 160 ms and more. To do so, the mask would have to dramatically broaden the probability distribution for the probe so that it overlapped with that of the much earlier target and, if this were the case, there should be more reversals for the conditions with shorter intervals between the target and the probe where there would be even more overlap. This did not happen: of the 9 participants showing high levels of reversals for late probes (Figure 4). Five of them show higher peak levels of reversals for longer vs. shorter target to probe SOAs (i.e., S.B., green peak higher than blue; S.C., red peak higher than blue).

Second, Kresevic et al. (2016) proposed that their data are consistent with perceptual insensitivity: the neural onset transient for a stimulus near to/during saccade time may be suppressed, leading to temporal ambiguity and necessitating a TOJ inference based on other cues than the unreliable temporal signals. For the majority of participants this would be apparent as a decrease in performance toward chance level, but, depending on biases in the inferential process (e.g., individual differences in assumptions about the temporally ambiguous stimulus, or in the assignment of attention), a subset of participants

could show more systematic (substantially above chance) reporting of reversals, a feature apparent in each of the pertinent data sets [current Figure 3; as well as (Morrone et al., 2005; Kresevic et al., 2016)]. A related account is that the visual disruption (mask or saccade) decreases the effective contrast/salience of stimuli, an effect that would be strongest for the stimulus closest in the time to the disruption. It has previously been shown that, in a simple TOJ task, a lower contrast stimulus is often perceived as having occurred before an earlier, higher contrast stimulus (Bachmann, Põder, & Luiga, 2004), although their finding of temporal reversal was restricted to short (<50 ms) SOAs. Kresevic et al. (2016) tested whether this might account for temporal reversals in their paradigm by repeating the experiment but replacing the TOJ task with a relative salience judgment. They found saccade-related suppression of salience, with timing matching the generation of reversals, supporting the above hypothesis. However, they actually found that salience suppression was more robust than temporal reversals across participants, and so concluded that additional factors must contribute on a participant-specific basis. Nonetheless, salience suppression remains plausible as a contributing factor in the generation of reversals in our mask-based paradigm.

An additional argument against the contribution of general temporal imprecision is that the results calculated only from the higher confidence trials show the same reversals and timing (Figure 5A). Furthermore, when comparing participants who frequently perceived reversals to those who did not perceive the illusion, confidence ratings did not differ (Figure 5B). These data suggest that while subjectively the temporal order of stimuli appeared clear to participants, a subset of them nevertheless consistently reported the wrong order, suggesting an illusion rather than an imprecision. To illustrate this we refer to the demonstration video of the stimulus paradigm in the supplementary materials (Supplementary Video 1). The illusion is best seen with the video set to loop repeatedly. Fixation should be maintained on the cross at the left of the window, with attention focused on the yellow (rightmost) bar. The task is to judge the order in which the red and yellow bars appear: a temporal reversal would be evident if the yellow bar were perceived first. Participants who do report reversals do not report difficulty in perceiving both target and probe (once accustomed to the stimuli and attending to the correct spatial location).

Another factor to consider is the potential role of "prior entry," whereby an

attended stimulus gains a temporal advantage in processing, and can be perceived as occurring before an earlier stimulus (Hikosaka, Miyauchi, & Shimojo, 1993; Spence & Parise, 2010), superficially similar to the temporal reversals described here. However, the absence of temporal advantage for the probe in our control (no mask) task showed no evidence of bias favoring the yellow probe over the red target in our stimuli. There are several other paradigms involving temporal reversals that deserve mention, namely masked priming (Scharlau, 2008), attentional blink (Akyürek et al., 2012; Spalek, Lagroix, Yanko, & Di Lollo, 2012), and motion-induced blindness (Wu, Busch, Fabre-Thorpe, & VanRullen, 2009). While having some resemblance to our paradigm we think that all of these examples are fundamentally different from the effects that we observe. In the masked priming paradigm of Scharlau (2007) the temporal order of a prime-mask and a subsequent stimulus is probed. No mask is presented that influences the two TOJ stimuli. In contrast we probe temporal order of two stimuli that are followed by a full field mask which has notable results as can be seen in our findings. Attentional blink phenomena are usually measured using rapid serial visual presentation and can be observed at SOA's of more than 100 ms. We observe reversals for much smaller SOA's between Probe and Target, starting at 30 ms and reaching full effectivity at 50 ms (see Figure 2C). Under very specific conditions motion induced blindness can result in temporal reversal of an inhibited and a flashed object. However, since all of our stimuli are clearly visible and at no point of time under the influence of motion induced inhibition we find it difficult to see clear parallels to our findings.

A last potential confound that we want to address are unintentional eye movements during the experiment. Saccades that are time-locked to the stimuli or mask could have potentially resulted in the pattern that we observed through actual peri-saccadic effects as described in the literature (Morrone et al., 2005). However, eye movements that are triggered by the onset of the stimuli should result in very similar patterns in experimental and control conditions. Instead we find that the mask was crucial to reveal reversal effects. It is conceivable that the mask itself triggered eye movements but it is unlikely that this could give rise to our results for two reasons: (1) the mask was a full field noise mask without features that could draw attention. It is therefore highly unlikely that attention would be drawn enough to elicit frequent and consistent eye movements that would be necessary to result in a saccadic effect. (2) if the mask indeed elicited reliable saccades we would expect the reversals to follow the patterns

that were previously observed in the literature (Morrone et al., 2005; Kresevic et al., 2016), namely a peak reversal around 50 ms before saccade onset. Assuming a saccadic reaction time of 100–200 ms in response to our mask, we should expect the peak reversal to happen around 50–150 ms after mask onset, which we clearly show to not be the case, with our peak reversal happening at 10–20 ms prior to mask.

Reversals were reported even for the longest intervals tested between the first and second stimulus (160 ms). From the shape of the curves in Figures 2, 3, this range could plausibly extend tens of ms beyond this. The original report of perisaccadic reversals also included reversals for grouped data from inter-stimulus intervals of 76–200 ms (Morrone et al., 2005). These values put the temporal reversal phenomenon into the category of illusions which seem to emphasize the re-writeable nature of conscious perception (Eagleman & Sejnowski, 2000; Scharnowski et al., 2009; Herzog, Kammer, & Scharnowski, 2016): 160 ms is ample time for the signal from the onset of the first stimulus to be processed by much of the cortex, and yet the subsequent appearance of the second stimulus can still be perceived as occurring first.

In particular, Zimmermann et al. (2014) have suggested that peri-saccadic/masking effects reflect a correspondence process that links targets of interest across interruptions in visual input. We would like to close by proposing a model of the temporal aspects of that process. We suggest that after a visual disruption, the representation of the scene must be updated by linking each item that had been attended prior to the disruption to its post-disruption version. Because this process is serial (at least, for items within a certain spatial scope), items are updated, thus perceived, one by one. Because this updating process most likely relies on delayed feedback from higher order areas (Enns & Di Lollo, 2000; Fahrenfort, Scholte, & Lamme, 2007; Binda et al., 2009), visual disruption shortly after the probe might interfere with the updating process of the target but not with the probe. It is possible that this disruption causes the updating of the target to be delayed to later position in the sequential updating process and thus its perception is delayed. We assume that the rate at which attention deals with each item in turn is linked to neuronal oscillations in the theta (4–8 Hz) or alpha (8–12 Hz) frequency bands (VanRullen et al., 2007; Busch & VanRullen, 2010; Landau & Fries, 2012; Fiebelkorn et al., 2013). Directly supporting the link between these lines of argument, we recently described a

correlation between the phase of a theta frequency oscillation and the amount of perisaccadic mislocalization observed across trials (McLelland et al., 2016). Different theories of oscillatory processing have in common the idea that discrete items would be processed one by one, serially, either across (Fries, 2015) or within (Lisman & Jensen, 2013) the cycles of a slow oscillation. A dependency on the oscillatory phase might also explain why illusory reversals are not experienced in every trial. We speculate here that this serial nature of processing could underlie the finding of temporal reversals.

6.6 Conclusion

In conclusion, we have shown that masking can result in a perceptual reversal of the temporal order of a pair of brief events. This is reminiscent of the temporal reversal previously described around the onset of saccades, although we cannot demonstrate here that there is a common underlying mechanism. This mask-based paradigm may nonetheless be very useful in exploring mechanisms of temporal order perception at fast timescales, because it affords greater temporal control and repeatability than equivalent saccadic paradigms.

Chapter 7

General Discussion

Evidently the brain needs to implement several stages of complexity reduction to handle the vast amount of incoming information. In this thesis I provide evidence that this is partially done via multiple periodic sampling mechanisms that collect, transform and transfer information rhythmically. These sampling mechanisms appear to differ in their properties in a hierarchical fashion, potentially reflecting the increasing complexity that generally governs the visual processing pipeline. During my doctorate I tried to show that these processes are intrinsically linked to neural oscillations and that we can measure their hidden states by probing behavior in a dynamic fashion. More specifically I aimed at expanding on the current literature by applying much needed causal methods using non-invasive brain stimulation methods and visual entrainment sequences. I was able to demonstrate that oscillations have profound effects on attention and temporal perception, and presented supporting evidence that their supposed functional role in vision might generalize to other modalities.

I aimed to answer the following research questions:

1. Is the occipital alpha rhythm causally involved in discretely sampling visual information? (**chapter II and III**)
2. Is there a link between oscillatory activity and rhythmic sampling in the somato-sensory system?(**chapter IV**)
3. Can we manipulate theta rhythmic activity to modulate attentional sampling? (**chapter V and VI**)

7.1 Is the occipital alpha rhythm causally involved in discretely sampling visual information?

The experiments in chapter II and III were aimed at directly interfering with the occipital alpha rhythm through rhythmic entrainment and observing the resulting effect on time perception. In chapter II we used a rhythmic visual stimulus to control the oscillatory alpha phase which allowed us to probe it's perceptual consequences on a visual illusion called the flash-lag effect (FLE). In the FLE a static stimulus that is briefly flashed next to a moving stimulus, is perceived to "lag" behind the moving stimulus. The FLE is assumed to be caused by a discrete periodic updating process that operates in the alpha band (Chakravarthi & Vanrullen, 2012; Schneider, 2018). In our first study we aimed at providing causal evidence for this hypothesis. We found that the perceived lag was dependent on the phase of the background entrainer, supporting the idea that the alpha rhythm instantiates discrete windows that are used to sample and to update stimulus positions.

In chapter III I present a study that used a similar entrainment paradigm. Here we used alpha rhythmic TMS to entrain 10 Hz oscillations. After entrainment we presented 2 stimuli on which participants performed a temporal order judgement (TOJ) task. Based on the hypothesis of discrete perception (VanRullen & Koch, 2003; VanRullen, 2016) we hypothesized that the TOJ performance should be modulated by the phase of the entrained oscillation. Underlying this assumption is the fact that alpha phase was shown to determine if two stimuli in close temporal proximity were perceived as simultaneous or sequential (Valera et al., 1981; Milton & Pleydell-Pearce, 2016; Ronconi et al., 2018). Similarly to these studies we found that TOJ-performance was modulated at 10 Hz indicating a dependency on alpha phase.

The two studies on discrete perception use two different means of entrainment to show effects on two different measures of relative timing perception. What follows is a critical assessment as well as a discussion on the conclusions that we can draw from our results. The two entrainment studies, while showing strong and convincing results, are limited by a few methodological and conceptual difficulties. First of all both studies make strong claims about the causal

relationship between alpha oscillations and discrete perception. However to irrefutably solidify this claim we would have had to perform EEG measurements and show that alpha phase is indeed modulated and directly correlated with perceptual outcome. While this would have been beneficial we are nevertheless confident that our conclusions are valid because of the following reasons. Visual entrainment and rhythmic TMS have shown to be efficient in controlling power and phase of oscillatory alpha activity (Romei et al., 2010; Thut et al., 2011; Spaak et al., 2014; Ronconi et al., 2018). Our stimulation procedure closely mimics the procedures applied in these studies. It would therefore be surprising if alpha oscillations would not be entrained in our case. Moreover it is important to consider how and at which cortical location we effectively entrain alpha oscillations and which conclusion this lets us draw about the cortical origin of our effect. In the case of visual entrainment it is plausible that multiple areas along the visual pathway get entrained, starting from the LGN and reaching up to the multitude of areas to which the LGN and V1 project (Schmid et al., 2010). By applying TMS directly to the primary visual cortex we are somewhat able to exclude the LGN, a highly connected area, and its projections from the list of potential candidates. In the future it might be beneficial to precisely locate a neural correlate of temporal perception instead of relying on behavioral reports. A potential way to investigate this might be through concurrent fMRI and EEG measures or intracranial recordings.

Another tricky issue to address is that of experimentally differentiating between "soft" and "hard" versions of discrete perception. In both cases the fluctuations in time perception are caused by fluctuations in excitability. In the "hard" version excitability directly influences time perception by implementing discrete perceptual windows. In the "soft" version excitability indirectly causes changes in time perception e.g. by reducing visibility of a stimulus in a sequence and thus biasing participants to report the more visible stimulus as occurring first. While an "all or nothing" modulation of behavior would strongly favour the "hard" version it is not likely that we will ever be able to measure such. This is simply because of the fact that the brain is a noisy organ and that measuring behavior can only ever approximate the true underlying perception. Given the distinction between hard and soft it is key to design tasks that allow us to control for excitability related changes in visibility. In the flash-lag study we tried to do this indirectly by choosing a task in which both stimuli (the cue and the clock hand) should be equally affected by the alpha phase at the time of our

probe. In the TMS study we were able to make a far stronger point on this front. In the majority of trials we presented two stimuli and participants had to judge the temporal order. Sometimes however we presented only a single stimulus to which the participant had to respond with a "single stimulus" response. By measuring the number of single stimulus responses during two stimulus trials we could estimate how low versus high excitability influences stimulus visibility. We found that different alpha phases had no impact on stimulus visibility and could therefore exclude visibility fluctuations as a cause of our TOJ fluctuations. In addition to that our participants underwent extensive training sessions in which we artificially deteriorated the visibility of one of two stimuli. The intend was to discourage participants to rely on subjective visibility which might be affected by excitability. We are confident that our study assessed the problematic of excitability fluctuations as possible cause for relative timing perception in a convincing way and added significantly to the current pool of literature.

Why does the visual system discretize its input? Over time several hypothesis have been brought forward in this regard. On the one hand I forward that precise temporal relationships (SOA's smaller than 100 ms) might not be behaviorally important enough to be made consciously available. Our visual scene tends to stay relatively stable over time and behaviorally meaningful changes usually occur over longer time periods. This can be nicely demonstrated by watching manipulated videos in which the frames are randomized every 100 ms, thus destroying temporal relationships in a similar fashion as the visual system presumably does. These altered videos do look strange but the "story" as well as the causal relationships between events stay to the largest part interpretable and comprehensible. If the brain can afford to discard information that is not relevant then it will most likely do so. This is the argument of complexity reduction in temporal perception. On a computational level concentrating neural activity to certain time points might be more energy efficient and might allow for more effective neural communication (Varela, Lachaux, Rodriguez, & Martinerie, 2001; Schroeder & Lakatos, 2009; Fries, 2015).

Where should we go from here on in the field of discrete perception? An important question that will need to be answered in the future is how exactly neurons encode relative timing using their most basic and important means of communication: spikes. Intuitively one would think the sequential presentation of stimuli naturally separates them in time in the brain as well. Interestingly how-

ever previous models have proposed that spiking neuronal ensembles that encode stimulus information through their firing latencies produce far more human-like behavior. (Thorpe, Delorme, & Van Rullen, 2001). If this was the case then the information contained in the relative timing between spikes would be pre-occupied with stimulus features and could not encode relative stimulus timing, at least within short intervals. This would be loosely similar to something like a Heisenberg uncertainly principle for latency codes. You can either measure what is encoded OR when it's encoded. Importantly a crucial assumption of these models is that spiking latencies need a reference of sorts (VanRullen & Thorpe, 2002). It is plausible that the phase of neural oscillations provides this reference which might in turn mean that all spikes relative to a phase within one oscillatory cycle encode stimulus features and cannot encode time (Masquelier, Hugues, Deco, & Thorpe, 2009). This kind of model would predict fluctuations in relative timing perception at a frequency of specific oscillations, just as we showed in our studies. Unfortunately we have little evidence on how exactly the brain encodes relative time and so further research is needed. Spike latency models might be an interesting direction to pursue in this regard.

One of the most interesting remaining questions, and also one of the most hard ones to solve, is how the brain "qualia"-tively fills the gaps between discrete snapshots. Although I do not have an answer to it there is an analogy that might help us understand how our brain might achieve this occlusion. Our visual scene contains a blind spot corresponding to the location where our retina connects to our optical nerve. There is no visual information coming from this part of the visual field and still, somehow our brain is perfectly able to generate the illusion that our visual field is complete. Perhaps it is this kind of mechanism, not in space but in time, that might give rise to our impression of continuous visual flow.

7.2 Is there a link between oscillatory activity and rhythmic sampling in the somatosensory system?

The studies in chapter II and III demonstrated how oscillations modulate the excitability and therefore the gating of information in the visual cortex. In

Chapter III we explored which effects these neural rhythms have on ongoing stimulus processing. Previous work in our lab has shown that the impulse response function (IRF) calculated by cross-correlating white noise luminance sequences and the corresponding EEG contains strong and long lasting reverbrations at 10 Hz (VanRullen & Macdonald, 2012). We replicated these findings in the somatosensory system using vibrotactile stimulation. We found the oscillatory frequency of the IRF's to be correlated to the resonance frequency of the somatosensory system at 25 Hz. Our findings demonstrate that these IRFs are a more general transmodal signature of cortical processing, potentially related to complexity reduction mechanisms, sequence learning and/or predictive coding (Chang et al., 2017; Alamia & VanRullen, 2019).

A striking feature of perceptual echoes is that they link strong oscillatory activity directly to active stimulus processing in frequency bands that usually desynchronize as a result of stimulation (Pfurtscheller, 1981; Pfurtscheller et al., 2002; Cheyne et al., 2003; Gaetz & Cheyne, 2006). While certain frequencies, like the gamma band, are known to increase during stimulus processing, alpha (and arguably beta) is currently understood as a mostly inhibitory signature because of it's reliable opposite behavior. (Başar et al., 1997; Klimesch, Sauseng, & Hanslmayr, 2007; Jensen & Mazaheri, 2010; Mathewson et al., 2011). The discrepancy between endogenous alpha/beta and IRF alpha/beta can be explained in several ways.

One might assume that IRF alpha/beta and endogenous alpha/beta are generated by different populations, the former being functionally significant for stimulus processing and the latter being of inhibitory nature. This however leaves several questions open. Why do we observe no alpha/beta oscillatory activity in single trial ERP's? And why do both rhythmic signatures share such close resemblance in frequency and topography? Intuitively such strong similarities might make functional separation difficult but not impossible.

The alpha component in the IRF is not simply explained by a general increase in endogenous alpha but could instead be explained by an increase in phase locking (Chang et al., 2017). Due to the nature of the cross-correlation we must interpret the echo reverbrations as phase locked to single luminance increments. It is therefore conceivable that all luminance increments give rise to perceptual echoes but since they are slightly shifted to each other they cancel out in the raw

time course. Perceptual echoes might be a common occurrence in electrophysiological studies but might never have been discovered before due to these reasons.

Recently two new studies have shed light on the functional significance of perceptual echoes. Repeated presentation of the same luminance sequences leads to an increase in echo alpha power (Chang et al., 2017). They interpret the echoes as signatures of sequence learning. A secondary study by Alamia and VanRullen proposed a new model of echo generation in which these previous findings neatly integrate (Alamia & VanRullen, 2019). Using a simple hierarchical predictive coding model with inhibitory feedback Alamia and VanRullen showed that biologically plausible communication delays leads to identical perceptual echoes to those found in human EEG. Furthermore they showed that the oscillatory IRF's behaved like travelling waves, a previously shown effect (Lozano-Soldevilla and VanRullen, 2019), moved from anterior to posterior areas when no visual stimulation was present and reversed their direction when stimulation was present, both in the model and in human EEG (Lozano-Soldevilla & VanRullen, 2019). These findings make an interesting point that the IRF's might be a signature of predictive coding. The changes in echo amplitude demonstrated in the findings by Chang et. al. can therefore be interpreted as a change in predictability of the luminance sequence. These findings are relatively new but nevertheless promising. More research, especially into the spatial component of oscillatory activity as well as its causal role might help to understand these processes more.

Previous attempts to find similar echoes in the auditory domain were not successful (İlhan & VanRullen, 2012). Potential explanations for this are manifold. The authors used high frequency carrier waves that were amplitude modulated in a random fashion. Similar to the visual system the stimulus was designed to interact with the first stage of neural processing. The low-level architecture of the auditory system however is substantially different from that of the other two domains. Raw auditory signals undergo a mechanical frequency decomposition in the cochlea before being interpreted by sub-cortical structures like the cochlear nuclei and finally by the auditory cortex (Ehret & Romand, 1997). If the perceptual echoes are a higher level cortical phenomenon involving feedback loops and neural oscillations, the stimulus design to elicit auditory echoes might have to be more complex, potentially in the syllable or even semantic domain. This makes designing white noise sequences difficult.

What is the relationship between perceptual echoes and rhythmic perception? If we could quantify the neural representation (or auto-correlation) of static objects that are sampled at a certain rhythm then we would see periodic fluctuations in the amount of neural representation of this object. And these fluctuations should appear at the same frequency as our sampling rhythm. Principally the perceptual echoes represent this effect by quantifying the amount of correlation between the input and the EEG and demonstrating it's oscillatory behavior. There are however two important differences. For one the correlation between EEG and stimulus measure the similarity between sequences and not static features. And second the IRF correlation is represented in lags and not real time. At the present moment the relationship between discrete sampling and perceptual echoes is not one that we can make confident claims about.

7.3 Can we manipulate theta rhythmic activity to modulate attentional sampling?

The experiment in chapter V investigated the rhythmic nature of attentional selection. In order to tightly link the observed behavioral rhythm to neuronal oscillations we designed our experiment to closely mimic a previous study in which this relationship was established in macaques. Only a handful of studies in the attentional literature have found intracranial neural oscillations that directly correlated with attention in the 4 to 8 Hz band in humans or macaques (Helfrich et al., 2018; Kienitz et al., 2018; Spyropoulos et al., 2018; Fiebelkorn et al., 2018). Our experiment provides a neat link between these studies, especially the study by Kienitz et. al. and the more frequently found behavioral oscillations in behavioral and EEG studies in humans. Replicating Kienitz findings in humans was therefore an important step to better understand how oscillations enable facilitation of stimulus processing.

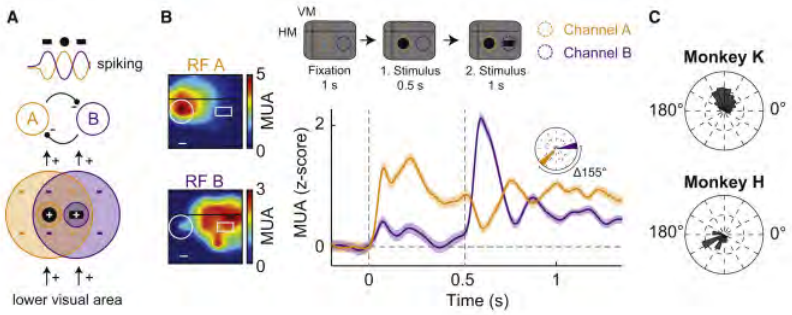

Figure 6. Theta rhythmic neuronal activity resulting from receptive field interactions. Reproduced from Kienitz et. al. (2018)

While the findings by Kienitz are very intriguing they nevertheless raise many questions about how the brain uses oscillations to select relevant stimuli. According to their findings stimuli in close proximity that fall in overlapping receptive fields of separate neurons are subject to an oscillatory competition that fluctuates at 4 Hz (Figure 6). But how does this mechanism work for stimuli that are further apart? What if more than two stimuli have to be attended? What if irrelevant stimuli lie on the opposite site of the off-surround of the receptive field which also benefits from the periodic increase in spiking activity? In theory the visual system contain neurons that encompass extremely large receptive fields, even spanning over separate visual fields (Hubel & Wiesel, 1962; Sanderson, Bishop, & Darian-Smith, 1971). However this increased size should lead to a less and less precise stimulus selection as more and more irrelevant information is covered by the receptive fields. On the other hand it has been found that receptive fields in V4 and other regions respond to a variety of curved contours, complex patterns and asymmetric shapes (Hubel & Wiesel, 1968; De Valois, Albrecht, & Thorell, 1982; Ben Hamed, Duhamel, Bremmer, & Graf, 2001). This could hypothetically enable the visual system to isolate relatively complex patterns and involve them in mutual rhythmic inhibition using only 2 neurons as was shown by Kienitz et al. It has been proposed that the sampling of more than 2 stimuli leads to a decrease in the rate in which individual stimuli are sampled (Holcombe & Chen, 2013). One could imagine that given three or more stimuli, the neurons processing the respective receptive fields would engage in a 3-way mutual rhythmic inhibition at a 2.6 Hz rhythm. All in all the findings by Kienitz are very insightful but do not fully explain how rhythmic attention samples more complex scenes and multiform objects.

Another important finding to discuss is that the theta rhythmic effect was found in V4 and not like in other studies in PFC (Helfrich et al., 2018; Spyropoulos et al., 2018; Fiebelkorn et al., 2018; Gaillard et al., 2020). This raises the question whether theta rhythmic activity was induced in a stimulus dependent bottom-up fashion or if the oscillatory activity was driven or modulated by higher level areas like the FEF. Microstimulation of the FEF has been shown to modulate responses in V4 in corresponding receptive fields, indicating that V4 receives top-down signals from the FEF (Moore & Armstrong, 2003). How much of the observed effects can be explained by these signals remains to be seen however.

Chapter VI was concerned with a peri-saccadic distortion of temporal order perception. We proposed that a likely mechanical cause for our observations is that full field flashes trigger saccadic mechanisms related to displacement and suppression. This makes intuitive sense because saccades are the most frequent and probable reason for brief and intense global changes in our visual stream. Notably out of the three types of signals that have functional relevance for saccadic mechanisms of visual stability, reafference, proprioception and corollary discharge, reafference and proprioception have been described as the least significant ones. This claim has been challenged by recent findings that replicate traditional peri-saccadic illusions solely by manipulating reafferent signals like stimulus position, flicker and full field masks (Mackay, 1970; O'Regan, 1984; Ostendorf et al., 2006; Terao et al., 2008; Zimmermann, Fink, & Cavanagh, 2013; Zimmermann et al., 2014). What then is the role of these saccadic mechanisms triggered by reafferent signals? Saccades introduce violent shifts in our visual field which need to be stabilized (Wurtz, 2008). Watching shaky camera footage intuitively makes the need for this mechanism very clear. There is two questions to be addressed here. One is how the brain knows that the world remained stable after a saccade. The second is how the brain creates the impression that the world is stable despite violent changes. The latter is far more difficult and will not be discussed here. A popular theory on how the visual system solves the former problem is the transsacadic memory hypothesis (Deubel, Schneider, & Bridgeman, 2002; Deubel, Bridgeman, & Schneider, 2004; Deubel, 2004). According to this idea the visual system stores the features of a saccadic target in memory before the saccade. After the saccade, the stored features can be compared the the features of the target. If they are the same then the world can be assumed to have remained stable. Without going into de-

tail there is a bit of evidence that supports this theory (Wolf, Hauske, & Lupp, 1980; Moore, Tolias, & Schiller, 1998; Kusunoki & Goldberg, 2003; Mathôt & Theeuwes, 2010). Another way to describe this process is that after the saccade the visual system needs to reconstruct the location and timing of events based on information from before and after the saccade (Zimmermann et al., 2014). We have proposed a possible interpretation our findings: objects are sampled sequentially and are transferred to a memory storage containing position, features and relative timing of the two discrete events (Melcher, 2009). The mask triggers saccadic mechanisms that initiate reconstruction of these features under the erroneous assumption that a saccade has been made (Zimmermann et al., 2014). The misinformed reconstruction then leads to errors in perception and in our case specifically time perception since objects have been sampled stored as discrete temporal events that can be reversed. I would like to extend this interpretation by proposing that the erroneous reconstruction of object position (peri-saccadic displacement) and object features could also give rise to the observed effect on temporal order judgements. Object position and features are also subject to illusions in the time surrounding saccades (Ross et al., 1997; Lappe et al., 2000; Morrone et al., 2005; Herwig & Schneider, 2014). Temporal order judgements require the observer to identify separate objects before judgements about relative timing can be made. If object features, object position or both would be misattributed this could lead to reliable reversals in reported temporal order as we observed them in our experiment. Especially changes in object position have been shown to go unnoticed for displacements for up to a third of the saccade, potentially aiding in disguising positional swaps (Bridgeman et al., 1975). Which of these factors gives rise to our findings cannot be disentangled based on our results and requires further experimentation. Given previous work that related peri-saccadic errors and attentional fluctuations to the phase of theta oscillations (McLelland et al., 2016; Chota et al., 2018; Kienitz et al., 2018) and the fact that attention plays such a big role in saccadic mechanisms (Melcher, 2009) it is likely that attentional sampling and our interference with its oscillatory mechanism plays a role in these peri-saccadic reversals of time.

7.4 On oscillations as cause or consequence

The work I have been presenting here makes a strong case for the causal role that oscillations play in visual perception. One might get the impression that

the brain implemented oscillatory mechanisms to solve a multitude of problems like information collection and complexity reduction. How much of a causal role oscillations play however is debated.

Experiments, among others from our own lab, have shown that in order to create oscillatory systems it could be sufficient to implement very simple inhibitory feedback loops. This suggests that oscillations might be more of a by-product of other ongoing processes than an intended mechanism. Indeed it is not immediately evident which lower brain function could not be implemented if oscillations were not present. Evidently these propositions rise many interesting and important questions that we as oscillation enthusiasts will have to answer at one point. I think it is possible that oscillations might have emerged from other processes that involved inhibitory feedback loops like traditional predictive coding (Bastos et al., 2012; Alamia & VanRullen, 2019). However I do not think that this means that they do not have a function now. Given that oscillatory activity somehow suddenly emerged I would find it surprising if the brain did not find a way to leverage the temporal structure that they provide. Oscillations might even be a phenomenon that impair functionality in the brain. After all information theory tells us that a perfectly synchronized system carries the minimum amount of information. Whatever of the two it is, I think that a highly sophisticated system like the brain will adapt to rhythmic activity, most likely in a rhythmic fashion. The end product of this long evolutionary adaptation process might result in an actual causal role of oscillations in important brain functioning.

7.5 Conclusion

The collection of studies in this thesis support the idea that neuronal oscillations at multiple frequency bands are causally involved in the process of selecting and processing information. I have shown that we can manipulate oscillatory activity and that this has effects on the dynamics of the sampling process as well as the perceptual outcome. My findings cover two dominant frequency bands, alpha and theta, each with dissociable functional mechanisms. Moreover I was able to provide support for a link between oscillatory activity and periodic information processing in the tactile domain. In conclusion my work highlights the close and causal relationship between oscillatory activity and neural sampling.

7.6 Moving on: De-synchronizing oscillatory activity

What could be the next step in probing the causal role of neural oscillations? In the last years me and other researchers have started to shed light on this question with a series of experiments that directly increase oscillatory activity using non-invasive brain stimulation methods or neurofeedback training programs (Hanslmayr, Sauseng, Doppelmayr, Schabus, & Klimesch, 2005; Romei et al., 2010; Thut et al., 2011). While being extremely insightful, these experiments have almost all only been able to increase oscillatory activity up until now. This presents an incredibly interesting opportunity since, given that oscillations are assumed to actively implement basic neural mechanisms, their absence should lead to severe changes in cognitive functioning. This is supported by the fact that the most notable visual perceptual changes e.g. under the influence of psychoactive substances, are accompanied by strong desynchronization of low frequency oscillations (Kometer, Schmidt, Jäncke, & Vollenweider, 2013). From a medical perspective neuronal de-synchronization might provide us with the means to more efficiently treat mental disorders like ADHD which is characterized by a disability to reduce alpha oscillations in task contexts (Lenartowicz, Mazaheri, Jensen, & Loo, 2018). It appears that a vast number of fields, both fundamental and clinical, would benefit from a way to dynamically up- or down regulate oscillatory activity in a non-invasive fashion.

We could potentially achieve neural synchronization and de-synchronization using an online EEG-TMS neurofeedback approach that I envisioned and prototyped in the last year of my PhD. The general approach is to record the EEG and analyze the phase of an a priori chosen frequency e.g. the alpha band in an ongoing fashion. The instantaneous phase will inform us about the current state of the underlying oscillatory population. Strong oscillatory power is assumed to reflect a large synchronized population. Given that we detect a certain phase in the EEG signal we can trigger a TMS pulse that is administered directly to a pre-selected area that we record the EEG signal from. TMS pulses are assumed to lead to a phase reset in a small population of neurons. Stimulating at certain phases of the oscillation should therefore lead to an increase in oscillatory power because we recruit more neurons into the common oscillation. On the other hand, stimulating at the opposite phase should lead to a decrease in

oscillatory power because we reset the phase of a subpopulation to the opposite phase compared to the dominant oscillation. By selecting the appropriate phase we are able to synchronize or de-synchronize oscillatory power at a selected frequency band on demand, and in turn increase or decrease the functionality of the underlying oscillation. A similar approach has already been done by Huang et. al. who used visual stimulation to increase or decrease alpha power (Huang et al., 2019) (Figure 7).

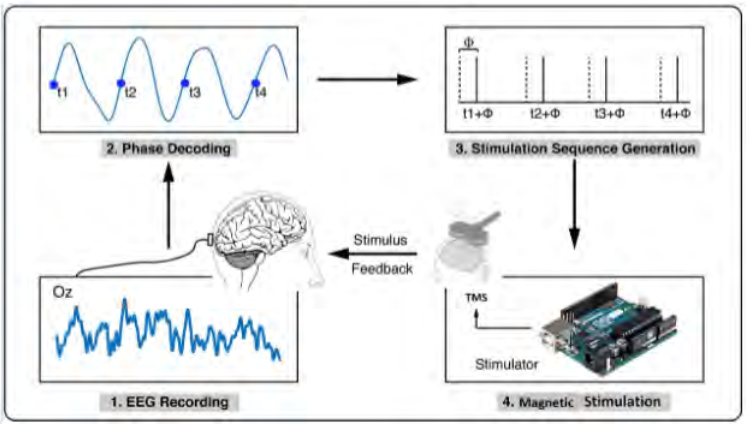

Figure 7. Neural Synchronization and De-synchronization via external magnetic phase-dependent neurofeedback. Adapted from

We collected data for 4 subjects using this novel approach. The TMS-EEG neurofeedback system was continuously recording 200 ms data segments from channel Pz and performed an online fourier transform. 10 Hz phase angles were extracted and TMS pulses were administered at 1 out of 4 different phases (0˚,90˚,180˚,270˚) corresponding to 4 experimental conditions. In a 5th control condition we replayed the tms sequence from 2 trials ago, therefore tms pulses should have a random relationship to the underlying alpha phase. Trials were 12 seconds long, starting with a cue that indicated near-threshold target locations (left/right), followed by an 8 second long tms-window in which between 3 and 18 tms pulses were applied. Targets could appear only in the last 4 seconds. The number of tms pulses per trial varied depending on if the algorithm detected high enough alpha power to extract a reliable phase in a given 200 ms window. The TMS coil localization procedure was identical to the one described

in chapter III.

We hypothesized that one of the stimulated phases should lead to synchronization of alpha oscillations while the opposite phase should lead to a de-synchronization. We could confirm this in preliminary data of 4 subjects (Figure 8 Row 2). Furthermore we hypothesized that trials in which de-synchronization took place should show better behavioral performance compared to synchronized trials. Although performance correlated with alpha power modulation this effect was driven mostly by high alpha power leading to decreased performance compared to the replay condition and not by performance increases due to de-synchronization (Figure 8 Row 3, Column 4). Data collection is ongoing and will allow us to statistically access our findings.

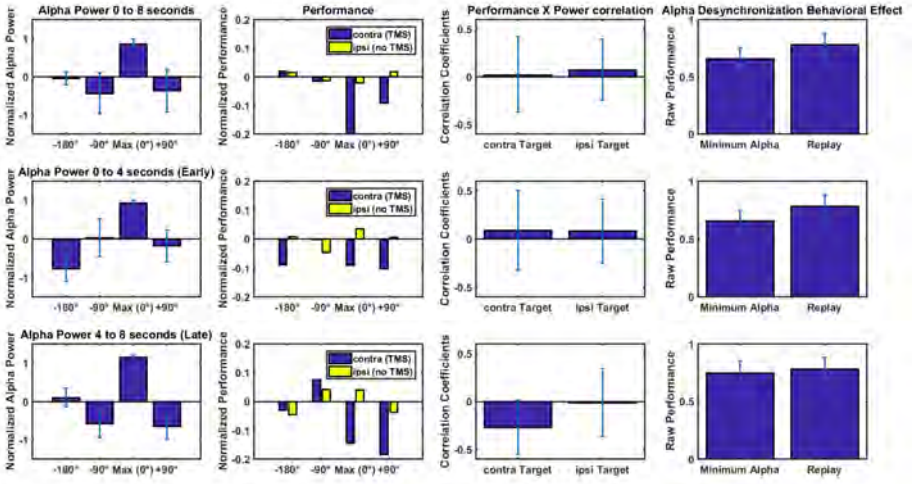

Figure 8. *Grand average of phase dependent alpha power modulation and behavioral performance.* Separate rows depict data taken from different times during the 8 second long stimulation window. **Row 1** (0 to 8 seconds) **Row 2** (0 to 4 seconds) **Row 3** (4 to 8 seconds). We decided for this separation because targets were always presented in the late (4 to 8 second) window. In addition we observed stronger alpha power in the early window (0 to 4 seconds) compared to the late window. **Column 1**. We calculated the mean alpha power for respective phase conditions (peak,trough,ascending,descending) for individual subjects. Although we observed a relatively consistent relationship between phase and alpha power on an individual level (Opposite phases resulted in opposite effects on power), subjects differed in the exact phase condition that led to maximal synchronization/de-synchronization). The circular nature of our phase condition allowed us to realign our individual data to the phase condition with the highest alpha synchronization (O°). We observe that stimulation at opposite phase (180 °) tends to result in alpha power decreases in the first 4 seconds when alpha power was high. **Column 2**. Performance relative to Replay condition. Overall TMS seems to have a detrimental effect on behavioral performance in the contralateral hemifield. **Column 3**. We correlated alpha power and behavioral performance within our 4 phase conditions on an individual basis. Displayed are the mean correlation coefficients. In the Late time window (during target presentation) alpha power negatively correlated with detection performance in line with previous findings. **Column 4.**. Can we increase target detection by de-synchronizing alpha oscillations? Conditions in which alpha power was maximally de-synchronized do not show improved performance compared to the replay condition. Power-Behavior correlation seems to be mostly driven by inhibitory effects of high alpha power.

Appendix

References

Akyürek, E. G., Eshuis, S. A. H., Nieuwenstein, M. R., Saija, J. D., Başkent, D., & Hommel, B. (2012, December). Temporal target integration underlies performance at Lag 1 in the attentional blink. *Journal of Experimental Psychology. Human Perception and Performance*, *38*(6), 1448–1464. doi: 10.1037/a0027610

Alamia, A., & VanRullen, R. (2019, October). Alpha oscillations and traveling waves: Signatures of predictive coding? *PLOS Biology*, *17*(10), e3000487. Retrieved 2020-08-07, from `https://journals.plos.org/plosbiology/article?id=10.1371/journal.pbio.3000487` (Publisher: Public Library of Science) doi: 10.1371/journal.pbio.3000487

Anstis, S. M. (1978). Apparent Movement. In S. M. Anstis et al. (Eds.), *Perception* (pp. 655–673). Berlin, Heidelberg: Springer. Retrieved 2020-09-01, from `https://doi.org/10.1007/978-3-642-46354-9_21` doi: 10.1007/978-3-642-46354-9_21

Astrand, E., Wardak, C., Baraduc, P., & Ben Hamed, S. (2016, July). Direct Two-Dimensional Access to the Spatial Location of Covert Attention in Macaque Prefrontal Cortex. *Current Biology*, *26*(13), 1699–1704. Retrieved 2020-09-18, from `http://www.sciencedirect.com/science/article/pii/S0960982216304080` doi: 10.1016/j.cub.2016.04.054

Başar, E., Başar-Eroglu, C., Karakaş, S., & Schürmann, M. (2001, January). Gamma, alpha, delta, and theta oscillations govern cognitive processes. *International Journal of Psychophysiology: Official Journal of the International Organization of Psychophysiology*, *39*(2-3), 241–248.

Başar, E., Schürmann, M., Başar-Eroglu, C., & Karakaş, S. (1997, June). Alpha oscillations in brain functioning: an integrative theory. *International Journal of Psychophysiology*, *26*(1), 5–29. Retrieved 2020-05-06, from `http://www.sciencedirect.com/science/article/pii/`

S0167876097007538 doi: 10.1016/S0167-8760(97)00753-8

Babiloni, C., Vecchio, F., Bultrini, A., Luca Romani, G., & Rossini, P. M. (2006, December). Pre- and poststimulus alpha rhythms are related to conscious visual perception: a high-resolution EEG study. *Cerebral Cortex (New York, N.Y.: 1991)*, *16*(12), 1690–1700. doi: 10.1093/cercor/bhj104

Bachmann, T., Põder, E., & Luiga, I. (2004, February). Illusory reversal of temporal order: the bias to report a dimmer stimulus as the first. *Vision Research*, *44*(3), 241–246. Retrieved 2020-03-27, from http://www.sciencedirect.com/science/article/pii/S0042698903006886 doi: 10.1016/j.visres.2003.10.012

Bastos, A. M., Usrey, W. M., Adams, R. A., Mangun, G. R., Fries, P., & Friston, K. J. (2012, November). Canonical microcircuits for predictive coding. *Neuron*, *76*(4), 695–711. doi: 10.1016/j.neuron.2012.10.038

Baumgarten, T. J., Schnitzler, A., & Lange, J. (2015, September). Beta oscillations define discrete perceptual cycles in the somatosensory domain. *Proceedings of the National Academy of Sciences*, *112*(39), 12187–12192. Retrieved 2020-08-05, from https://www.pnas.org/content/112/39/12187 (Publisher: National Academy of Sciences Section: Biological Sciences) doi: 10.1073/pnas.1501438112

Ben Hamed, S., Duhamel, J.-R., Bremmer, F., & Graf, W. (2001, September). Representation of the visual field in the lateral intraparietal area of macaque monkeys: a quantitative receptive field analysis. *Experimental Brain Research*, *140*(2), 127–144. Retrieved 2020-09-14, from https://doi.org/10.1007/s002210100785 doi: 10.1007/s002210100785

Berger, H. (1931, December). Über das Elektrenkephalogramm des Menschen. *Archiv für Psychiatrie und Nervenkrankheiten*, *94*(1), 16–60. Retrieved 2020-03-23, from https://link.springer.com/article/10.1007/BF01835097 doi: 10.1007/BF01835097

Binda, P., Cicchini, G. M., Burr, D. C., & Morrone, M. C. (2009, October). Spatiotemporal Distortions of Visual Perception at the Time of Saccades. *Journal of Neuroscience*, *29*(42), 13147–13157. Retrieved 2020-03-27, from https://www.jneurosci.org/content/29/42/13147 doi: 10.1523/JNEUROSCI.3723-09.2009

Bonnefond, M., & Jensen, O. (2012, October). Alpha Oscillations Serve to Protect Working Memory Maintenance against Anticipated Distracters. *Current Biology*, *22*(20), 1969–1974. Retrieved 2018-11-12, from http://www.sciencedirect.com/science/article/pii/S0960982212009943 doi:

10.1016/j.cub.2012.08.029

Brainard, D. H. (1997, January). The Psychophysics Toolbox. *Spatial Vision*, *10*(4), 433–436. Retrieved 2020-03-27, from https://brill.com/view/journals/sv/10/4/article-p433_15.xml doi: 10.1163/156856897X00357

Bridgeman, B., Hendry, D., & Stark, L. (1975, June). Failure to detect displacement of the visual world during saccadic eye movements. *Vision Research*, *15*(6), 719–722. Retrieved 2020-03-27, from http://www.sciencedirect.com/science/article/pii/0042698975902904 doi: 10.1016/0042-6989(75)90290-4

Brown, L., & Li, X. (2005, March). Confidence intervals for two sample binomial distribution. *Journal of Statistical Planning and Inference*, *130*(1), 359–375. Retrieved 2020-03-27, from http://www.sciencedirect.com/science/article/pii/S037837580400271X doi: 10.1016/j.jspi.2003.09.039

Busch, N. A., Dubois, J., & VanRullen, R. (2009, June). The phase of ongoing EEG oscillations predicts visual perception. *The Journal of Neuroscience: The Official Journal of the Society for Neuroscience*, *29*(24), 7869–7876. doi: 10.1523/JNEUROSCI.0113-09.2009

Busch, N. A., & VanRullen, R. (2010, September). Spontaneous EEG oscillations reveal periodic sampling of visual attention. *Proceedings of the National Academy of Sciences*, *107*(37), 16048–16053. Retrieved 2020-03-27, from https://www.pnas.org/content/107/37/16048 doi: 10.1073/pnas.1004801107

Buzsaki, G. (2006). *Rhythms of the Brain*. Oxford University Press. (Google-Books-ID: ldz58irprjYC)

Callaway, E., & Yeager, C. L. (1960, December). Relationship between reaction time and electroencephalographic alpha phase. *Science (New York, N.Y.)*, *132*(3441), 1765–1766.

Chakravarthi, R., & Vanrullen, R. (2012, June). Conscious updating is a rhythmic process. *Proceedings of the National Academy of Sciences of the United States of America*, *109*(26), 10599–10604. doi: 10.1073/pnas.1121622109

Chang, A. Y.-C., Schwartzman, D. J., VanRullen, R., Kanai, R., & Seth, A. K. (2017). Visual Perceptual Echo Reflects Learning of Regularities in Rapid Luminance Sequences. *The Journal of Neuroscience*. doi: 10.1523/JNEUROSCI.3714-16.2017

Cheyne, D., Gaetz, W., Garnero, L., Lachaux, J.-P., Ducorps, A., Schwartz,

D., & Varela, F. J. (2003, October). Neuromagnetic imaging of cortical oscillations accompanying tactile stimulation. *Brain Research. Cognitive Brain Research*, *17*(3), 599–611. doi: 10.1016/s0926-6410(03)00173-3

Chota, S., Luo, C., Crouzet, S. M., Boyer, L., Kienitz, R., Schmid, M. C., & VanRullen, R. (2018, October). Rhythmic fluctuations of saccadic reaction time arising from visual competition. *Scientific Reports*, *8*(1), 15889. Retrieved 2020-06-26, from `https://www.nature.com/articles/s41598-018-34252-7` doi: 10.1038/s41598-018-34252-7

Chota, S., & VanRullen, R. (2019). Visual Entrainment at 10 Hz Causes Periodic Modulation of the Flash Lag Illusion. *Frontiers in Neuroscience*, *13*. Retrieved 2019-04-09, from `https://www.frontiersin.org/articles/10.3389/fnins.2019.00232/full` doi: 10.3389/fnins.2019.00232

Clark, A. (2013, June). Whatever next? Predictive brains, situated agents, and the future of cognitive science. *The Behavioral and Brain Sciences*, *36*(3), 181–204. doi: 10.1017/S0140525X12000477

Clayton, M. S., Yeung, N., & Cohen Kadosh, R. (2015, April). The roles of cortical oscillations in sustained attention. *Trends in Cognitive Sciences*, *19*(4), 188–195. Retrieved 2020-07-17, from `http://www.sciencedirect.com/science/article/pii/S1364661315000285` doi: 10.1016/j.tics.2015.02.004

Cohen, M. X., & Gulbinaite, R. (2017, February). Rhythmic entrainment source separation: Optimizing analyses of neural responses to rhythmic sensory stimulation. *NeuroImage*, *147*, 43–56. Retrieved 2020-07-06, from `http://www.sciencedirect.com/science/article/pii/S105381191630653X` doi: 10.1016/j.neuroimage.2016.11.036

Crone, N. E., Miglioretti, D. L., Gordon, B., Sieracki, J. M., Wilson, M. T., Uematsu, S., & Lesser, R. P. (1998, December). Functional mapping of human sensorimotor cortex with electrocorticographic spectral analysis. I. Alpha and beta event-related desynchronization. *Brain*, *121*(12), 2271–2299. Retrieved 2020-07-01, from `https://academic.oup.com/brain/article/121/12/2271/371495` (Publisher: Oxford Academic) doi: 10.1093/brain/121.12.2271

Crouzet, S. M., & VanRullen, R. (2017, February). The rhythm of attentional stimulus selection during visual competition. *bioRxiv*, 105239. Retrieved 2020-03-27, from `https://www.biorxiv.org/content/10.1101/105239v1` doi: 10.1101/105239

Davidson, M. J., Alais, D., van Boxtel, J. J., & Tsuchiya, N. (2018, December).

Attention periodically samples competing stimuli during binocular rivalry. *eLife*, *7*, e40868. Retrieved 2020-07-18, from https://doi.org/10.7554/eLife.40868 doi: 10.7554/eLife.40868

Deubel, H. (2004, March). Localization of targets across saccades: Role of landmark objects. *Visual Cognition*, *11*(2-3), 173–202. Retrieved 2020-08-20, from https://doi.org/10.1080/13506280344000284 (Publisher: Routledge _eprint: https://doi.org/10.1080/13506280344000284) doi: 10.1080/13506280344000284

Deubel, H., Bridgeman, B., & Schneider, W. X. (2004, July). Different effects of eyelid blinks and target blanking on saccadic suppression of displacement. *Perception & Psychophysics*, *66*(5), 772–778. Retrieved 2020-08-20, from https://doi.org/10.3758/BF03194971 doi: 10.3758/BF03194971

Deubel, H., Schneider, W. X., & Bridgeman, B. (1996, April). Postsaccadic target blanking prevents saccadic suppression of image displacement. *Vision Research*, *36*(7), 985–996. Retrieved 2020-03-27, from http://www.sciencedirect.com/science/article/pii/0042698995002030 doi: 10.1016/0042-6989(95)00203-0

Deubel, H., Schneider, W. X., & Bridgeman, B. (2002, January). Transsaccadic memory of position and form. In J. Hyona, D. P. Munoz, W. Heide, & R. Radach (Eds.), *Progress in Brain Research* (Vol. 140, pp. 165–180). Elsevier. Retrieved 2020-08-20, from http://www.sciencedirect.com/science/article/pii/S0079612302400490 doi: 10.1016/S0079-6123(02)40049-0

De Valois, R. L., Albrecht, D. G., & Thorell, L. G. (1982, January). Spatial frequency selectivity of cells in macaque visual cortex. *Vision Research*, *22*(5), 545–559. Retrieved 2020-08-17, from http://www.sciencedirect.com/science/article/pii/0042698982901134 doi: 10.1016/0042-6989(82)90113-4

DeWeerd, P., Peralta, M. R., Desimone, R., & Ungerleider, L. G. (1999, August). Loss of attentional stimulus selection after extrastriate cortical lesions in macaques. *Nature Neuroscience*, *2*(8), 753–758. Retrieved 2020-03-27, from https://www.nature.com/articles/nn0899_753 doi: 10.1038/11234

Dubois, J., & VanRullen, R. (2011, May). Visual Trails: Do the Doors of Perception Open Periodically? *PLoS Biology*, *9*(5). Retrieved 2020-07-17, from https://www.ncbi.nlm.nih.gov/pmc/articles/PMC3091843/ doi: 10.1371/journal.pbio.1001056

Dugué, L., Marque, P., & VanRullen, R. (2011, August). The phase of ongoing oscillations mediates the causal relation between brain excitation and visual perception. *The Journal of Neuroscience: The Official Journal of the Society for Neuroscience*, *31*(33), 11889–11893. doi: 10.1523/JNEUROSCI.1161-11.2011

Dugué, L., McLelland, D., Lajous, M., & VanRullen, R. (2015, December). Attention searches nonuniformly in space and in time. *Proceedings of the National Academy of Sciences*, *112*(49), 15214–15219. Retrieved 2020-06-26, from `https://www.pnas.org/content/112/49/15214` doi: 10.1073/pnas.1511331112

Dugué, L., Roberts, M., & Carrasco, M. (2016, June). Attention Reorients Periodically. *Current Biology*, *26*(12), 1595–1601. Retrieved 2020-03-27, from `https://www.cell.com/current-biology/abstract/S0960-9822(16)30399-2` doi: 10.1016/j.cub.2016.04.046

Dugué, L., & VanRullen, R. (2017, March). Transcranial Magnetic Stimulation Reveals Intrinsic Perceptual and Attentional Rhythms. *Frontiers in Neuroscience*, *11*. Retrieved 2018-11-12, from `https://www.ncbi.nlm.nih.gov/pmc/articles/PMC5366344/` doi: 10.3389/fnins.2017.00154

Eagleman, D. M., & Sejnowski, T. J. (2000, March). Motion Integration and Postdiction in Visual Awareness. *Science*, *287*(5460), 2036–2038. Retrieved 2018-11-12, from `http://science.sciencemag.org/content/287/5460/2036` doi: 10.1126/science.287.5460.2036

Ehret, A. V. N. G., & Romand, L. d. N. R. (1997). *The Central Auditory System*. Oxford University Press.

Enns, J. T., & Di Lollo, V. (2000, September). What's new in visual masking? *Trends in Cognitive Sciences*, *4*(9), 345–352. Retrieved 2020-06-26, from `http://www.sciencedirect.com/science/article/pii/S1364661300015205` doi: 10.1016/S1364-6613(00)01520-5

Fahrenfort, J. J., Scholte, H. S., & Lamme, V. a. F. (2007, August). Masking Disrupts Reentrant Processing in Human Visual Cortex. *Journal of Cognitive Neuroscience*, *19*(9), 1488–1497. Retrieved 2020-03-27, from `https://www.mitpressjournals.org/doi/10.1162/jocn.2007.19.9.1488` doi: 10.1162/jocn.2007.19.9.1488

Fekete, T., Van de Cruys, S., Ekroll, V., & van Leeuwen, C. (2018, January). In the interest of saving time: a critique of discrete perception. *Neuroscience of Consciousness*, *2018*(1). Retrieved 2019-01-30, from `https://academic.oup.com/nc/article/2018/1/niy003/4978127` doi: 10.1093/

nc/niy003

Fiebelkorn, I. C., Foxe, J. J., Butler, J. S., Mercier, M. R., Snyder, A. C., & Molholm, S. (2011, July). Ready, Set, Reset: Stimulus-Locked Periodicity in Behavioral Performance Demonstrates the Consequences of Cross-Sensory Phase Reset. *Journal of Neuroscience*, *31*(27), 9971–9981. Retrieved 2020-03-27, from https://www.jneurosci.org/content/31/27/9971 doi: 10.1523/JNEUROSCI.1338-11.2011

Fiebelkorn, I. C., & Kastner, S. (2018, December). A Rhythmic Theory of Attention. *Trends in Cognitive Sciences*. Retrieved 2019-01-09, from http://www.sciencedirect.com/science/article/pii/S136466131830281X doi: 10.1016/j.tics.2018.11.009

Fiebelkorn, I. C., Pinsk, M. A., & Kastner, S. (2018). A Dynamic Interplay within the Frontoparietal Network Underlies Rhythmic Spatial Attention. *Neuron*, *99*(4), 842–853.e8. doi: 10.1016/j.neuron.2018.07.038

Fiebelkorn, I. C., Saalmann, Y. B., & Kastner, S. (2013, December). Rhythmic Sampling within and between Objects despite Sustained Attention at a Cued Location. *Current Biology*, *23*(24), 2553–2558. Retrieved 2020-03-27, from https://www.cell.com/current-biology/abstract/S0960-9822(13)01338-9 doi: 10.1016/j.cub.2013.10.063

Foxe, J. J., & Snyder, A. C. (2011). The Role of Alpha-Band Brain Oscillations as a Sensory Suppression Mechanism during Selective Attention. *Frontiers in Psychology*, *2*. Retrieved 2018-11-12, from https://www.frontiersin.org/articles/10.3389/fpsyg.2011.00154/full doi: 10.3389/fpsyg.2011.00154

Fransen, A. M. M., Dimitriadis, G., van Ede, F., & Maris, E. (2016, March). Distinct alpha- and beta-band rhythms over rat somatosensory cortex with similar properties as in humans. *Journal of Neurophysiology*, *115*(6), 3030–3044. Retrieved 2020-07-01, from https://journals.physiology.org/doi/full/10.1152/jn.00507.2015 (Publisher: American Physiological Society) doi: 10.1152/jn.00507.2015

Fries, P. (2015, October). Rhythms For Cognition: Communication Through Coherence. *Neuron*, *88*(1), 220–235. Retrieved 2020-07-10, from https://www.ncbi.nlm.nih.gov/pmc/articles/PMC4605134/ doi: 10.1016/j.neuron.2015.09.034

Friston, K. (2005, April). A theory of cortical responses. *Philosophical Transactions of the Royal Society B: Biological Sciences*, *360*(1456), 815–836. Retrieved 2020-08-07, from https://royalsocietypublishing.org/doi/

10.1098/rstb.2005.1622 (Publisher: Royal Society) doi: 10.1098/rstb.2005.1622

Fuggetta, G., Fiaschi, A., & Manganotti, P. (2005, October). Modulation of cortical oscillatory activities induced by varying single-pulse transcranial magnetic stimulation intensity over the left primary motor area: A combined EEG and TMS study. *NeuroImage*, *27*(4), 896–908. Retrieved 2020-06-26, from http://www.sciencedirect.com/science/article/pii/S1053811905003289 doi: 10.1016/j.neuroimage.2005.05.013

Gaetz, W., & Cheyne, D. (2006, April). Localization of sensorimotor cortical rhythms induced by tactile stimulation using spatially filtered MEG. *NeuroImage*, *30*(3), 899–908. doi: 10.1016/j.neuroimage.2005.10.009

Gaillard, C., Ben Hadj Hassen, S., Di Bello, F., Bihan-Poudec, Y., Van-Rullen, R., & Ben Hamed, S. (2020, February). Prefrontal attentional saccades explore space rhythmically. *Nature Communications*, *11*(1), 925. Retrieved 2020-09-14, from https://www.nature.com/articles/s41467-020-14649-7 (Number: 1 Publisher: Nature Publishing Group) doi: 10.1038/s41467-020-14649-7

Haegens, S., Nácher, V., Luna, R., Romo, R., & Jensen, O. (2011, November). Alpha-Oscillations in the monkey sensorimotor network influence discrimination performance by rhythmical inhibition of neuronal spiking. *Proceedings of the National Academy of Sciences of the United States of America*, *108*, 19377–82. doi: 10.1073/pnas.1117190108

Hanslmayr, S., Aslan, A., Staudigl, T., Klimesch, W., Herrmann, C. S., & Bäuml, K.-H. (2007, October). Prestimulus oscillations predict visual perception performance between and within subjects. *NeuroImage*, *37*(4), 1465–1473. doi: 10.1016/j.neuroimage.2007.07.011

Hanslmayr, S., Sauseng, P., Doppelmayr, M., Schabus, M., & Klimesch, W. (2005, March). Increasing Individual Upper Alpha Power by Neurofeedback Improves Cognitive Performance in Human Subjects. *Applied Psychophysiology and Biofeedback*, *30*(1), 1–10. Retrieved 2020-07-13, from http://link.springer.com/10.1007/s10484-005-2169-8 doi: 10.1007/s10484-005-2169-8

Hanslmayr, S., Volberg, G., Wimber, M., Dalal, S. S., & Greenlee, M. W. (2013, November). Prestimulus Oscillatory Phase at 7 Hz Gates Cortical Information Flow and Visual Perception. *Current Biology*, *23*(22), 2273–2278. Retrieved 2020-03-27, from https://www.cell.com/current-biology/abstract/S0960-9822(13)01136-6 doi: 10.1016/j.cub.2013.09.020

Harter, M. R. (1967). Excitability cycles and cortical scanning: A review of two hypotheses of central intermittency in perception. *Psychological Bulletin*, *68*(1), 47–58. (Place: US Publisher: American Psychological Association) doi: 10.1037/h0024725

Helfrich, R. F., Fiebelkorn, I. C., Szczepanski, S. M., Lin, J. J., Parvizi, J., Knight, R. T., & Kastner, S. (2018, August). Neural mechanisms of sustained attention are rhythmic. *Neuron*, *99*(4), 854–865.e5. Retrieved 2020-07-17, from `https://www.ncbi.nlm.nih.gov/pmc/articles/PMC6286091/` doi: 10.1016/j.neuron.2018.07.032

Helfrich, R. F., Schneider, T. R., Rach, S., Trautmann-Lengsfeld, S. A., Engel, A. K., & Herrmann, C. S. (2014, February). Entrainment of Brain Oscillations by Transcranial Alternating Current Stimulation. *Current Biology*, *24*(3), 333–339. Retrieved 2020-06-26, from `http://www.sciencedirect.com/science/article/pii/S096098221301600X` doi: 10.1016/j.cub.2013.12.041

Herring, J. D., Thut, G., Jensen, O., & Bergmann, T. O. (2015, October). Attention Modulates TMS-Locked Alpha Oscillations in the Visual Cortex. *The Journal of Neuroscience: The Official Journal of the Society for Neuroscience*, *35*(43), 14435–14447. doi: 10.1523/JNEUROSCI.1833-15.2015

Herrmann, C. S. (2001, April). Human EEG responses to 1–100 Hz flicker: resonance phenomena in visual cortex and their potential correlation to cognitive phenomena. *Experimental Brain Research*, *137*(3), 346–353. Retrieved 2018-11-12, from `https://doi.org/10.1007/s002210100682` doi: 10.1007/s002210100682

Herwig, A., & Schneider, W. X. (2014). Predicting object features across saccades: Evidence from object recognition and visual search. *Journal of Experimental Psychology: General*, *143*(5), 1903–1922. (Place: US Publisher: American Psychological Association) doi: 10.1037/a0036781

Herzog, M. H., Kammer, T., & Scharnowski, F. (2016, April). Time Slices: What Is the Duration of a Percept? *PLOS Biology*, *14*(4), e1002433. Retrieved 2020-03-27, from `https://journals.plos.org/plosbiology/article?id=10.1371/journal.pbio.1002433` doi: 10.1371/journal.pbio.1002433

Hikosaka, O., Miyauchi, S., & Shimojo, S. (1993, June). Focal visual attention produces illusory temporal order and motion sensation. *Vision Research*, *33*(9), 1219–1240. doi: 10.1016/0042-6989(93)90210-n

Hoffman, K. L., Dragan, M. C., Leonard, T. K., Micheli, C., Montefusco-

Siegmund, R., & Valiante, T. A. (2013). Saccades during visual exploration align hippocampal 3–8 Hz rhythms in human and non-human primates. *Frontiers in Systems Neuroscience*, *7*. Retrieved 2020-07-17, from https://www.frontiersin.org/articles/10.3389/fnsys.2013.00043/full doi: 10.3389/fnsys.2013.00043

Hogendoorn, H. (2016, May). Voluntary Saccadic Eye Movements Ride the Attentional Rhythm. *Journal of Cognitive Neuroscience*, *28*(10), 1625–1635. Retrieved 2020-06-26, from https://doi.org/10.1162/jocn_a_00986 doi: 10.1162/jocn_a_00986

Hogendoorn, H., & Burkitt, A. N. (2019, March). Predictive Coding with Neural Transmission Delays: A Real-Time Temporal Alignment Hypothesis. *eNeuro*, *6*(2). Retrieved 2020-04-03, from https://www.eneuro.org/content/6/2/ENEURO.0412-18.2019 doi: 10.1523/ENEURO.0412-18.2019

Holcombe, A. O., & Chen, W.-Y. (2013, January). Splitting attention reduces temporal resolution from 7 Hz for tracking one object to \textless3 Hz when tracking three. *Journal of Vision*, *13*(1), 12–12. Retrieved 2020-06-26, from https://jov.arvojournals.org/article.aspx?articleid=2121116 doi: 10.1167/13.1.12

Huang, G., Liu, J., Li, L., Zhang, L., Zeng, Y., Ren, L., ... Zhang, Z. (2019). A novel training-free externally-regulated neurofeedback (ER-NF) system using phase-guided visual stimulation for alpha modulation. *NeuroImage*, *189*, 688–699. doi: 10.1016/j.neuroimage.2019.01.072

Hubel, D. H., & Wiesel, T. N. (1962, January). Receptive fields, binocular interaction and functional architecture in the cat's visual cortex. *The Journal of Physiology*, *160*(1), 106–154.2. Retrieved 2020-08-17, from https://www.ncbi.nlm.nih.gov/pmc/articles/PMC1359523/

Hubel, D. H., & Wiesel, T. N. (1968). Receptive fields and functional architecture of monkey striate cortex. *The Journal of Physiology*, *195*(1), 215–243. Retrieved 2020-08-17, from https://physoc.onlinelibrary.wiley.com/doi/abs/10.1113/jphysiol.1968.sp008455 (_eprint: https://physoc.onlinelibrary.wiley.com/doi/pdf/10.1113/jphysiol.1968.sp008455) doi: 10.1113/jphysiol.1968.sp008455

Jensen, O., Bonnefond, M., & VanRullen, R. (2012, April). An oscillatory mechanism for prioritizing salient unattended stimuli. *Trends in Cognitive Sciences*, *16*(4), 200–206. Retrieved 2018-11-12, from http://www.sciencedirect.com/science/article/pii/S1364661312000575 doi:

10.1016/j.tics.2012.03.002

Jensen, O., Gips, B., Bergmann, T. O., & Bonnefond, M. (2014, July). Temporal coding organized by coupled alpha and gamma oscillations prioritize visual processing. *Trends in Neurosciences*, *37*(7), 357–369. Retrieved 2020-08-06, from http://www.sciencedirect.com/science/article/pii/S0166223614000605 doi: 10.1016/j.tins.2014.04.001

Jensen, O., & Mazaheri, A. (2010). Shaping Functional Architecture by Oscillatory Alpha Activity: Gating by Inhibition. *Frontiers in Human Neuroscience*, *4*. Retrieved 2018-11-12, from https://www.frontiersin.org/articles/10.3389/fnhum.2010.00186/full doi: 10.3389/fnhum.2010.00186

Johnson, M. G., & Henley, T. B. (2013). *Reflections on the Principles of Psychology: William James After A Century*. Psychology Press. (Google-Books-ID: aQ9jAjO4DTcC)

Jokisch, D., & Jensen, O. (2007, March). Modulation of Gamma and Alpha Activity during a Working Memory Task Engaging the Dorsal or Ventral Stream. *Journal of Neuroscience*, *27*(12), 3244–3251. Retrieved 2018-11-12, from http://www.jneurosci.org/content/27/12/3244 doi: 10.1523/JNEUROSCI.5399-06.2007

Kelly, S. P., Lalor, E. C., Reilly, R. B., & Foxe, J. J. (2006, June). Increases in Alpha Oscillatory Power Reflect an Active Retinotopic Mechanism for Distracter Suppression During Sustained Visuospatial Attention. *Journal of Neurophysiology*, *95*(6), 3844–3851. Retrieved 2018-11-12, from https://www.physiology.org/doi/full/10.1152/jn.01234.2005 doi: 10.1152/jn.01234.2005

Kerzel, D. (2010). The Fröhlich effect: past and present. In R. Nijhawan & B. Khurana (Eds.), *Space and Time in Perception and Action* (pp. 321–337). Cambridge: Cambridge University Press. Retrieved 2018-11-12, from https://www.cambridge.org/core/product/identifier/CBO9780511750540A030/type/book_part doi: 10.1017/CBO9780511750540.019

Kienitz, R., Schmiedt, J. T., Shapcott, K. A., Kouroupaki, K., Saunders, R. C., & Schmid, M. C. (2018, August). Theta Rhythmic Neuronal Activity and Reaction Times Arising from Cortical Receptive Field Interactions during Distributed Attention. *Current Biology*, *28*(15), 2377–2387.e5. Retrieved 2020-03-27, from http://www.sciencedirect.com/science/article/pii/S0960982218307541 doi: 10.1016/j.cub.2018.05.086

Kilavik, B. E., Zaepffel, M., Brovelli, A., MacKay, W. A., & Riehle, A. (2013, July). The ups and downs of beta oscillations in sensorimotor cortex. *Experimental Neurology*, *245*, 15–26. Retrieved 2020-07-01, from http://www.sciencedirect.com/science/article/pii/S0014488612003767 doi: 10.1016/j.expneurol.2012.09.014

Kitazawa, S., Moizumi, S., Okuzumi, A., Saito, F., Shibuya, S., Takahashi, T., ... Yamamoto, S. (n.d.). *Reversal of subjective temporal order due to sensory and motor integrations.* Oxford University Press. Retrieved 2020-06-26, from https://www.oxfordscholarship.com/view/10.1093/acprof:oso/9780199231447.001.0001/acprof-9780199231447-chapter-4

Klimesch, W. (1999, April). EEG alpha and theta oscillations reflect cognitive and memory performance: a review and analysis. *Brain Research Reviews*, *29*(2), 169–195. Retrieved 2018-11-12, from http://www.sciencedirect.com/science/article/pii/S0165017398000563 doi: 10.1016/S0165-0173(98)00056-3

Klimesch, W. (2012, December). Alpha-band oscillations, attention, and controlled access to stored information. *Trends in Cognitive Sciences*, *16*(12), 606–617. Retrieved 2018-11-12, from http://www.sciencedirect.com/science/article/pii/S1364661312002434 doi: 10.1016/j.tics.2012.10.007

Klimesch, W., Sauseng, P., & Hanslmayr, S. (2007, January). EEG alpha oscillations: The inhibition–timing hypothesis. *Brain Research Reviews*, *53*(1), 63–88. Retrieved 2018-11-12, from http://www.sciencedirect.com/science/article/pii/S016501730600083X doi: 10.1016/j.brainresrev.2006.06.003

Klimesch, W., Sauseng, P., Hanslmayr, S., Gruber, W., & Freunberger, R. (2007, January). Event-related phase reorganization may explain evoked neural dynamics. *Neuroscience & Biobehavioral Reviews*, *31*(7), 1003–1016. Retrieved 2020-06-26, from http://www.sciencedirect.com/science/article/pii/S0149763407000334 doi: 10.1016/j.neubiorev.2007.03.005

Kometer, M., Schmidt, A., Jäncke, L., & Vollenweider, F. X. (2013, June). Activation of Serotonin 2A Receptors Underlies the Psilocybin-Induced Effects on alpha Oscillations N170 Visual-Evoked Potentials and Visual Hallucinations. *Journal of Neuroscience*, *33*(25), 10544–10551. Retrieved 2020-07-10, from https://www.jneurosci.org/content/33/25/

10544 (Publisher: Society for Neuroscience Section: Articles) doi: 10.1523/JNEUROSCI.3007-12.2013

Kresevic, J. L., Marinovic, W., Johnston, A., & Arnold, D. H. (2016, August). Time order reversals and saccades. *Vision Research*, *125*, 23–29. Retrieved 2020-03-27, from http://www.sciencedirect.com/science/article/pii/S0042698916300232 doi: 10.1016/j.visres.2016.04.005

Kusunoki, M., & Goldberg, M. E. (2003, March). The Time Course of Perisaccadic Receptive Field Shifts in the Lateral Intraparietal Area of the Monkey. *Journal of Neurophysiology*, *89*(3), 1519–1527. Retrieved 2020-08-18, from https://journals.physiology.org/doi/full/10.1152/jn.00519.2002 (Publisher: American Physiological Society) doi: 10.1152/jn.00519.2002

Landau, A. N., & Fries, P. (2012, June). Attention Samples Stimuli Rhythmically. *Current Biology*, *22*(11), 1000–1004. Retrieved 2020-03-27, from https://www.cell.com/current-biology/abstract/S0960-9822(12)00341-7 doi: 10.1016/j.cub.2012.03.054

Landau, A. N., Schreyer, H. M., van Pelt, S., & Fries, P. (2015, August). Distributed Attention Is Implemented through Theta-Rhythmic Gamma Modulation. *Current Biology*, *25*(17), 2332–2337. Retrieved 2020-03-27, from https://www.cell.com/current-biology/abstract/S0960-9822(15)00882-9 doi: 10.1016/j.cub.2015.07.048

Lappe, M., Awater, H., & Krekelberg, B. (2000, February). Postsaccadic visual references generate presaccadic compression of space. *Nature*, *403*(6772), 892–895. doi: 10.1038/35002588

Lee, H., Simpson, G. V., Logothetis, N. K., & Rainer, G. (2005, January). Phase Locking of Single Neuron Activity to Theta Oscillations during Working Memory in Monkey Extrastriate Visual Cortex. *Neuron*, *45*(1), 147–156. Retrieved 2020-03-27, from https://www.cell.com/neuron/abstract/S0896-6273(04)00841-4 doi: 10.1016/j.neuron.2004.12.025

Lenartowicz, A., Mazaheri, A., Jensen, O., & Loo, S. K. (2018, January). Aberrant Modulation of Brain Oscillatory Activity and Attentional Impairment in Attention-Deficit/Hyperactivity Disorder. *Biological Psychiatry: Cognitive Neuroscience and Neuroimaging*, *3*(1), 19–29. Retrieved 2020-07-14, from http://www.sciencedirect.com/science/article/pii/S2451902217301714 doi: 10.1016/j.bpsc.2017.09.009

İlhan, B., & VanRullen, R. (2012, November). No Counterpart of Visual Perceptual Echoes in the Auditory System. *PLOS ONE*, *7*(11),

e49287. Retrieved 2020-07-01, from https://journals.plos.org/plosone/article?id=10.1371/journal.pone.0049287 (Publisher: Public Library of Science) doi: 10.1371/journal.pone.0049287

Linares, D., Holcombe, A. O., & White, A. L. (2009, December). Where is the moving object now? Judgments of instantaneous position show poor temporal precision (SD = 70 ms). *Journal of Vision*, *9*(13), 9–9. Retrieved 2018-11-12, from https://jov.arvojournals.org/article.aspx?articleid=2193411 doi: 10.1167/9.13.9

Lisman, J. E., & Jensen, O. (2013, March). The Theta-Gamma Neural Code. *Neuron*, *77*(6), 1002–1016. Retrieved 2020-06-26, from http://www.sciencedirect.com/science/article/pii/S0896627313002316 doi: 10.1016/j.neuron.2013.03.007

Lozano-Soldevilla, D., & VanRullen, R. (2019, January). The Hidden Spatial Dimension of Alpha: 10-Hz Perceptual Echoes Propagate as Periodic Traveling Waves in the Human Brain. *Cell Reports*, *26*(2), 374–380.e4. Retrieved 2020-09-21, from http://www.sciencedirect.com/science/article/pii/S2211124718320035 doi: 10.1016/j.celrep.2018.12.058

Lőrincz, M. L., Kékesi, K. A., Juhász, G., Crunelli, V., & Hughes, S. W. (2009, September). Temporal Framing of Thalamic Relay-Mode Firing by Phasic Inhibition during the Alpha Rhythm. *Neuron*, *63*(5), 683–696. Retrieved 2018-11-12, from https://www.ncbi.nlm.nih.gov/pmc/articles/PMC2791173/ doi: 10.1016/j.neuron.2009.08.012

Macdonald, J. S. P., Cavanagh, P., & VanRullen, R. (2014, January). Attentional sampling of multiple wagon wheels. *Attention, Perception, & Psychophysics*, *76*(1), 64–72. Retrieved 2020-03-27, from https://doi.org/10.3758/s13414-013-0555-5 doi: 10.3758/s13414-013-0555-5

Mackay, D. M. (1970, August). Mislocation of Test Flashes during Saccadic Image Displacements. *Nature*, *227*(5259), 731–733. Retrieved 2020-02-06, from https://www.nature.com/articles/227731a0 doi: 10.1038/227731a0

Makeig, S., Westerfield, M., Jung, T.-P., Enghoff, S., Townsend, J., Courchesne, E., & Sejnowski, T. J. (2002, January). Dynamic Brain Sources of Visual Evoked Responses. *Science*, *295*(5555), 690–694. Retrieved 2020-06-26, from https://science.sciencemag.org/content/295/5555/690 doi: 10.1126/science.1066168

Masquelier, T., Hugues, E., Deco, G., & Thorpe, S. J. (2009, October). Oscillations, Phase-of-Firing Coding, and Spike Timing-Dependent Plastic-

ity: An Efficient Learning Scheme. *Journal of Neuroscience*, *29*(43), 13484–13493. Retrieved 2020-08-12, from https://www.jneurosci.org/content/29/43/13484 doi: 10.1523/JNEUROSCI.2207-09.2009

Mathewson, K. E., Fabiani, M., Gratton, G., Beck, D. M., & Lleras, A. (2010, April). Rescuing stimuli from invisibility: Inducing a momentary release from visual masking with pre-target entrainment. *Cognition*, *115*(1), 186–191. doi: 10.1016/j.cognition.2009.11.010

Mathewson, K. E., Gratton, G., Fabiani, M., Beck, D. M., & Ro, T. (2009, March). To See or Not to See: Prestimulus alpha Phase Predicts Visual Awareness. *Journal of Neuroscience*, *29*(9), 2725–2732. Retrieved 2018-11-12, from http://www.jneurosci.org/content/29/9/2725 doi: 10.1523/JNEUROSCI.3963-08.2009

Mathewson, K. E., Lleras, A., Beck, D. M., Fabiani, M., Ro, T., & Gratton, G. (2011, May). Pulsed Out of Awareness: EEG Alpha Oscillations Represent a Pulsed-Inhibition of Ongoing Cortical Processing. *Frontiers in Psychology*, *2*. Retrieved 2018-11-12, from https://www.ncbi.nlm.nih.gov/pmc/articles/PMC3132674/ doi: 10.3389/fpsyg.2011.00099

Mathôt, S., & Theeuwes, J. (2010). Evidence for the predictive remapping of visual attention. *Experimental Brain Research*, *200*(1), 117–122. Retrieved 2020-08-18, from https://research.vu.nl/en/publications/evidence-for-the-predictive-remapping-of-visual-attention-2 (Publisher: Springer Verlag) doi: 10.1007/s00221-009-2055-3

McLelland, D., Lavergne, L., & VanRullen, R. (2016, July). The phase of ongoing EEG oscillations predicts the amplitude of peri-saccadic mislocalization. *Scientific Reports*, *6*(1), 1–8. Retrieved 2020-03-27, from https://www.nature.com/articles/srep29335 doi: 10.1038/srep29335

Melcher, D. (2009, June). Selective attention and the active remapping of object features in trans-saccadic perception. *Vision Research*, *49*(10), 1249–1255. Retrieved 2020-08-20, from http://www.sciencedirect.com/science/article/pii/S0042698908001454 doi: 10.1016/j.visres.2008.03.014

Melcher, D., & Colby, C. L. (2008, December). Trans-saccadic perception. *Trends in Cognitive Sciences*, *12*(12), 466–473. Retrieved 2020-03-27, from https://www.cell.com/trends/cognitive-sciences/abstract/S1364-6613(08)00232-5 doi: 10.1016/j.tics.2008.09.003

Milton, A., & Pleydell-Pearce, C. W. (2016). The phase of pre-stimulus alpha oscillations influences the visual perception of stimulus timing. *NeuroImage*, *133*, 53–61. doi: 10.1016/j.neuroimage.2016.02.065

Moore, T., & Armstrong, K. M. (2003, January). Selective gating of visual signals by microstimulation of frontal cortex. *Nature*, *421*(6921), 370–373. Retrieved 2020-09-21, from https://www.nature.com/articles/nature01341 (Number: 6921 Publisher: Nature Publishing Group) doi: 10.1038/nature01341

Moore, T., Tolias, A. S., & Schiller, P. H. (1998, July). Visual representations during saccadic eye movements. *Proceedings of the National Academy of Sciences*, *95*(15), 8981–8984. Retrieved 2020-08-20, from https://www.pnas.org/content/95/15/8981 (Publisher: National Academy of Sciences Section: Biological Sciences) doi: 10.1073/pnas.95.15.8981

Morrone, M. C., Ross, J., & Burr, D. (2005, July). Saccadic eye movements cause compression of time as well as space. *Nature Neuroscience*, *8*(7), 950–954. Retrieved 2020-06-26, from https://www.nature.com/articles/nn1488 doi: 10.1038/nn1488

Muller, G. R., Neuper, C., & Pfurtscheller, G. (2001, January). Resonance-like“ Frequencies of Sensorimotor Areas Evoked by Repetitive Tactile Stimulation - Resonanzeffekte in sensomotorischen Arealen, evoziert durch rhythmische taktile Stimulation. *Biomedical Engineering / Biomedizinische Technik*, *46*(7-8), 186–190. Retrieved 2020-07-02, from https://www.degruyter.com/view/journals/bmte/46/7-8/article-p186.xml (Publisher: De Gruyter Section: Biomedical Engineering / Biomedizinische Technik) doi: 10.1515/bmte.2001.46.7-8.186

Murakami, I. (2001, November). A flash-lag effect in random motion. *Vision Research*, *41*(24), 3101–3119. Retrieved 2018-11-12, from http://www.sciencedirect.com/science/article/pii/S0042698901001936 doi: 10.1016/S0042-6989(01)00193-6

Nakamura, K., Mikami, A., & Kubota, K. (1991, October). Unique oscillatory activity related to visual processing in the temporal pole of monkeys. *Neuroscience Research*, *12*(1), 293–299. Retrieved 2020-03-27, from http://www.sciencedirect.com/science/article/pii/016801029190119J doi: 10.1016/0168-0102(91)90119-J

Newcombe, R. G. (1998, April). Interval estimation for the difference between independent proportions: comparison of eleven methods. *Statistics in Medicine*, *17*(8), 873–890. doi: 10.1002/(sici)1097-0258(19980430)17:8⟨873::aid-sim779⟩3.0.co;2-i

O'Regan, J. K. (1984, January). Retinal versus extraretinal influences in flash localization during saccadic eye movements in the presence of a

visible background. *Perception & Psychophysics*, *36*(1), 1–14. Retrieved 2020-02-06, from https://doi.org/10.3758/BF03206348 doi: 10.3758/BF03206348

Osipova, D., Hermes, D., & Jensen, O. (2008). Gamma power is phase-locked to posterior alpha activity. *PloS One*, *3*(12), e3990. doi: 10.1371/journal.pone.0003990

Ostendorf, F., Fischer, C., Gaymard, B., & Ploner, C. J. (2006, February). Perisaccadic mislocalization without saccadic eye movements. *Neuroscience*, *137*(3), 737–745. doi: 10.1016/j.neuroscience.2005.09.032

Otero-Millan, J., Troncoso, X. G., Macknik, S. L., Serrano-Pedraza, I., & Martinez-Conde, S. (2008, October). Saccades and microsaccades during visual fixation, exploration, and search: Foundations for a common saccadic generator. *Journal of Vision*, *8*(14), 21–21. Retrieved 2020-03-27, from http://jov.arvojournals.org/article.aspx?articleid=2193271 doi: 10.1167/8.14.21

Paus, T., Sipila, P. K., & Strafella, A. P. (2001, October). Synchronization of Neuronal Activity in the Human Primary Motor Cortex by Transcranial Magnetic Stimulation: An EEG Study. *Journal of Neurophysiology*, *86*(4), 1983–1990. Retrieved 2020-06-26, from https://journals.physiology.org/doi/full/10.1152/jn.2001.86.4.1983 doi: 10.1152/jn.2001.86.4.1983

Pfurtscheller, G. (1981, March). Central beta rhythm during sensorimotor activities in man. *Electroencephalography and Clinical Neurophysiology*, *51*(3), 253–264. Retrieved 2020-08-06, from http://www.sciencedirect.com/science/article/pii/0013469481901395 doi: 10.1016/0013-4694(81)90139-5

Pfurtscheller, G., & Lopes da Silva, F. H. (1999, November). Event-related EEG/MEG synchronization and desynchronization: basic principles. *Clinical Neurophysiology*, *110*(11), 1842–1857. Retrieved 2020-07-01, from http://www.sciencedirect.com/science/article/pii/S1388245799001418 doi: 10.1016/S1388-2457(99)00141-8

Pfurtscheller, G., Stancák, A., & Neuper, C. (1996, November). Event-related synchronization (ERS) in the alpha band — an electrophysiological correlate of cortical idling: A review. *International Journal of Psychophysiology*, *24*(1), 39–46. Retrieved 2020-03-25, from http://www.sciencedirect.com/science/article/pii/S0167876096000669 doi: 10.1016/S0167-8760(96)00066-9

Pfurtscheller, G., Woertz, M., Müller, G., Wriessnegger, S., & Pfurtscheller, K. (2002, April). Contrasting behavior of beta event-related synchronization and somatosensory evoked potential after median nerve stimulation during finger manipulation in man. *Neuroscience Letters*, *323*(2), 113–116. Retrieved 2020-08-06, from http://www.sciencedirect.com/science/article/pii/S0304394002001192 doi: 10.1016/S0304-3940(02)00119-2

Pitts, W., & McCulloch, W. S. (1947, September). How we know universals the perception of auditory and visual forms. *The bulletin of mathematical biophysics*, *9*(3), 127–147. Retrieved 2020-09-02, from https://doi.org/10.1007/BF02478291 doi: 10.1007/BF02478291

Ploner, M., Gross, J., Timmermann, L., Pollok, B., & Schnitzler, A. (2006, September). Oscillatory activity reflects the excitability of the human somatosensory system. *NeuroImage*, *32*(3), 1231–1236. Retrieved 2020-07-01, from http://www.sciencedirect.com/science/article/pii/S1053811906006641 doi: 10.1016/j.neuroimage.2006.06.004

Rao, R. P. N., & Ballard, D. H. (1999, January). Predictive coding in the visual cortex: a functional interpretation of some extra-classical receptive-field effects. *Nature Neuroscience*, *2*(1), 79–87. Retrieved 2020-04-01, from http://www.nature.com/articles/nn0199_79 doi: 10.1038/4580

Regan, D. (1977, November). Steady-state evoked potentials. *JOSA*, *67*(11), 1475–1489. Retrieved 2020-07-16, from https://www.osapublishing.org/josa/abstract.cfm?uri=josa-67-11-1475 (Publisher: Optical Society of America) doi: 10.1364/JOSA.67.001475

Rohenkohl, G., & Nobre, A. C. (2011, October). Alpha Oscillations Related to Anticipatory Attention Follow Temporal Expectations. *Journal of Neuroscience*, *31*(40), 14076–14084. Retrieved 2018-11-12, from http://www.jneurosci.org/content/31/40/14076 doi: 10.1523/JNEUROSCI.3387-11.2011

Rollenhagen, J. E., & Olson, C. R. (2005, November). Low-Frequency Oscillations Arising From Competitive Interactions Between Visual Stimuli in Macaque Inferotemporal Cortex. *Journal of Neurophysiology*, *94*(5), 3368–3387. Retrieved 2020-03-27, from https://journals.physiology.org/doi/full/10.1152/jn.00158.2005 doi: 10.1152/jn.00158.2005

Romei, V., Gross, J., & Thut, G. (2010, June). On the Role of Prestimulus Alpha Rhythms over Occipito-Parietal Areas in Visual Input Regulation: Correlation or Causation? *Journal of Neuroscience*, *30*(25), 8692–8697. Retrieved 2018-11-12, from http://www.jneurosci.org/content/

30/25/8692 doi: 10.1523/JNEUROSCI.0160-10.2010

Romei, V., Gross, J., & Thut, G. (2012, May). Sounds Reset Rhythms of Visual Cortex and Corresponding Human Visual Perception. *Current Biology*, *22*(9), 807–813. Retrieved 2020-06-26, from http://www.sciencedirect.com/science/article/pii/S0960982212003120 doi: 10.1016/j.cub.2012.03.025

Ronconi, L., Busch, N. A., & Melcher, D. (2018, August). Alpha-band sensory entrainment alters the duration of temporal windows in visual perception. *Scientific Reports*, *8*(1), 11810. Retrieved 2018-11-12, from https://www.nature.com/articles/s41598-018-29671-5 doi: 10.1038/s41598-018-29671-5

Ronconi, L., & Melcher, D. (2017, November). The Role of Oscillatory Phase in Determining the Temporal Organization of Perception: Evidence from Sensory Entrainment. *Journal of Neuroscience*, *37*(44), 10636–10644. Retrieved 2020-06-26, from https://www.jneurosci.org/content/37/44/10636 doi: 10.1523/JNEUROSCI.1704-17.2017

Rosanova, M., Casali, A., Bellina, V., Resta, F., Mariotti, M., & Massimini, M. (2009, June). Natural Frequencies of Human Corticothalamic Circuits. *Journal of Neuroscience*, *29*(24), 7679–7685. Retrieved 2020-06-26, from https://www.jneurosci.org/content/29/24/7679 doi: 10.1523/JNEUROSCI.0445-09.2009

Ross, J., Morrone, M. C., & Burr, D. C. (1997, April). Compression of visual space before saccades. *Nature*, *386*(6625), 598–601. doi: 10.1038/386598a0

Samaha, J., & Postle, B. R. (2015, November). The Speed of Alpha-Band Oscillations Predicts the Temporal Resolution of Visual Perception. *Current Biology*, *25*(22), 2985–2990. Retrieved 2018-11-12, from https://www.cell.com/current-biology/abstract/S0960-9822(15)01235-X doi: 10.1016/j.cub.2015.10.007

Sanderson, K. J., Bishop, P. O., & Darian-Smith, I. (1971, August). The properties of the binocular receptive fields of lateral geniculate neurons. *Experimental Brain Research*, *13*(2), 178–207. Retrieved 2020-08-17, from https://doi.org/10.1007/BF00234085 doi: 10.1007/BF00234085

Sato, T., Kawamura, T., & Iwai, E. (1980, February). Responsiveness of inferotemporal single units to visual pattern stimuli in monkeys performing discrimination. *Experimental Brain Research*, *38*(3), 313–319. Retrieved 2020-03-27, from https://doi.org/10.1007/BF00236651 doi:

10.1007/BF00236651

Sauseng, P., Klimesch, W., Stadler, W., Schabus, M., Doppelmayr, M., Hanslmayr, S., ... Birbaumer, N. (2005, December). A shift of visual spatial attention is selectively associated with human EEG alpha activity. *European Journal of Neuroscience*, *22*(11), 2917–2926. Retrieved 2018-11-12, from https://onlinelibrary.wiley.com/doi/abs/10.1111/j.1460-9568.2005.04482.x doi: 10.1111/j.1460-9568.2005.04482.x

Savers, B. M., Beagley, H. A., & Henshall, W. R. (1974, February). The Mechanism of Auditory Evoked EEG Responses. *Nature*, *247*(5441), 481–483. Retrieved 2020-06-26, from https://www.nature.com/articles/247481a0 doi: 10.1038/247481a0

Scharlau, I. (2008, July). Temporal processes in prime–mask interaction: Assessing perceptual consequences of masked information. *Advances in Cognitive Psychology*, *3*(1-2), 241–255. Retrieved 2020-03-06, from https://www.ncbi.nlm.nih.gov/pmc/articles/PMC2864975/ doi: 10.2478/v10053-008-0028-x

Scharnowski, F., Rüter, J., Jolij, J., Hermens, F., Kammer, T., & Herzog, M. H. (2009, June). Long-lasting modulation of feature integration by transcranial magnetic stimulation. *Journal of Vision*, *9*(6), 1–1. Retrieved 2020-06-26, from https://jov.arvojournals.org/article.aspx?articleid=2204003 doi: 10.1167/9.6.1

Schmid, M. C., Mrowka, S. W., Turchi, J., Saunders, R. C., Wilke, M., Peters, A. J., ... Leopold, D. A. (2010, July). Blindsight depends on the lateral geniculate nucleus. *Nature*, *466*(7304), 373–377. Retrieved 2018-12-17, from https://www.nature.com/articles/nature09179 doi: 10.1038/nature09179

Schneider, K. A. (2018). The Flash-Lag, Fröhlich and Related Motion Illusions Are Natural Consequences of Discrete Sampling in the Visual System. *Frontiers in Psychology*, *9*. Retrieved 2018-11-12, from https://www.frontiersin.org/articles/10.3389/fpsyg.2018.01227/full doi: 10.3389/fpsyg.2018.01227

Schroeder, C. E., & Lakatos, P. (2009, January). Low-frequency neuronal oscillations as instruments of sensory selection. *Trends in neurosciences*, *32*(1). Retrieved 2020-08-06, from https://www.ncbi.nlm.nih.gov/pmc/articles/PMC2990947/ doi: 10.1016/j.tins.2008.09.012

Schwab, K., Ligges, C., Jungmann, T., Hilgenfeld, B., Haueisen, J.,

& Witte, H. (2006, November). Alpha entrainment in human electroencephalogram and magnetoencephalogram recordings. *NeuroReport*, *17*(17), 1829–1833. Retrieved 2020-06-26, from https://journals.lww.com/neuroreport/Abstract/2006/11270/Alpha_entrainment_in_human_electroencephalogram.15.aspx doi: 10.1097/01.wnr.0000246326.89308.ec

Schwenk, J. C. B., VanRullen, R., & Bremmer, F. (2020, August). Dynamics of Visual Perceptual Echoes Following Short-Term Visual Deprivation. *Cerebral Cortex Communications*, *1*(1). Retrieved 2020-09-01, from https://academic.oup.com/cercorcomms/article/1/1/tgaa012/5818880 (Publisher: Oxford Academic) doi: 10.1093/texcom/tgaa012

Seth, A. K. (2014, April). A predictive processing theory of sensorimotor contingencies: Explaining the puzzle of perceptual presence and its absence in synesthesia. *Cognitive Neuroscience*, *5*(2), 97–118. Retrieved 2020-08-07, from https://doi.org/10.1080/17588928.2013.877880 (Publisher: Routledge _eprint: https://doi.org/10.1080/17588928.2013.877880) doi: 10.1080/17588928.2013.877880

Sheinberg, D. L., & Logothetis, N. K. (1997, April). The role of temporal cortical areas in perceptual organization. *Proceedings of the National Academy of Sciences*, *94*(7), 3408–3413. Retrieved 2020-03-27, from https://www.pnas.org/content/94/7/3408 doi: 10.1073/pnas.94.7.3408

Simonson, E., & Brozek, J. (1952, July). Flicker fusion frequency; background and applications. *Physiological Reviews*, *32*(3), 349–378. doi: 10.1152/physrev.1952.32.3.349

Snyder, A. Z. (1992, May). Steady-state vibration evoked potentials: description of technique and characterization of responses. *Electroencephalography and Clinical Neurophysiology/Evoked Potentials Section*, *84*(3), 257–268. Retrieved 2020-07-02, from http://www.sciencedirect.com/science/article/pii/016855979290007X doi: 10.1016/0168-5597(92)90007-X

Solis-Escalante, T., Müller-Putz, G. R., Pfurtscheller, G., & Neuper, C. (2012, June). Cue-induced beta rebound during withholding of overt and covert foot movement. *Clinical Neurophysiology*, *123*(6), 1182–1190. Retrieved 2020-08-06, from http://www.sciencedirect.com/science/article/pii/S1388245712000594 doi: 10.1016/j.clinph.2012.01.013

Song, K., Meng, M., Chen, L., Zhou, K., & Luo, H. (2014, April). Behavioral Oscillations in Attention: Rhythmic alpha Pulses Mediated through theta

Band. *Journal of Neuroscience*, *34*(14), 4837–4844. Retrieved 2020-03-27, from https://www.jneurosci.org/content/34/14/4837 doi: 10.1523/JNEUROSCI.4856-13.2014

Spaak, E., Lange, F. P. d., & Jensen, O. (2014, March). Local Entrainment of Alpha Oscillations by Visual Stimuli Causes Cyclic Modulation of Perception. *Journal of Neuroscience*, *34*(10), 3536–3544. Retrieved 2018-11-12, from http://www.jneurosci.org/content/34/10/3536 doi: 10.1523/JNEUROSCI.4385-13.2014

Spalek, T. M., Lagroix, H. E. P., Yanko, M. R., & Di Lollo, V. (2012, April). Perception of temporal order is impaired during the time course of the attentional blink. *Journal of Experimental Psychology. Human Perception and Performance*, *38*(2), 402–413. doi: 10.1037/a0025050

Spence, C., & Parise, C. (2010, March). Prior-entry: A review. *Consciousness and Cognition*, *19*(1), 364–379. Retrieved 2020-06-26, from http://www.sciencedirect.com/science/article/pii/S1053810009001871 doi: 10.1016/j.concog.2009.12.001

Spyropoulos, G., Bosman, C. A., & Fries, P. (2018, June). A theta rhythm in macaque visual cortex and its attentional modulation. *Proceedings of the National Academy of Sciences*, *115*(24), E5614–E5623. Retrieved 2020-09-14, from https://www.pnas.org/content/115/24/E5614 (Publisher: National Academy of Sciences Section: PNAS Plus) doi: 10.1073/pnas.1719433115

Stroud, J. M. (1956). The fine structure of psychological time. In *Information theory in psychology: problems and methods* (pp. 174–207). New York, NY, US: Free Press.

Tamura, H., & Tanaka, K. (2001, May). Visual Response Properties of Cells in the Ventral and Dorsal Parts of the Macaque Inferotemporal Cortex. *Cerebral Cortex*, *11*(5), 384–399. Retrieved 2020-03-27, from https://academic.oup.com/cercor/article/11/5/384/385889 doi: 10.1093/cercor/11.5.384

Terao, M., Watanabe, J., Yagi, A., & Nishida, S. (2008, May). Reduction of stimulus visibility compresses apparent time intervals. *Nature Neuroscience*, *11*(5), 541–542. Retrieved 2020-06-26, from https://www.nature.com/articles/nn.2111 doi: 10.1038/nn.2111

Thorpe, S., Delorme, A., & Van Rullen, R. (2001, July). Spike-based strategies for rapid processing. *Neural Networks*, *14*(6), 715–725. Retrieved 2020-07-14, from http://www.sciencedirect.com/science/article/

pii/S0893608001000831 doi: 10.1016/S0893-6080(01)00083-1

Thut, G., Nietzel, A., Brandt, S. A., & Pascual-Leone, A. (2006, September). Alpha-Band Electroencephalographic Activity over Occipital Cortex Indexes Visuospatial Attention Bias and Predicts Visual Target Detection. *Journal of Neuroscience*, *26*(37), 9494–9502. Retrieved 2020-03-25, from https://www.jneurosci.org/content/26/37/9494 doi: 10.1523/JNEUROSCI.0875-06.2006

Thut, G., Veniero, D., Romei, V., Miniussi, C., Schyns, P., & Gross, J. (2011, July). Rhythmic TMS Causes Local Entrainment of Natural Oscillatory Signatures. *Current Biology*, *21*(14), 1176–1185. Retrieved 2018-11-12, from http://www.sciencedirect.com/science/article/pii/S0960982211006075 doi: 10.1016/j.cub.2011.05.049

Tobimatsu, S., Zhang, Y. M., & Kato, M. (1999, November). Steady-state vibration somatosensory evoked potentials: physiological characteristics and tuning function. *Clinical Neurophysiology*, *110*(11), 1953–1958. Retrieved 2020-07-02, from http://www.sciencedirect.com/science/article/pii/S1388245799001467 doi: 10.1016/S1388-2457(99)00146-7

Tuladhar, A. M., Huurne, N. t., Schoffelen, J.-M., Maris, E., Oostenveld, R., & Jensen, O. (2007, August). Parieto-occipital sources account for the increase in alpha activity with working memory load. *Human Brain Mapping*, *28*(8), 785–792. Retrieved 2018-11-12, from https://onlinelibrary.wiley.com/doi/abs/10.1002/hbm.20306 doi: 10.1002/hbm.20306

Valera, F. J., Toro, A., Roy John, E., & Schwartz, E. L. (1981, January). Perceptual framing and cortical alpha rhythm. *Neuropsychologia*, *19*(5), 675–686. Retrieved 2018-11-12, from http://www.sciencedirect.com/science/article/pii/0028393281900051 doi: 10.1016/0028-3932(81)90005-1

van Diepen, R. M., Cohen, M. X., Denys, D., & Mazaheri, A. (2015, March). Attention and Temporal Expectations Modulate Power, Not Phase, of Ongoing Alpha Oscillations. *Journal of Cognitive Neuroscience*, *27*(8), 1573–1586. Retrieved 2018-11-12, from https://doi.org/10.1162/jocn_a_00803 doi: 10.1162/jocn_a_00803

van Noordt, S. J. R., Desjardins, J. A., Gogo, C. E. T., Tekok-Kilic, A., & Segalowitz, S. J. (2017, January). Cognitive control in the eye of the beholder: Electrocortical theta and alpha modulation during response preparation in a cued saccade task. *NeuroImage*, *145*, 82–95. Retrieved

2020-07-17, from http://www.sciencedirect.com/science/article/pii/S105381191630533X doi: 10.1016/j.neuroimage.2016.09.054

VanRullen, R. (2013, December). Visual Attention: A Rhythmic Process? *Current Biology*, *23*(24), R1110–R1112. Retrieved 2020-03-23, from http://www.sciencedirect.com/science/article/pii/S0960982213013924 doi: 10.1016/j.cub.2013.11.006

VanRullen, R. (2016). Perceptual Cycles. *Trends in Cognitive Sciences*, *20*(10), 723–735. doi: 10.1016/j.tics.2016.07.006

VanRullen, R. (2018, August). Attention Cycles. *Neuron*, *99*(4), 632–634. Retrieved 2020-09-16, from http://www.sciencedirect.com/science/article/pii/S0896627318306792 doi: 10.1016/j.neuron.2018.08.006

VanRullen, R., Carlson, T., & Cavanagh, P. (2007, December). The blinking spotlight of attention. *Proceedings of the National Academy of Sciences*, *104*(49), 19204–19209. Retrieved 2020-03-23, from https://www.pnas.org/content/104/49/19204 doi: 10.1073/pnas.0707316104

Vanrullen, R., & Dubois, J. (2011). The psychophysics of brain rhythms. *Frontiers in Psychology*, *2*, 203. doi: 10.3389/fpsyg.2011.00203

VanRullen, R., & Koch, C. (2003, May). Is perception discrete or continuous? *Trends in Cognitive Sciences*, *7*(5), 207–213.

VanRullen, R., & Macdonald, J. S. P. (2012, June). Perceptual echoes at 10 Hz in the human brain. *Current biology: CB*, *22*(11), 995–999. doi: 10.1016/j.cub.2012.03.050

VanRullen, R., & Thorpe, S. J. (2002, October). Surfing a spike wave down the ventral stream. *Vision Research*, *42*(23), 2593–2615. Retrieved 2020-08-12, from http://www.sciencedirect.com/science/article/pii/S0042698902002985 doi: 10.1016/S0042-6989(02)00298-5

VanRullen, R., Zoefel, B., & Ilhan, B. (2014, May). On the cyclic nature of perception in vision versus audition. *Philosophical Transactions of the Royal Society of London. Series B, Biological Sciences*, *369*(1641), 20130214. doi: 10.1098/rstb.2013.0214

Varela, F., Lachaux, J.-P., Rodriguez, E., & Martinerie, J. (2001, April). The brainweb: Phase synchronization and large-scale integration. *Nature Reviews Neuroscience*, *2*(4), 229–239. Retrieved 2020-08-14, from https://www.nature.com/articles/35067550 (Number: 4 Publisher: Nature Publishing Group) doi: 10.1038/35067550

Vialatte, F.-B., Maurice, M., Dauwels, J., & Cichocki, A. (2010, April). Steady-state visually evoked potentials: Focus on essential paradigms and fu-

ture perspectives. *Progress in Neurobiology*, *90*(4), 418–438. Retrieved 2020-07-01, from http://www.sciencedirect.com/science/article/pii/S0301008209001853 doi: 10.1016/j.pneurobio.2009.11.005

Vijayan, S., & Kopell, N. J. (2012, November). Thalamic model of awake alpha oscillations and implications for stimulus processing. *Proceedings of the National Academy of Sciences*, *109*(45), 18553–18558. Retrieved 2018-11-12, from http://www.pnas.org/content/109/45/18553 doi: 10.1073/pnas.1215385109

Voytek, B., Canolty, R. T., Shestyuk, A., Crone, N. E., Parvizi, J., & Knight, R. T. (2010, October). Shifts in Gamma Phase–Amplitude Coupling Frequency from Theta to Alpha Over Posterior Cortex During Visual Tasks. *Frontiers in Human Neuroscience*, *4*. Retrieved 2018-11-12, from https://www.ncbi.nlm.nih.gov/pmc/articles/PMC2972699/ doi: 10.3389/fnhum.2010.00191

Wang, X.-J. (2010, July). Neurophysiological and Computational Principles of Cortical Rhythms in Cognition. *Physiological reviews*, *90*(3), 1195–1268. Retrieved 2020-04-01, from https://www.ncbi.nlm.nih.gov/pmc/articles/PMC2923921/ doi: 10.1152/physrev.00035.2008

Watson, A. B., & Pelli, D. G. (1983, March). Quest: A Bayesian adaptive psychometric method. *Perception & Psychophysics*, *33*(2), 113–120. Retrieved 2020-03-27, from https://doi.org/10.3758/BF03202828 doi: 10.3758/BF03202828

Wertheimer, M. (1912). *Experimentelle Studien über das Sehen von Bewegung*. Barth. (Google-Books-ID: EREUnQEACAAJ)

White, P. A. (2018, April). Is conscious perception a series of discrete temporal frames? *Consciousness and Cognition*, *60*, 98–126. Retrieved 2019-01-30, from http://www.sciencedirect.com/science/article/pii/S1053810018300047 doi: 10.1016/j.concog.2018.02.012

Wolf, W., Hauske, G., & Lupp, U. (1980, January). Interaction of pre- and postsaccadic patterns having the same coordinates in space. *Vision Research*, *20*(2), 117–125. Retrieved 2020-08-20, from http://www.sciencedirect.com/science/article/pii/0042698980901534 doi: 10.1016/0042-6989(80)90153-4

Womelsdorf, T., Johnston, K., Vinck, M., & Everling, S. (2010, March). Theta-activity in anterior cingulate cortex predicts task rules and their adjustments following errors. *Proceedings of the National Academy of Sciences*, *107*(11), 5248–5253. Retrieved 2020-07-17, from https://www.pnas.org/

content/107/11/5248 doi: 10.1073/pnas.0906194107

Wu, C. T., Busch, N. A., Fabre-Thorpe, M., & VanRullen, R. (2009). The Temporal Interplay between Conscious and Unconscious Perceptual Streams. *Current Biology*, *19*(23), 2003–2007. Retrieved 2020-01-08, from https://www.mendeley.com/catalogue/temporal-interplay-between-conscious-unconscious-perceptual-streams/ doi: 10.1016/j.cub.2009.10.017

Wurtz, R. H. (2008, September). Neuronal mechanisms of visual stability. *Vision Research*, *48*(20), 2070–2089. Retrieved 2020-08-18, from http://www.sciencedirect.com/science/article/pii/S0042698908001727 doi: 10.1016/j.visres.2008.03.021

Zhao, M., Gersch, T. M., Schnitzer, B. S., Dosher, B. A., & Kowler, E. (2012, December). Eye movements and attention: The role of pre-saccadic shifts of attention in perception, memory and the control of saccades. *Vision research*, *74*, 40–60. Retrieved 2020-07-17, from https://www.ncbi.nlm.nih.gov/pmc/articles/PMC3623695/ doi: 10.1016/j.visres.2012.06.017

Zimmermann, E., Born, S., Fink, G. R., & Cavanagh, P. (2014, December). Masking produces compression of space and time in the absence of eye movements. *Journal of Neurophysiology*, *112*(12), 3066–3076. doi: 10.1152/jn.00156.2014

Zimmermann, E., Fink, G., & Cavanagh, P. (2013, April). Perifoveal spatial compression. *Journal of Vision*, *13*(5), 21–21. Retrieved 2020-08-20, from https://jov.arvojournals.org/article.aspx?articleid=2121618 (Publisher: The Association for Research in Vision and Ophthalmology) doi: 10.1167/13.5.21

7.7 Acknowledgements

I owe much gratitude to **Rufin** for his invaluable support, insights and patience in the last years. Often I came to your office with unfocused and chaotic ideas and you managed to frame them and bounce back the interesting parts to me. You helped me become more methodological, express myself better, think big and appreciate a proper work wake balance. Many good memories about my time in Toulouse will be about our sessions at the cable and our funny lab meetings. Thanks for being a fantastic mentor.

I would like to thank **Zoe** for making my arrival in France so much easier. **Carmen** for her quick and efficient problem solving capabilities and **Maxime** for his masterful tinkering and for introducing me to the world of 3D printing. Much gratitude also goes to **Claire**, **Pier** and **Simon** who kept things running smoothly, always wearing a smile.

There is many people that I met in Toulouse that have contributed to me keeping my sanity and staying productive, either through fruitful scientific discussion or the opposite. Thanks to **Romain, Yseult, Zhaoyang, Victor, Mariam, Rasa, Sasskia, Nicolas, Giulio, Jakub, Mario, Aimen, Matthieu, Callum, Anna**.

Ook mijn tweede familie, **Jan** en **Carmen**, wil ik bedanken dat jullie mij hebben ontvangen met open armen.

I had the luck to start my first work as a young researcher under the supervision of **Jim** who has been an incredibly encouraging and humorous teacher. Many of the ideas that are present in this manuscript are inspired by you in one way or the other.

Ich möchte mich speziell bei **Kim** und **Joe** bedanken, die ich beide leider nicht oft genug gesehen habe in den letzten Jahren. Ihr wart meine ersten Freunde an der Uni und seit es bis heute geblieben.

A special place in my heart will always be dedicated to my Dungeons and Dragons group. **Milad** (Milok), **Benjamin** (Neb), **Bhavin** (Schaitaan) and **Dimitri** (Gurundir). You have provided me with much happiness and amazing memories during our fantastic adventures.

Special gratitude goes to the ones that I have journeyed with for the longest, **Can** and **Andrea**. Thank you **Can** for always being the first station to bounce crazy ideas off. Thank you for always being there to discuss science and private things alike. **Andrea** thank you for always being the second station to bounce ideas off. You were always a beacon of happiness and inspiration to the entire lab and a role model in many ways to me.

Ganz egal wie stressig, anstrengend oder enttäuschend die Arbeit manchmal sein konnte, es gab einen Ort an dem ich immer vollkommen relaxen konnte. Meine Heimat in Börtlingen war immer ein Ruhepol für mich. Danke **Mama** und **Papa**, dass ihr immer da wart um mich aufzufangen, zu füttern und mit mir über die Dinge zu diskutieren auf die es am Ende wirklich ankommt. **Papa**, dir speziell habe ich meine experimentierfreudigkeit and mein Interesse an der Wissenschaft zu verdanken. Ohne dich hätte ich diesen fantastischen Weg nie eingeschlagen. **Mama**, du hast das einzigartige Talent die Dinge immer von einem aussergewöhnlichen Blickwinkel zu betrachten. Du hast mich mit einem gesunden Selbstbewusstsein und kritischem Auge gesegnet. Ich kann euch beiden dafür nicht genug danken.

Esther und **Matthews**. Ohne euch wäre meine Kindheit leer gewesen. Ihr habt mir beigebracht wie man teilt, schenkt, aufheitert und verzeiht. Falls sich irgendjemand fragt warum ich so witzig bin, das habe ich euch zwei zu verdanken.

The most important person during my thesis was you **Kelly**. You provided the basis and support upon which everything else was built. You guided me through difficult decisions, helped me reflect and to understand myself better and kicked my ass at exactly the right times. In the last 5 years I became a better person through you. I'm very happy that we are together in this to tackle everything that life might throw at us in the future. I love you.